POLARITY REVERSAL CATALYSIS AND ENANTIOSELECTIVE

HYDROGEN-ATOM TRANSFER

A thesis submitted for the degree of Doctor

of Philosophy of the University of London

by

PEARL LING HO MOK

Department of Chemistry,

University College London,

20 Gordon Street,

London WC1H 0AJ.

December 1992

ProQuest Number: 10046085

All rights reserved

INFORMATION TO ALL USERS
The quality of this reproduction is dependent upon the quality of the copy submitted.

In the unlikely event that the author did not send a complete manuscript
and there are missing pages, these will be noted. Also, if material had to be removed,
a note will indicate the deletion.

ProQuest 10046085

Published by ProQuest LLC(2016). Copyright of the Dissertation is held by the Author.

ABSTRACT

This thesis is divided into two sections:

Section A

Polarity reversal catalysis (PRC) is a method by which sluggish abstraction of electron deficient hydrogen by electrophilic radicals, such as t-butoxyl radical ($Bu^tO\cdot$), can be accelerated.

In this section of the thesis, the effect of PRC by amine-alkylborane complexes on hydrogen-atom transfer from ketones was studied. ESR spectroscopy was used to monitor the radical reaction products. t-Butyl methyl ether was found to be 30 times more reactive than acetone towards hydrogen-atom abstraction by $Bu^tO\cdot$ at 190 K, and this difference is attributed entirely to polar effects. In contrast, the highly-nucleophilic amine-boryl radical $Me_3N\rightarrow\dot{B}HThx$ abstracts hydrogen very much <u>more rapidly</u> from acetone than from the ether.

Competitive abstraction from the two different types of α-C-H groups in methyl isopropyl ketone $MeC(O)CHMe_2$ by amine-alkylboryl radicals which have differing steric demands has also been quantified.

Specific alkyl radicals can be generated for ESR studies at low temperature by UV irradiation of a solution containing di-t-butyl peroxide, trimethylamine-butylborane, and the corresponding alkyl chloride. This procedure complements the "triethylsilane method" of Hudson and Jackson for alkyl radical generation from bromoalkanes.

Section B

This section describes the application of PRC to bring about enantioselective α-hydrogen-atom abstraction from esters of the type $R^1R^2CHCO_2R^3$ using optically active amine-alkylboranes to catalyse the reaction of t-butoxyl radicals. This procedure has been used to bring about kinetic resolution of such esters. The bis(isopinocampheylborane) complex of N,N,N',N'-tetramethyl-ethylenediamine and some of its derivatives were investigated as optically active polarity reversal catalysts. After partial consumption of the substrate, the amount remaining and its enantiomeric excess (ee) have been used to derive enantioselectivity constants $(k_{R/S}/k_{S/R})$ for α-hydrogen-atom abstraction from a variety of esters. Enantioselectivity is sensitive to the substituent bulk at the 2-position of the pinene moiety of the catalyst, and varies considerably with the structure of the substrate. The highest selectivity was observed for hydrogen abstraction from dimethyl 2,2-dimethyl-1,3-dioxolane-*trans*-dicarboxylate, when after 75% consumption of initially-racemic ester at 183 K, the residual substrate showed an ee of 97%. A transition state model is proposed to account for the observed enantioselectivities.

In addition, ESR spectroscopy has been used, for the first time, to measure the relative rates of the <u>elementary</u> enantioselective hydrogen-atom abstraction reactions of optically active amine-boryl radicals.

ACKNOWLEDGEMENTS

I would like to express my sincere thanks to my supervisor, Dr. Brian Roberts, for his continual guidance, encouragement and patience during the course of this project. Thanks are also due to Dang, Neil, Parveen for their fruitful discussions, and Claude for his kindness.

I would like to thank my family for their constant financial support, and the Department of Chemistry U.C.L. and U.C.L. for providing scholarships.

Finally, thanks to Neil for his patience and assistance in the preparation of this thesis.

CONTENTS

Chapter 3   Experimental

SECTION B : POLARITY REVERSAL CATALYSIS OF ENANTIOSELECTIVE

HYDROGEN-ATOM ABSTRACTION

Chapter 4   Introduction   72

Chapter 5   Kinetic Resolution of Esters

Chapter 6   Experimental

Chapter 7   ESR Spectroscopic Studies of Enantioselective
Hydrogen-Atom Abstraction Reactions

Chapter 8   Experimental

Chapter 9   Electron Spin Resonance Spectroscopy

SECTION A : POLARITY REVERSAL CATALYSIS OF HYDROGEN-ATOM ABSTRACTION

CHAPTER 1

INTRODUCTION

1.1 Polar Effects in Radical Reactions

Although the reactions of neutral free radicals are less subject to polar influences than ionic reactions, such factors can still strongly affect the courses of homolytic processes. The importance of polar effects in influencing the reactions of uncharged free radicals has been recognised for over forty years.[1] A striking illustration of the operation of polar effects can be seen in the phenomenon of alternating radical co-polymerisation. This is the property of certain monomer pairs, for example styrene and maleic anhydride, of forming a co-polymer in which the monomer units tend to alternate along the chain.[1]

It is also well-established that polar factors play an important role in determining the chemo- and regio-selectivities of hydrogen atom transfer reactions of the type (1.1).[1-4] In valence

$$\overset{\bullet}{A} + H\text{-}B \longrightarrow A\text{-}H + \overset{\bullet}{B} \qquad (1.1)$$
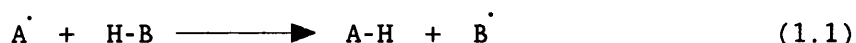
bond terms, the transition state for such direct atom transfer reactions can be represented as a hybrid of the canonical structures **1a-d** and the stability of the transition state will increase as the contribution from the ionic structures **1c** or **1d** increases. As a

$$[\ \overset{\bullet}{A}\ H\text{-}B\ ] \longleftrightarrow [\ A\text{-}H\ \overset{\bullet}{B}\ ] \longleftrightarrow [\ A^+\ H\ B^-\ ] \longleftrightarrow [\ A^-\ \overset{\bullet}{H}\ B^+\ ]$$

$$\textbf{1a} \qquad\qquad \textbf{1b} \qquad\qquad \textbf{1c} \qquad\qquad \textbf{1d}$$
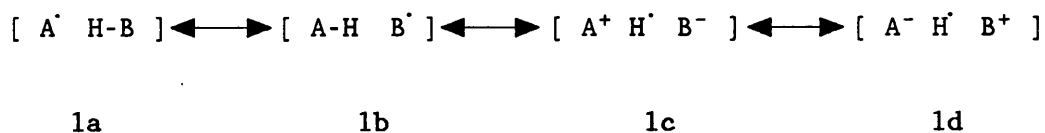
result, the activation energies for a series of <u>similarly</u> <u>exothermic</u> hydrogen atom abstraction reactions would be expected to decrease as the properties of the attacking and departing radicals become more mutually conducive to the participation of charge-transfer structures of the types **1c** or **1d**. Thus, if Nuc· and El· are nucleophilic and electrophilic radicals, respectively, polar effects will favour abstraction of hydrogen from H-Nuc by El· and from H-El by Nuc·, but abstraction of hydrogen from H-Nuc by Nuc· or from H-El by El· will both be disfavoured.*

Similar conclusions may be arrived at by consideration of the frontier molecular orbital interactions in the reactants.[5] The unpaired electron in A· is in a singly occupied molecular orbital (SOMO) which can interact with both the highest occupied molecular orbital (HOMO) and with the lowest unoccupied molecular orbital (LUMO) of the hydrogen donor HB, as shown in Figure **1.1**. Both of these interactions are net stabilising and the extent of stabilisation depends upon the reciprocal of the energy difference between the SOMO and the HOMO or LUMO of HB.

Radicals with a high-energy SOMO (nucleophilic radicals) will react readily with molecules which have a low-energy LUMO, and radicals with a low-energy SOMO (electrophilic radicals) will react

---

*The descriptions "electrophilic" and "nucleophilic" are relative terms. In general, whether a radical A· behaves as a net electrophile [structure **1d** more important than **1c**] or a net nucleophile [structure **1c** more important than **1d**] in reaction (1.1) will depend on the nature of B· (*i.e.* on the electronegativity difference between A· and B·).

preferentially with molecules having a high-energy HOMO. This is
illustrated by considering the reactions of the methyl radical and
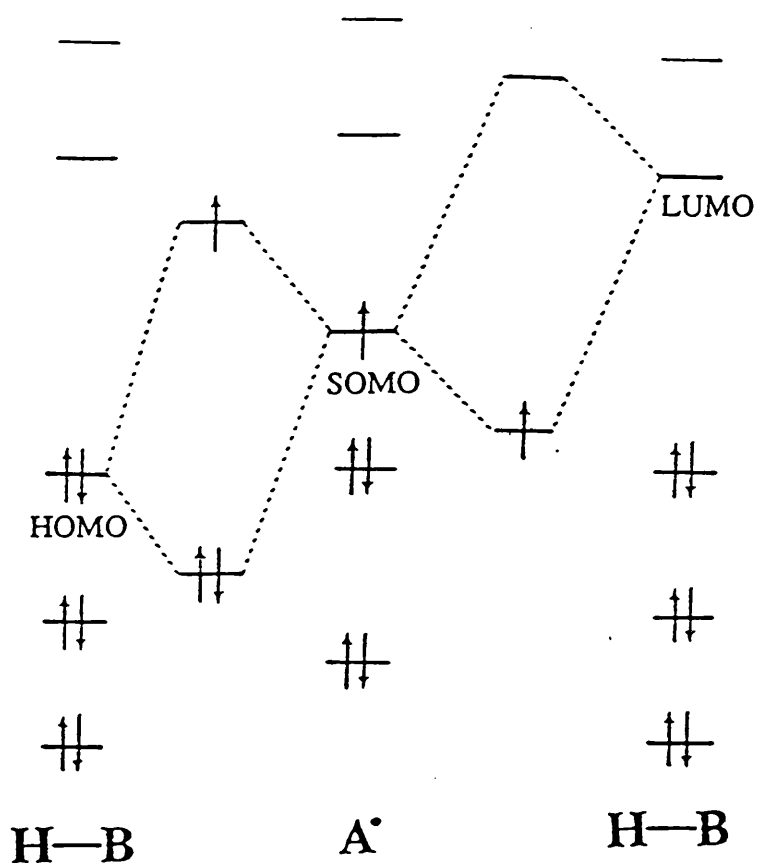
Figure 1.1 : Schematic diagram showing the interactions between the
frontier molecular orbitals of A· and H-B.

the chlorine atom with propanoic acid $(CH_3CH_2CO_2H)$.[6] Methyl radicals
preferentially attack hydrogen atoms on C-2 of the acid; on the other
hand, chlorine atoms preferentially attack the hydrogen atoms
attached to C-3. Quantitatively in the gas phase, methyl radicals
attack an electron deficient α-hydrogen 7.8 times faster than a more
electron rich β-hydrogen, whereas chlorine radicals attack an
α-hydrogen 30 times slower than a β-hydrogen. The methyl radical has
a much higher energy SOMO (lower ionisation potential) than the
chlorine atom. Because of the presence of the electron withdrawing

carboxyl group, the C-2-H σ bonding orbital (the HOMO) and the σ^* orbital (the LUMO) will be relatively low in energy. Conversely, the C-3-H σ and σ^* orbitals will be relatively high in energy, because the CO_2H group is more remote and the CH_2CO_2H group is a mild electron donor. The orbital interactions are therefore those shown in Figure 1.2. The interactions A for the chlorine atom and C for
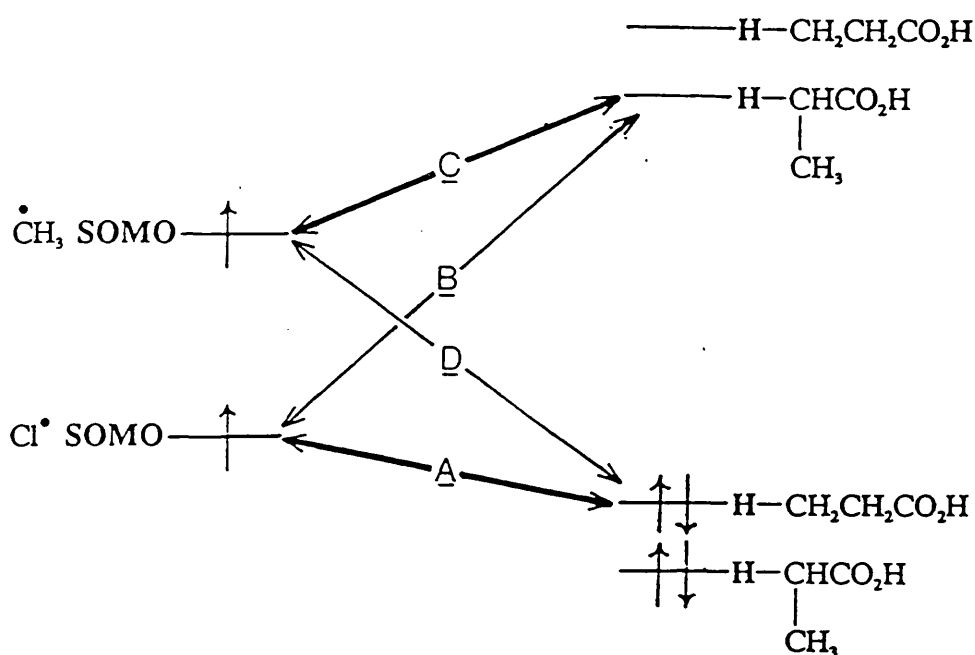
Figure 1.2 : Schematic diagram showing the frontier orbital interactions for the attack of methyl and chlorine radicals on propanoic acid.

the methyl radical are more effective than B and D respectively, because the energy differences between the relevant orbitals are smaller. Thus, as from the valence bond analysis given before, we conclude that the hydrogen abstractions (1.2) and (1.3) will be favoured by polar effects, while reactions (1.4) and (1.5) will not.

$$El^{\bullet} \; + \; H\text{-}Nuc \; \longrightarrow \; H\text{-}El \; + \; Nuc^{\bullet} \qquad\qquad (1.2)$$

$$Nuc^{\bullet} \; + \; H\text{-}El \; \longrightarrow \; H\text{-}Nuc \; + \; El^{\bullet} \qquad\qquad (1.3)$$

$$El^{1\bullet} \; + \; H\text{-}El^2 \; \longrightarrow \; H\text{-}El^1 \; + \; El^{2\bullet} \qquad\qquad (1.4)$$

$$Nuc^{1\bullet} \; + \; H\text{-}Nuc^2 \; \longrightarrow \; H\text{-}Nuc^1 \; + \; Nuc^{2\bullet} \qquad\qquad (1.5)$$
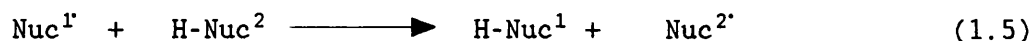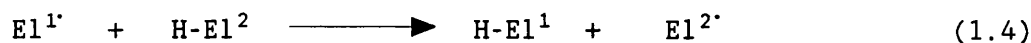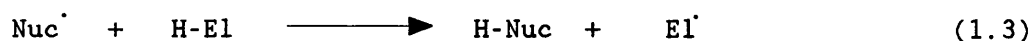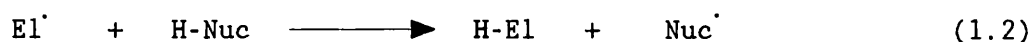
1.2 Polarity Reversal Catalysis (PRC)

The preceding analysis points to the concept of polarity reversal catalysis (PRC),[7-9] whereby the sluggish single step processes (1.4) and (1.5) are replaced by pairs of fast consecutive steps, as illustrated in equations (1.6) and (1.7) or (1.8) and (1.9) respectively. Both steps of each catalytic cycle are now facilitated by favourable polar effects. We may refer to the molecules H-Nuc and H-El as "donor" and "acceptor" catalysts, respectively.*

$$\left\{ \begin{array}{l} El^{1\bullet} \; + \; H\text{-}Nuc \; \longrightarrow \; H\text{-}El^1 \; + \; Nuc^{\bullet} \qquad\qquad (1.6) \\[2ex] Nuc^{\bullet} \; + \; H\text{-}El^2 \; \longrightarrow \; H\text{-}Nuc \; + \; El^{2\bullet} \qquad\qquad (1.7) \end{array} \right.$$

$$\left\{ \begin{array}{l} Nuc^{1\bullet} \; + \; H\text{-}El \; \longrightarrow \; H\text{-}Nuc^1 \; + \; El^{\bullet} \qquad\qquad (1.8) \\[2ex] El^{\bullet} \; + \; H\text{-}Nuc^2 \; \longrightarrow \; H\text{-}El \; + \; Nuc^{2\bullet} \qquad\qquad (1.9) \end{array} \right.$$
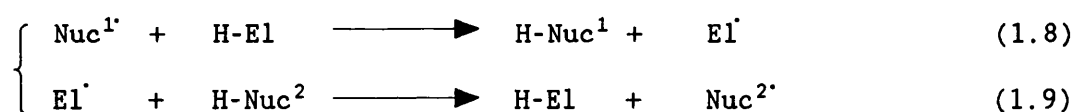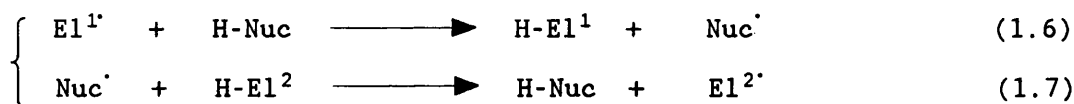
The t-butoxyl radical ($Bu^tO^{\bullet}$), which may be generated in solution by UV photolysis of di-t-butyl peroxide (DTBP) [equation (1.10)], is (like other alkoxyl radicals) a highly electrophilic

*In 1953 Barrett and Waters[10] reported that thiols catalyse the radical chain decarbonylation of aldehydes. Mayo[11] explained this effect of thiols in terms of what we refer to here as polarity reversal catalysis.

$$Bu^tOOBu^t \quad \xrightarrow{\quad h\nu \quad} \quad 2Bu^tO^{\cdot} \qquad\qquad (1.10)$$

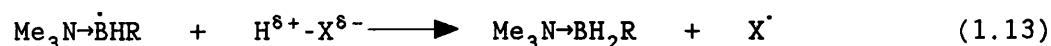species.[2-4] The ionisation potential and electron affinity of $Bu^tO^{\cdot}$ are 12 and 1.89 eV respectively, and as such its chemical reactivity is strongly influenced by polar factors. The rates of similarly-exothermic hydrogen atom abstraction reactions (1.11) will thus increase with the extent of charge transfer stabilisation of the

$$Bu^tO^{\cdot} \quad + \quad H\text{-}X \quad \xrightarrow{\quad\quad} \quad Bu^tOH \quad + \quad X^{\cdot} \qquad\qquad (1.11)$$

$$[Bu^tO^{\cdot} \quad H\text{-}X] \quad \longleftrightarrow \quad [Bu^tO\text{-}H \quad {}^{\cdot}X\ ] \quad \longleftrightarrow \quad [Bu^tO^{-} \quad {}^{\cdot}H \quad X^{+}]$$

$$\textbf{2a} \qquad\qquad\qquad \textbf{2b} \qquad\qquad\qquad \textbf{2c}$$
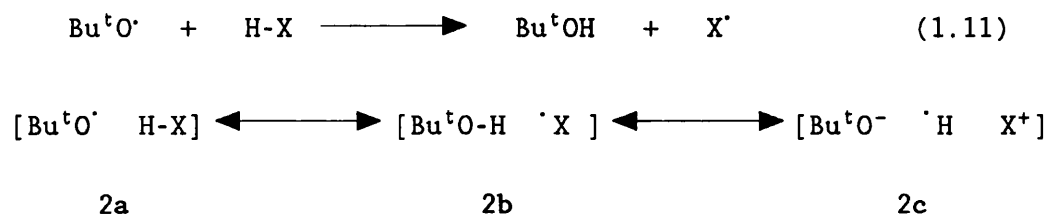
transition state **2**, as represented by the inclusion of structure **2c**. Thus, the rate of reaction (1.11) will increase with increasing stability of the cationic fragment X^{+}.

Abstraction of an electron deficient hydrogen (that is when X^{+} is relatively unstable and X^{-} relatively stable) by $Bu^tO^{\cdot}$ should be susceptible to PRC using an appropriate donor catalyst and it has been shown[7,9] that these reactions are catalysed by amine-alkylborane complexes such as trimethylamine-thexylborane [thexyl(Thx) = 1,1,2-trimethylpropyl]. In their presence the direct abstraction from $H^{\delta+}\text{-}X^{\delta-}$ is replaced by the catalytic cycle shown in equations (1.12) and (1.13). Both steps are facilitated by favourable polar

$$Bu^tO^{\cdot} \quad + \quad Me_3N{\to}BH_2R \quad \xrightarrow{\quad\quad} \quad Bu^tOH \quad + \quad Me_3N{\to}\dot{B}HR \qquad (1.12)$$

$$Me_3N{\to}\dot{B}HR \quad + \quad H^{\delta+}\text{-}X^{\delta-} \quad \xrightarrow{\quad\quad} \quad Me_3N{\to}BH_2R \quad + \quad X^{\cdot} \qquad (1.13)$$
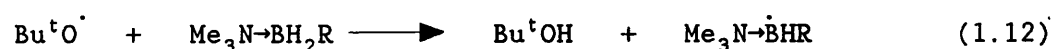
effects, the charge transfer structure **3** making an appreciable

contribution to the transition state for reaction (1.13).

$$[Me_3N{\rightarrow}BHR \quad \overset{\bullet}{H} \quad X^-] \qquad 3$$
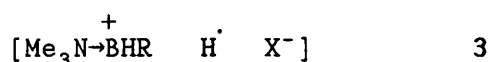
The control of regioselectivity that may be exercised using PRC can be strikingly illustrated by the reactions of tetrahydro-4*H*-pyran-4-one 4.[12] UV irradiation of a solution of 4 in DTBP at 268 K yields mainly the oxygen-conjugated radical 5 [equation (1.14)], as shown by ESR spectroscopy, while in the presence of trimethylamine-thexylborane as donor polarity reversal catalyst, the major product is the carbonyl-conjugated radical 6 [equation (1.15)].

$$(1.14)$$

$$(1.15)$$
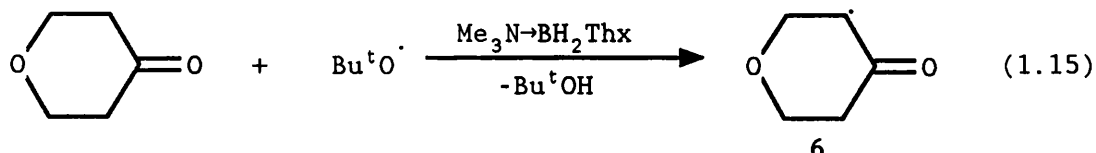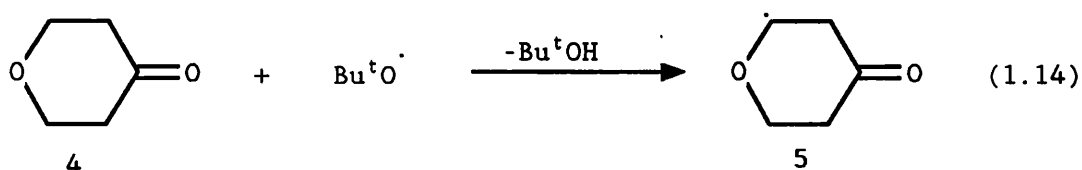
Abstraction of the electron deficient hydrogen α to the carbonyl group is brought about by the nucleophilic $Me_3N{\rightarrow}\overset{\bullet}{B}HThx$, instead of by the electrophilic $Bu^tO\cdot$.

The strengths of the H-El or H-Nuc bonds in acceptor or donor catalysts for hydrogen atom abstractions are crucial. Ideally, these should be such that the exothermicity of the uncatalysed reaction is split approximately equally between the two steps of the catalytic cycle, as illustrated for a donor catalyst in Figure 1.3

Donor catalysts will generally be built around metal(loid)-H bonds (as in $Me_3N{\rightarrow}BH_2R$), and steric or electronic substituent effects

can be used to modify their strengths and the selectivities of the derived metal(loid)-centred radicals.
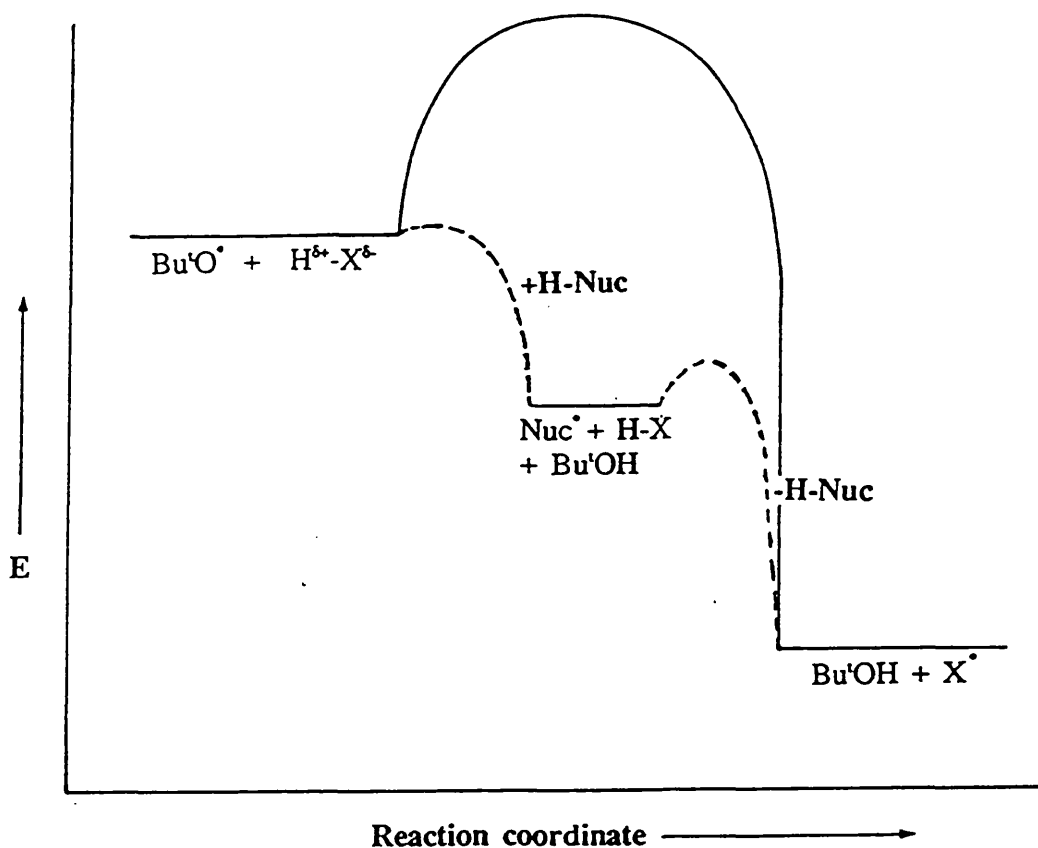
Figure 1.3 : Schematic potential energy diagram to illustrate the principle of PRC.

A number of amine-alkylborane complexes 7-13 have been prepared and investigated as "donor" polarity reversal catalysts.

The effect of polarity reversal catalysis on the reactions of $Bu^tO\cdot$ with a variety of esters has been studied by Vikram Paul in this Department.[13] The carbonyl group in a ketone, like that in an ester, is a powerful π-electron withdrawing substituent and should activate adjacent C-H groups towards abstraction by $Bu^tO\cdot$ in the presence of "donor" polarity reversal catalysts. In this section of

$Me_3N{\rightarrow}BH_2Thx$

7

$Me_3N{\rightarrow}BH_2Bu^n$

8

$Me_3N{\rightarrow}BH_2Bu^i$

9

$Me_3N{\rightarrow}BH_2Bu^s$
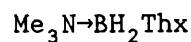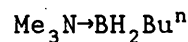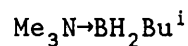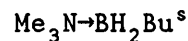
10
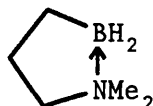
11
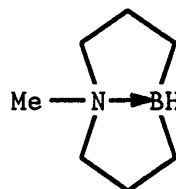
12
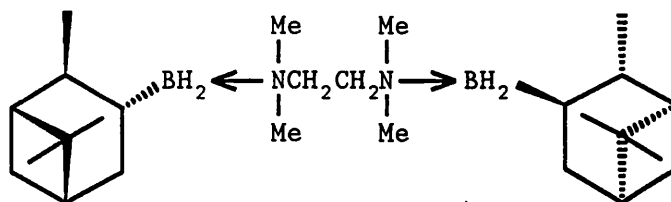
13

the thesis, abstraction of hydrogen by $Bu^tO\cdot$ from acetone, methyl isopropyl ketone, cyclobutanone, cyclopentanone and cyclohexanone under conditions of PRC using "donor" catalysts was investigated.

Since a knowledge of the properties of boron-centred radicals is important for understanding the application of ligated boranes as polarity reversal catalysts, a review of these properties is appropriate at this point.

1.3 Neutral Ligated Boryl Radicals

The ligated boryl radicals, $L{\rightarrow}\overset{\bullet}{B}X_2$ constitute an important class of boron-centred radicals. A wide variety of <u>neutral</u> ligated boryl radicals can be envisaged in which Lewis bases such as amines, phosphines, sulphides, and carbon monoxide are attached to the electron deficient $H_2B{\bullet}$. In fact, a wide variety of ligated boryl radicals have now been generated by hydrogen atom abstraction from the parent borane complexes [equation (1.16), where $L = R_3N$, R_2NH,

$$L{\rightarrow}BH_3 \xrightarrow{\quad -H^{\bullet}\quad} L{\rightarrow}\overset{\bullet}{B}H_2 \qquad\qquad (1.16)$$
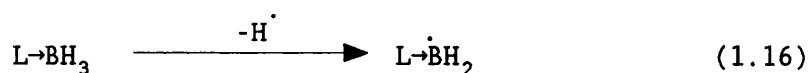
R_3P or R_2S] and the structures and reactivities of these have been investigated using ESR spectroscopy.[14-17]

While the phosphine- and sulphide-boryl radicals are, like $H_3B{\bullet}^-$, essentially planar at the radical centre, the amine-boryl radicals are strongly pyramidal at boron. These differences have been explained in terms of the greater electronegativity of nitrogen compared with hydrogen and of the ability of the R_3P[15] and R_2S[17] ligands to delocalise the unpaired electron from boron, whereas little delocalisation occurs onto an R_3N donor. Such delocalisation will be more extensive if the radical centre is planar.

1.4 Amine-Boryl Radicals

The amine-boranes and -boryl radicals are of particular interest because they afford a comparison with organic systems in which a C-C moiety is replaced by the isoelectronic $N{\rightarrow}B$ linkage.

Ammonia-borane ($H_3N{\rightarrow}BH_3$) is isoelectronic with ethane (H_3C-CH_3), and the two possible radicals formed by hydrogen atom abstraction from $H_3N{\rightarrow}BH_3$ will be isoelectronic with the ethyl radical.

t-Butoxyl radicals react with ammonia-borane or with primary, secondary, or tertiary amine-boranes to give amine-boryl radicals [equation (1.17)].[18,19] The ESR spectroscopic parameters for the

$$Bu^tO^{\cdot} \;+\; R_3N{\rightarrow}BH_3 \;\longrightarrow\; R_3N{\rightarrow}\overset{\cdot}{B}H_2 \;+\; Bu^tOH \qquad (1.17)$$
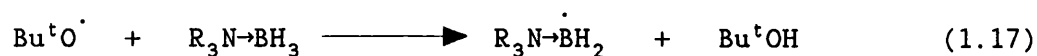
<div align="center">14</div>

ammonia-boryl radical 14 (R = H) are $a(^{11}B)$ 42.3, $a(2H_\alpha)$ 11.0, $a(^{14}N)$ 1.4, $a(3H_\beta)$ 11.0 G, and g 2.0023 at 269 K in t-butyl alcohol-dimethyl ether (4:1 v/v) solvent.[18] For comparison, the ethyl radical shows $a(2H_\alpha)$ 22.2 and $a(3H_\beta)$ 26.9 G. The large magnitude of the ^{11}B splitting and the relatively small α-proton hyperfine coupling constant show clearly that $H_3N{\rightarrow}\overset{\cdot}{B}H_2$ is pyramidal at boron, unlike ethyl radical[20] which is effectively planar at the radical centre.

It has been shown[14] that the equilibrium geometry at boron in the trimethylamine-boryl radical is also pyramidal, as shown in 15 (R
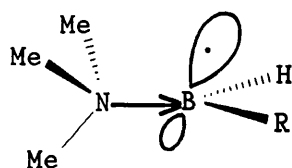
<div align="center">15</div>

= H), again on the basis of the magnitude and temperature dependencies of the ^{11}B and α-proton coupling constants and the effects of deuteriation at boron. The ESR parameters of the amine-alkylboryl radicals are also indicative of a non-planar

configuration at the radical centre.[9] The ^{11}B (I = 3/2, natural abundance 80.2%) splittings are large (*ca.* 60 G) and correspond to 8-9% unpaired electron population of the B-2s atomic orbital.[21] There is a small decrease in $a(^{11}B)$ with increasing temperature, which implies that the time-average configuration becomes more nearly planar at higher temperatures, as expected for a pyramidal equilibrium geometry. For example,[9] the ESR parameters for the trimethylamine-thexylboryl radical are $a(^{11}B)$ 59.9, $a(H_\alpha)$ 9.8 G, and g 2.0021 at 264 K in cyclopropane. The magnitude of $a(H_\alpha)$ is appreciably smaller than the value (15.2 G at 253 K) for the planar or nearly-planar borane radical anion $H_3B^{\cdot -}$,[22] again in accord with a pyramidal geometry for the amine-alkylboryl radicals. The sign of $a(H_\alpha)$ for **15** (R = alkyl) is almost certainly negative, corresponding to spin-polarisation as the predominant mechanism for spin-transmission to the α-proton.

The ^{11}B splittings for **15** (R = alkyl) are 15-20% larger than $a(^{11}B)$ for **15** (R = H) under similar conditions, suggesting that the time-average configuration of the latter deviates less from planarity at boron.

Secondary and primary amine-boryl radicals have been generated similarly and their chemical properties have been investigated. When the ligand is a secondary amine, although the amine-boryl radical **16** is the initial (kinetically-controlled) product of the reaction with t-butoxyl radicals, **16** subsequently abstracts hydrogen rapidly from the NH group of the parent amine-borane to give the more stable isomeric aminyl-borane radical **17** [equations (1.18) and (1.19)].[19]

$$\text{Bu}^t\text{O}^\bullet \quad + \quad \text{R}_2\text{NH}\rightarrow\text{BH}_3 \quad\longrightarrow\quad \text{R}_2\text{NH}\rightarrow\dot{\text{B}}\text{H}_2 \quad + \quad \text{Bu}^t\text{OH} \qquad (1.18)$$

16

$$\text{R}_2\text{NH}\rightarrow\dot{\text{B}}\text{H}_2 \quad + \quad \text{R}_2\text{NH}\rightarrow\text{BH}_3 \quad\longrightarrow\quad \text{R}_2\dot{\text{N}}\rightarrow\text{BH}_3 \quad + \quad \text{R}_2\text{NH}\rightarrow\text{BH}_3 \qquad (1.19)$$

17
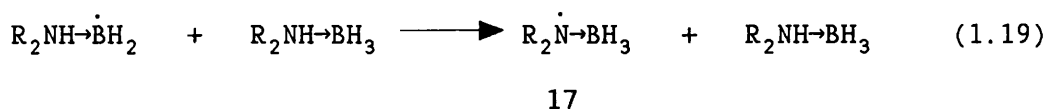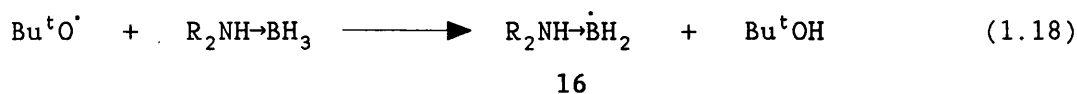
1.5 Reactions of Amine-Boryl Radicals with Alkyl Halides

The amine-boryl radicals[14,23] react rapidly with both alkyl chlorides and bromides to give alkyl radicals [equation (1.20)]. In

$$\text{R}_3\text{N}\rightarrow\dot{\text{B}}\text{H}_2 \quad + \quad \text{R}'\text{-Hal} \quad\longrightarrow\quad \text{R}^{''\bullet} \quad + \quad \text{R}_3\text{N}\rightarrow\text{BH}_2\text{Hal} \qquad (1.20)$$
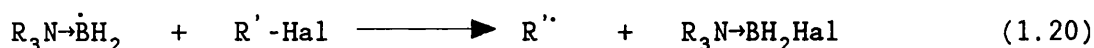
these reactions, $\text{R}_3\text{N}\rightarrow\dot{\text{B}}\text{H}_2$ behaves in a fashion similarly to trialkylsilyl radicals,[24-26] rather than like their isoelectronic alkyl-radical counterparts, reflecting the "diagonal" relationship between boron and silicon in the Periodic Table.

Both thermodynamic and polar factors are thought to be responsible for the higher reactivity of $\text{R}_3\text{N}\rightarrow\dot{\text{B}}\text{H}_2$ towards alkyl halides as compared with $\text{R}_3\text{C}\text{-}\dot{\text{C}}\text{H}_2$. It is likely that the transition state for dehalogenation of an alkyl halide by amine-boryl radical involves a large degree of charge transfer from $\text{R}_3\text{N}\rightarrow\dot{\text{B}}\text{H}_2$ to the halide and this will favour abstraction by the nucleophilic boron-centred radical [see **18a** and **18b**]. The bond to halogen is probably stronger

$$[\text{R}_3\text{N}\rightarrow\dot{\text{B}}\text{H}_2 \quad \text{R}'\text{-Hal} \quad\longleftrightarrow\quad \text{R}_3\text{N}\rightarrow\text{BH}_2^+ \quad \text{R}^{''} \quad \text{Hal}^-]$$
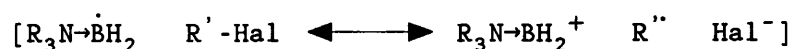
18a   **18b**

in $R_3N{\rightarrow}BH_2Hal$ than in R_3C-CH_2Hal, because of the metalloidal character of boron. Generally, the abstraction of bromine by a ligated boryl radical from an alkyl bromide is faster than the abstraction of chlorine from an alkyl chloride.[27]

1.6 β-Scission of Amine-Boryl Radicals

An important point which has to be considered when designing a donor polarity reversal catalyst is the possibility of β-scission of the amine-boryl radical involved.

As stated above, in bimolecular processes the chemical reactivity of an amine-boryl radical **19** resembles that of a silyl radical more closely than that of the isoelectronic alkyl radical. However, whereas alkylsilyl radicals do not undergo ready unimolecular β-scission, the amine-boryls do [equation (1.21)] and

$$R_3N{\rightarrow}\overset{\bullet}{B}H_2 \longrightarrow R^{\bullet} + R_2N{\Rightarrow}BH_2 \qquad (1.21)$$

19

much more readily than the isoelectronic alkyl radicals.[14]

The reactions of $Bu^tO^{\bullet}$ with aziridine- and azetidine-boranes **20** (n = 1 or 2) have been examined previously[14,27,28] using ESR spectroscopy and shown to lead ultimately to carbon-centred radicals **22**, formed by the ring-opening β-scission of intermediate amine-boryl radicals [equation (1.22)]. The aziridine-boryl radical thus resembles the isoelectronic cyclopropylmethyl radical, which undergoes ring opening to give the but-3-enyl radical.[29]

The acyclic t-butyldimethylamine-boryl radical **23** also undergoes rapid β-scission, now to produce $Bu^{t\bullet}$ [equation (1.23)].[14]

$$\text{20} \xrightarrow[-Bu^tOH]{Bu^tO^\bullet} \text{21} \longrightarrow \text{22} \qquad (1.22)$$

20   21   22

$$Bu^tMe_2N\text{-}\overset{\bullet}{B}H_2 \longrightarrow Bu^{t\bullet} + Me_2N{=}BH_2 \qquad (1.23)$$
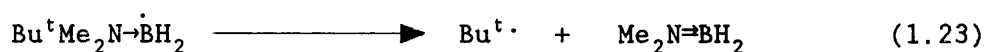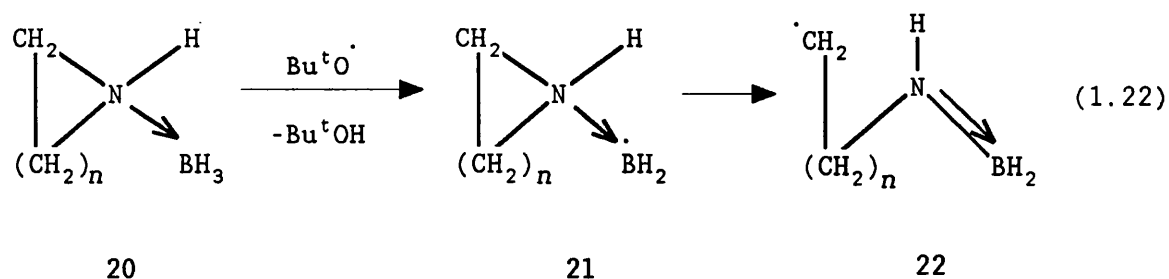
23

The isoelectronic alkyl radical $Bu^tMe_2C\text{-}\overset{\bullet}{C}H_2$ shows no sign of β-scission under similar conditions. β-Scission also takes place rapidly for $Pr^i{}_2EtN\text{-}\overset{\bullet}{B}H_2$, to give the isopropyl radical, although the rate of cleavage is *ca.* 3.7 times slower than that of 23 at 221 K[30] and both are slower than the ring opening of the aziridine-boryl radical.

The high rate of β-scission of amine-boryl radicals has been attributed to the thermodynamic favourability of this process, which is reflected in much lower activation energies for decomposition of the amine-boryls[30] as compared with the isoelectronic alkyl radicals, β-scission of which is much less favourable thermodynamically.

References to Chapter 1

1. C. Walling, "Free Radicals in Solution", Wiley, New York, 1957.

2. G. A. Russell in "Free Radicals", ed. J. K. Kochi, Wiley-Interscience, New York, 1973, Vol. 1, Ch. 7.

3. F. Minisci and A. Citterio, *Adv. Free Radical Chem.*, 1980, **6**, 65.

4. "Substituent Effects in Radical Chemistry", ed. H. G. Viehe, Z. Janousek and R. Merenyi, Reidel, Dordrecht, 1986.

5. I. Fleming, "Frontier Orbitals and Organic Chemical Reactions", Wiley-Interscience, London, 1976, Ch. 5, pp.186-188.

6. H. Magritte and A. Bruylants, *Ind. Chem. Belge*, 1957, **22**, 547.

7. V. Paul and B. P. Roberts, *J. Chem. Soc., Chem. Commun.*, 1987, 1322.

8. V. Paul, B. P. Roberts and C. A. S. Robinson, *J. Chem. Research (S)*, 1988, 264.

9. V. Paul and B. P. Roberts, *J. Chem. Soc., Perkin Trans. 2*, 1988, 1183.

10. K. E. J. Barrett and W. A. Waters, *Discuss. Faraday Soc.*, 1953, **14**, 221.

11. F. R. Mayo, *Discuss. Faraday Soc.*, 1953, **14**, 254.

12. V. Paul, B. P. Roberts and C. R. Willis, *J. Chem. Soc., Perkin Trans. 2*, 1989, 1953.

13. V. Paul, Ph. D. thesis, London, 1989, Ch. 4.

14. J. A. Baban, V. P. J. Marti and B. P. Roberts, *J. Chem. Soc., Perkin Trans. 2*, 1985, 1723.

15. J. A. Baban and B. P. Roberts, *J. Chem. Soc., Perkin Trans. 2*, 1984, 1717.

16. J. A. Baban and B. P. Roberts, *J. Chem. Soc., Perkin Trans. 2*, 1986, 1607.

17. J. A. Baban and B. P. Roberts, *J. Chem. Soc., Perkin Trans. 2*, 1987, 497.

18. J. A. Baban, V. P. J. Marti and B. P. Roberts, *J. Chem. Research (S)*, 1985, 90.

19. I. G. Green and B. P. Roberts, *J. Chem. Soc., Perkin Trans. 2*, 1986, 1597.

20. D. Griller, P. R. Marriott and K. F. Preston, *J. Chem. Phys.*, 1979, **71**, 3703.

21. M. C. R. Symons, "Chemical and Biochemical Aspects of Electron Spin Resonance Spectroscopy", Van Nostrand Reinhold, London, 1978.

22. J. R. M. Giles and B. P. Roberts, *J. Chem. Soc., Perkin Trans. 2*, 1982, 1699; 1983, 743.

23. V. P. J. Marti and B. P. Roberts, *J. Chem. Soc., Perkin Trans. 2*, 1986, 1613.

24. R. A. Jackson, "Essays On Free-Radical Chemistry Special Publication 24", The Chemical Society, 1970, Ch. 12.

25. A. Hudson, R. A. Jackson, *Chem. Commun.*, 1969, 1323.

26. C. Chatgilialoglu, K. U. Ingold and J. C. Scaiano, *J. Am. Chem. Soc.*, 1982, **104**, 5123.

27. J. A. Baban and B. P. Roberts, *J. Chem. Soc., Chem. Commun.*, 1983, 1224.

28. J. A. Baban and B. P. Roberts, *J. Chem. Soc., Chem. Commun.*, 1984, 850.

29. A. L. J. Beckwith and K. U. Ingold, "Rearrangements in Ground and Excited States", ed. P. de Mayo, Academic Press, New York,

1980, Vol. 1, Ch. 4.

30. J. A. Baban, J. P. Goddard and B. P. Roberts, *J. Chem. Research (S)*, 1986, 30.

CHAPTER 2

RESULTS AND DISCUSSION

2.1 Syntheses of Catalysts

Trimethylamine-thexylborane[1,2] **1** was prepared by the hydroboration of 2,3-dimethylbut-2-ene, using dimethyl sulphide-borane (BMS), followed by the addition of an excess of trimethylamine [equations (2.1) and (2.2)].

$$Me_2S{\rightarrow}BH_3 \quad + \quad Me_2C{=}CMe_2 \quad \longrightarrow \quad 1/2(Me_2CHCMe_2BH_2)_2 \quad + \quad Me_2S \qquad (2.1)$$

$$1/2(Me_2CHCMe_2BH_2)_2 \quad + \quad Me_3N \longrightarrow Me_3N{\rightarrow}BH_2CMe_2CMe_2H \qquad (2.2)$$
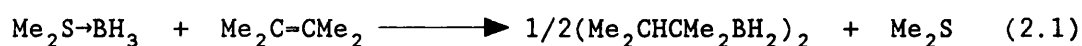
1

Trimethylamine-n-butylborane **2** was prepared by reduction of tri-n-butylboroxine with lithium aluminium hydride in the presence of excess trimethylamine, using the method of Hawthorne[3] [equation (2.3)]. The isomeric trimethylamine-isobutylborane **3** and

$$(Bu^nBO)_3 \quad \xrightarrow[\text{2. } Me_3N]{\text{1. } LiAlH_4} \quad Me_3N{\rightarrow}BH_2Bu^n \qquad (2.3)$$

2
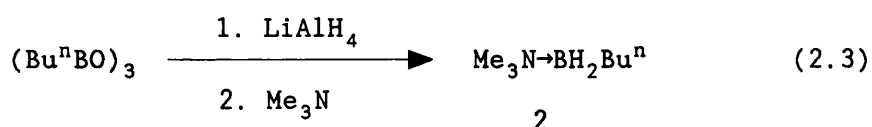
trimethylamine-s-butylborane **4** were prepared similarly from the corresponding trialkylboroxines.[3]

The amine-boranes **1**[2,4,5] and **2-4** are all good polarity reversal catalysts. The trimethylamine-butylboranes **2-4** have been shown[6] by ^{1}H NMR spectroscopy to be stable to hydrolysis after 1.5 h exposure to the atmosphere. In the case of trimethylamine-n-butylborane **2**, no change was detected even after 5 h of exposure. In comparison, **1** is

air-sensitive and hydrolyses very easily in the atmosphere to give thexylboronic acid 5 [see equation (2.4)]. This is presumably because

$$Me_3N{\rightarrow}BH_2Thx \;\rightleftharpoons\; Me_3N \;+\; BH_2THx \;\xrightarrow[{-2H_2}]{2H_2O}\; ThxB(OH)_2 \qquad (2.4)$$

<div align="center">5</div>

of the relatively large bulk of the thexyl group, which results in a weak N→B bond.

One way to increase the stability of the N→B linkage is by incorporating it into a ring system. 1-Methyl-cis-1-azonia-5-boratabicyclo[3.3.0]octane 6 has been synthesised by Parveen Kaushal[7] by heating $Et_3N{\rightarrow}BH_3$ with N-methyldiallylamine in refluxing xylene at ca. 140 °C in a sealed tube [equation (2.5)]. However, the yield was only 5%. The method was

$$(2.5)$$

<div align="center">6</div>
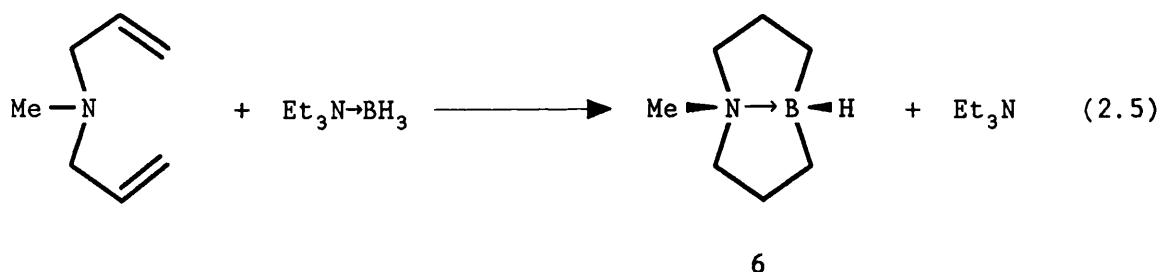
therefore modified in order to obtain a higher yield and, by heating $Et_3N{\rightarrow}BH_3$ with N-methyldiallylamine in refluxing benzene at ca. 190 °C using a pressure vessel, the yield was increased to 13%. However, the complex was slightly less pure than that obtained by the original route.

The complex 6 has also been prepared from N-methyldiallylamine and BMS. The sulphide-borane was added to N-methyldiallylamine in ether at 0 °C and, after stirring for a further one hour at room

temperature, the volatiles were removed under reduced pressure (10 Torr). The residual oil was then heated in benzene at ca. 190 °C for 3 h in a pressure vessel. However, the complex 6 synthesised this way was no purer than that from the previous method.

The first stage in the formation of 6 presumably involves formation of N-methyldiallylamine-borane 7, which then undergoes stepwise intramolecular hydroboration to give the bicyclic product 6 [equation (2.6)]. The impurity obtained was possibly

Me — N + Et₃N→BH₃ —benzene→ Me — N → BH₃
                        -Et₃N

7

(2.6)

Me — N → B — H

6
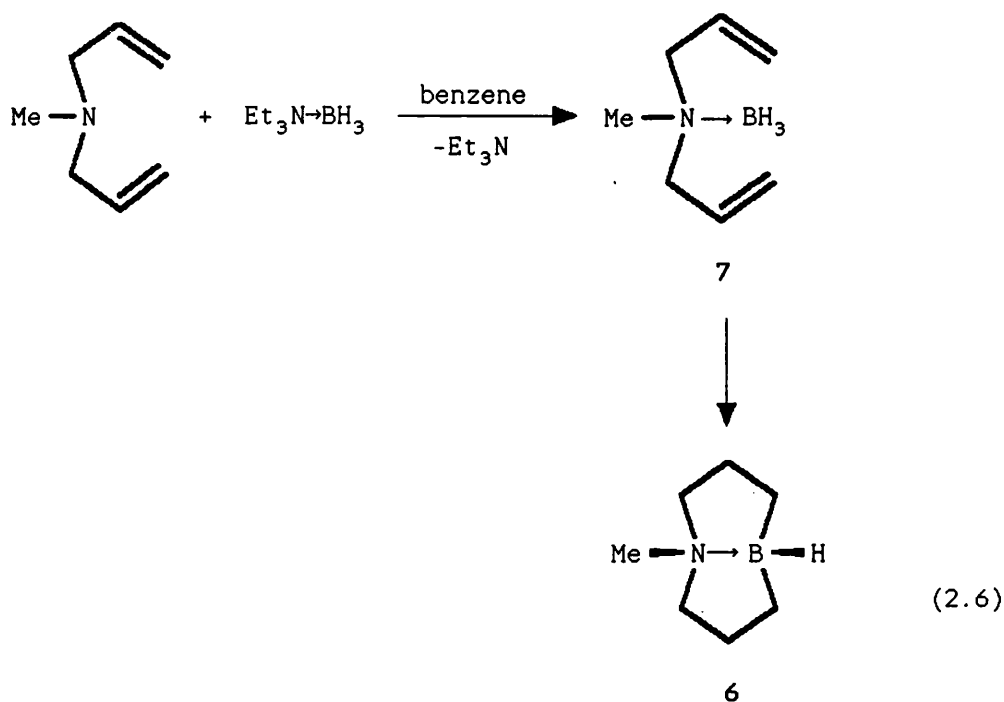
1-methyl-1,2-azaborolidine **8**, which would be formed by the elimination of propene from the intermediate **9** [equation (2.7)],[8,9]

Me — N→BH₂ ——→ Me — N⇒BH + ⟍⟋⟍ (2.7)

9   **8**
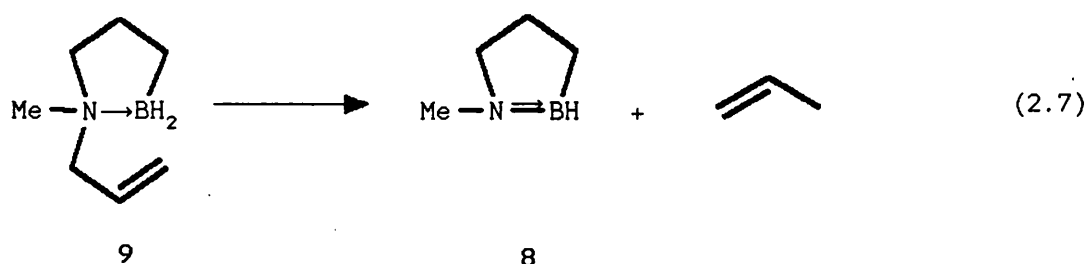
especially at high temperatures.

Cyclic N,N-dimethylglycinatoborane[10] 10 was synthesised from trimethylamine-iodoborane and N,N-dimethylglycine [equation (2.8)].

$$Me_2NCH_2CO_2H \ + \ Me_3N{\rightarrow}BH_2I \ \xrightarrow{\hspace{2cm}} \ \underset{\textstyle 10}{\text{[structure]}} \ + \ Me_3NHI \qquad (2.8)$$
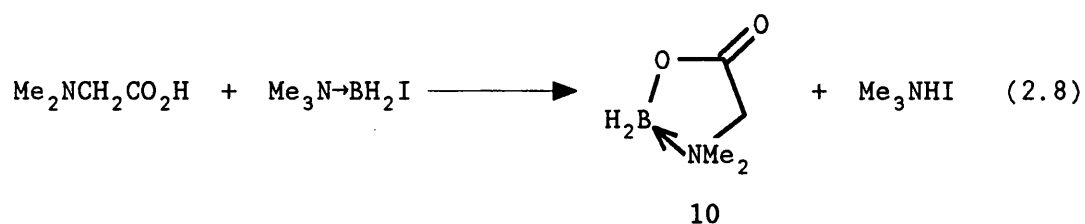
Unfortunately, despite its stability in air, the ability of 10 to act as a polarity reversal catalyst could not be successfully investigated because of its low solubility. The best solvents found for 10 were oxirane and a mixture of t-butyl alcohol and t-pentyl alcohol. However, in both cases the solubility was still so low that the compound was unsuitable for ESR work.

2.2 Catalysed Hydrogen-Atom Abstraction by t-Butoxyl Radicals from Ketones

2.2.1 From Acetone

It has been known for many years that t-butoxyl radicals abstract hydrogen from acetone only relatively slowly [equation (2.9)]. At first sight, this is surprising since the abstraction is

$$Bu^tO\cdot \quad + \quad Me_2CO \quad \longrightarrow \quad Bu^tOH \quad + \quad MeC(O)\dot{C}H_2 \qquad (2.9)$$
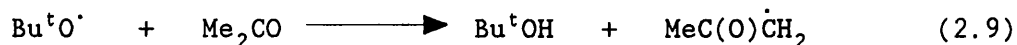
$$11$$

appreciably exothermic because the α-carbonylalkyl radical **11** is stabilised by conjugative delocalisation of the unpaired electron. The radical **11** may be represented as a resonance hybrid of canonical structures **12a** and **12b**, and delocalisation of the unpaired electron onto oxygen is responsible for the relatively high g-factors of α-carbonylalkyl radicals [the g-factor of **11** is 2.0045, as compared with 2.0026 for $H_3C\cdot$]. Because of this delocalisation onto oxygen the

12a   12b
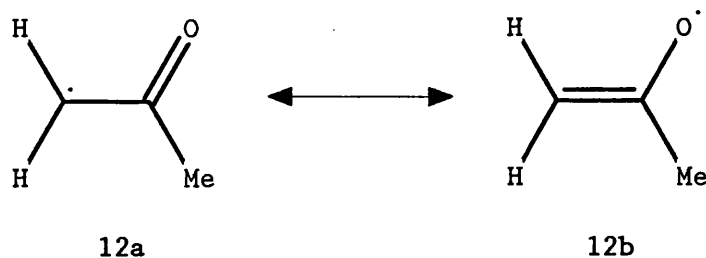
C_α-C_β bond order is greater than unity and there is an appreciable barrier to rotation about this bond (*ca.* 40 kJmol^{-1}) in radicals of this type.

The relatively large activation energy for reaction (2.9), despite its exothermicity, can be understood in terms of polar

effects, because it involves abstraction of electron deficient hydrogen by an electrophilic radical. Reaction (2.9) should therefore be an ideal candidate for catalysis by an amine-alkylborane complex and we set out to confirm this proposal.

When a solution of acetone (1.2 M) and DTBP (36% v/v)* in cyclopropane was photolysed in the microwave cavity of the ESR spectrometer at 201 K, only a very weak spectrum of the radical **11** was observed and other radicals were also present. Spectra of secondary product radicals could be formed by photo reactions of the ketone, for example photoreduction which would produce $CH_3\dot{C}(OH)CH_3$.[11]

In marked contrast, when the experiment was repeated in the presence of $Me_3N\text{-}BH_2Thx$ **1** (0.2 M), a very strong, clean spectrum of the radical **11** [$a(1H_\alpha)$ 20.04, $a(1H'_\alpha)$ 19.50, $a(3H_\gamma)$ ca. 0.1 G, and g 2.0045 at 201 K] alone was observed. A similar result was obtained with $Me_3N\text{-}BH_2Bu^n$ **2** as catalyst. In the absence of DTBP and UV irradiation, acetone (1.0 M) showed no sign of reacting with **2** (1.0 M) in C_6D_6 during 1 hour at room temperature or, subsequently after 1 hour at 50 °C, as judged by ^1H NMR spectroscopy.

The trimethylamine-alkylboranes thus act as efficient polarity reversal catalysts for the abstraction of hydrogen from acetone by t-butoxyl radicals, via the cycle of reactions (2.10) and (2.11).

Despite being less exothermic than reaction (2.9), reaction (2.11) proceeds much more rapidly. This is reasonable, since the transition state for abstraction of hydrogen from acetone by the

*In order to minimise the effects of light absorption by the carbonyl chromophore, the DTBP : ketone concentration ratio was kept large.

$$\left\{\begin{array}{l} Bu^tO^{\cdot} \ + \ Me_3N{\rightarrow}BH_2R \xrightarrow{\text{fast}} Bu^tOH \ + \ Me_3N{\rightarrow}\overset{\cdot}{B}HR \qquad (2.10) \\[2ex] Me_3N{\rightarrow}\overset{\cdot}{B}HR \ + \ Me_2CO \xrightarrow{\text{fast}} Me_3N{\rightarrow}BH_2R \ + \ MeC(O)\overset{\cdot}{C}H_2 \qquad (2.11) \end{array}\right.$$

$$\underline{\text{OVERALL}} \quad Bu^tO^{\cdot} \ + \ Me_2CO \xrightarrow{\text{fast}} Bu^tOH \ + \ MeC(O)\overset{\cdot}{C}H_2$$
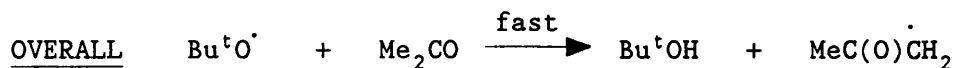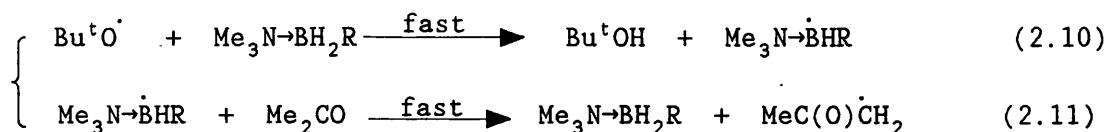
highly nucleophilic amine-alkylboryl radical will be strongly favoured by polar effects. The transition state for reaction (2.11) can be represented as a resonance hybrid of structures 13a-13c and the ionic structure 13c would be expected to make a major contribution. The ionisation potential of $Me_3N{\rightarrow}\overset{\cdot}{B}HR$ is low* and the electron affinity of an α-carbonylalkyl radical will be relatively large because of the high stability of the enolate ion produced by electron addition.

$$Me_3N{\rightarrow}\overset{\cdot}{B}HR \qquad H\text{-}CH_2COMe \quad \longleftrightarrow \quad Me_3N{\rightarrow}BHR\text{-}H \qquad {}^{\cdot}CH_2C(O)Me$$

$$\qquad\qquad 13a \qquad\qquad\qquad\qquad\qquad\qquad\qquad\qquad\qquad 13b$$

$$\overset{+}{Me_3N{\rightarrow}BHR} \qquad H^{\cdot} \qquad {}^{-}{:}CH_2C(O)Me$$

$$13c$$
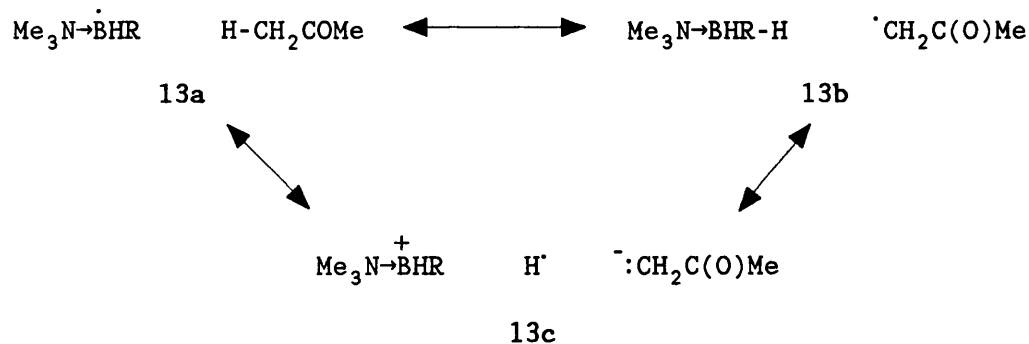
A competition experiment was carried out to determine the relative reactivities of acetone and t-butyl methyl ether towards hydrogen-atom abstraction by $Bu^tO^{\cdot}$. When a cyclopropane solution containing DTBP (35% v/v) and a 3:1 molar mixture of acetone (0.78 M)

*The calculated ionisation potential of $Me_3N{\rightarrow}\overset{\cdot}{B}HMe$ is 6.39 eV.[12]

and t-butyl methyl ether (0.26 M) was UV irradiated at 190 K in the presence of 1 (0.20 M), only the radical 11 was detected. When the experiment was repeated in the absence of the catalyst spectra of the radicals 11 and 14 were observed, together with secondary product radicals [equations (2.12) and (2.13)].

$$Bu^tO^\cdot \ + \ Me_2CO \ \xrightarrow{\ k_{2.12}\ } \ {}^\cdot CH_2C(O)Me \ + \ Bu^tOH \qquad (2.12)$$

11

$$Bu^tO^\cdot \ + \ Bu^tOMe \ \xrightarrow{\ k_{2.13}\ } \ Bu^tO\dot{C}H_2 \ + \ Bu^tOH \qquad (2.13)$$

14
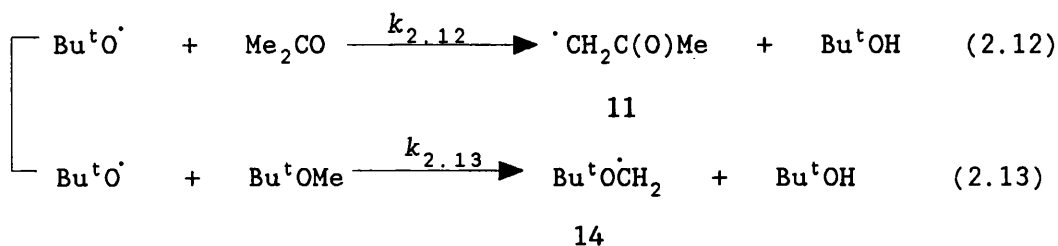
The radicals 11 and 14 are removed by reactions (2.14-2.16).

$$11 \ + \ 11 \ \xrightarrow{\ 2k_t^A\ } \Big]$$ (2.14)

$$11 \ + \ 14 \ \xrightarrow{\ k_x\ } \Big] \quad \begin{array}{l}\text{molecular}\\ \text{products}\end{array}$$ (2.15)

$$14 \ + \ 14 \ \xrightarrow{\ 2k_t^B\ } \Big]$$ (2.16)
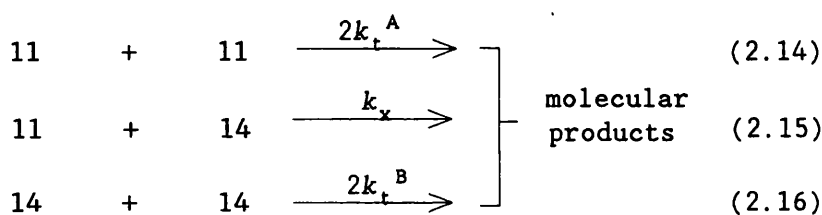
During continuous UV photolysis, a steady state will be established such that the rate of radical production is equal to the rate of their removal [equations (2.17) and (2.18)].

$$0 = d[11]/dt = k_{2.12}[Bu^tO^\cdot][Me_2CO] - 2k_t^A[11]^2 - k_x[11][14] \qquad (2.17)$$

$$0 = d[14]/dt = k_{2.13}[Bu^tO^\cdot][Bu^tOMe] - 2k_t^B[14]^2 - k_x[11][14] \qquad (2.18)$$

Assuming that the self- and cross-reactions of 11 and 14 are all diffusion-controlled and therefore effectively equal,[13] from equations (2.17) and (2.18) we obtain equation (2.19).

By computer simulation of the ESR spectra, it was found that [14]/[11] = 10.1 at 190 K and hence ($k_{2.13}/k_{2.12}$) is 30, $i.e.$ t-butyl methyl ether is 30 times more reactive than acetone towards

$$\frac{k_{2.12}[\text{Bu}^t\text{O}^\cdot][\text{Me}_2\text{CO}]}{k_{2.13}[\text{Bu}^t\text{O}^\cdot][\text{Bu}^t\text{OMe}]} = \frac{[11]}{[14]}\left(\frac{[11] + [14]}{[11] + [14]}\right)$$

$$i.e.\left(\frac{k_{2.12}}{k_{2.13}}\right) = \frac{[\text{Bu}^t\text{OMe}]}{[\text{Me}_2\text{CO}]} \times \frac{[\dot{C}H_2C(O)Me]}{[\text{Bu}^t\text{O}\dot{C}H_2]} \qquad (2.19)$$

hydrogen-atom abstraction by Bu^{t}O$^\cdot$ at 190 K. The value of [14]/[11] was unchanged when the [DTBP]:[acetone] ratio was doubled, keeping the [Me$_2$CO]:[Bu^{t}OMe] ratio constant, showing that reactions of photoexcited ketone are unimportant under these conditions.

The relatively high reactivity of Bu^{t}OMe compared to acetone can be understood by considering the transition states for the two reactions (2.12) and (2.13). Charge transfer to the t-butoxy moiety can be represented by inclusion of the two canonical structures **15** and **16**. Of the two cationic species, $^+$CH$_2$OBu^t is much more stable

[Bu^{t}O$^-$ H$^\cdot$ $^+$CH$_2$OBu^t]   [Bu^{t}O$^-$ H$^\cdot$ $^+$CH$_2$C(O)Me]

       15   **16**
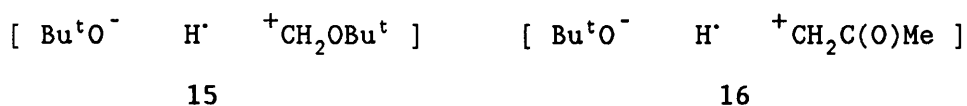
than $^+$CH$_2$C(O)Me, because in the former the positive charge is effectively delocalised onto oxygen (resonance structures **17a** and **17b**). In contrast, conjugative delocalisation of the positive charge

[$^+$CH$_2$-O-Bu^t] ⬌ [CH$_2$=$\overset{+}{O}$-Bu^t]

     17a   **17b**
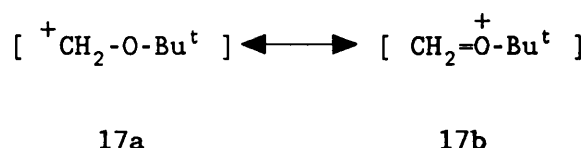
in $^+$CH$_2$-C(O)Me will be negligible and inductive <u>destabilisation</u> of the cation will dominate.

A similar experiment was carried out with a 1:4 molar mixture of t-butyl methyl ether and cyclopropyl methyl ketone. The radicals **14** and **18** were detected, but even with such a high concentration of

the ketone, hydrogen was abstracted mainly from the ether [equations (2.13) and (2.20)].

$$Bu^tO\cdot \quad + \quad Bu^tOMe \quad \xrightarrow{\;k_{2.13}\;} \quad Bu^tOH \quad + \quad Bu^tO\dot{C}H_2 \qquad (2.13)$$

14

$$Bu^tO\cdot \quad + \quad \underset{O}{\underset{\|}{C}}(C_3H_5)Me \quad \xrightarrow{\;k_{2.20}\;} \quad Bu^tOH \quad + \quad \underset{O}{\underset{\|}{C}}(C_3H_5)\dot{C}H_2 \qquad (2.20)$$

18
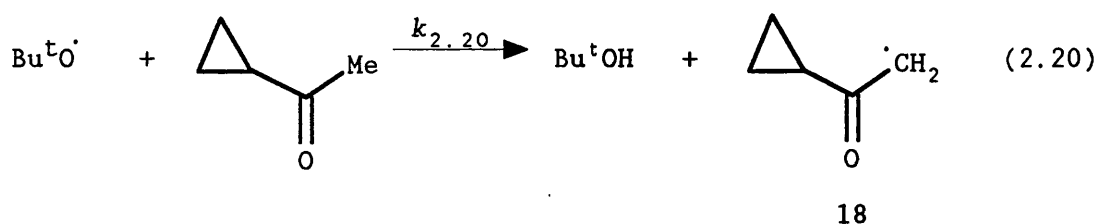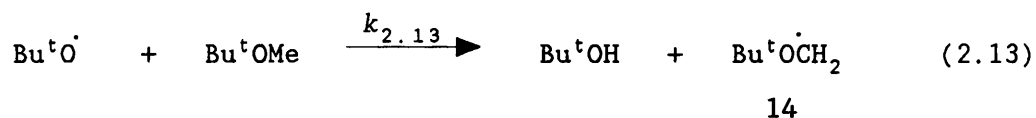
$$\left(\frac{k_{2.13}}{k_{2.20}}\right) = \frac{[Bu^tO\dot{C}H_2]}{[(C_3H_5)\text{-}C(O)\text{-}\dot{C}H_2]} \; X \; \frac{[(C_3H_5)\text{-}C(O)Me]}{[Bu^tOMe]} \qquad (2.21)$$

By computer simulation, $[Bu^tO\dot{C}H_2]/[(C_3H_5)\text{-}C(O)\text{-}\dot{C}H_2]$ was found to be 11.5 and therefore, from equation (2.21), $(k_{2.13}/k_{2.20})$ is $ca.$ 46. Combining this result with that obtained for acetone and Bu^tOMe, $(k_{2.12}/k_{2.20})$ is therefore 1.8, $i.e.$ acetone is nearly twice as reactive as cyclopropyl methyl ketone towards hydrogen-atom abstraction by $Bu^tO\cdot$. This is reasonable, because acetone has two methyl groups per molecule whereas cyclopropyl methyl ketone only has one, and so on a statistical basis, acetone should be twice as reactive.

2.2.2 From Methyl Isopropyl Ketone

Photolysis of a solution containing methyl isopropyl ketone (**19**, 0.85 M) and DTBP (36% v/v) in cyclopropane at 190 K afforded the spectrum of **20** shown in Figure **2.1** [$a(3H_\beta)$ 20.35, $a(3H'_\beta)$ 19.06, $a(3H_\gamma)$ 0.69 G, and g 2.0042 at 190 K]. However, in the presence of $Me_3N{\rightarrow}BH_2Thx$ **1** (0.20 M), the spectrum of the radical **21** [$a(H_\alpha)$ 19.94, $a(H'_\alpha)$ 19.60, $a(H_\gamma)$ 0.65, $a(6H_\delta)$ 0.28 G; g 2.0045, $g(21)$-$g(20)$ = 0.00027 at 190 K] along with a very low concentration of **20** was observed [equations (2.22) and (2.23)].

$$k_{2.22} \qquad (2.22)$$

$$k_{2.23} \qquad (2.23)$$
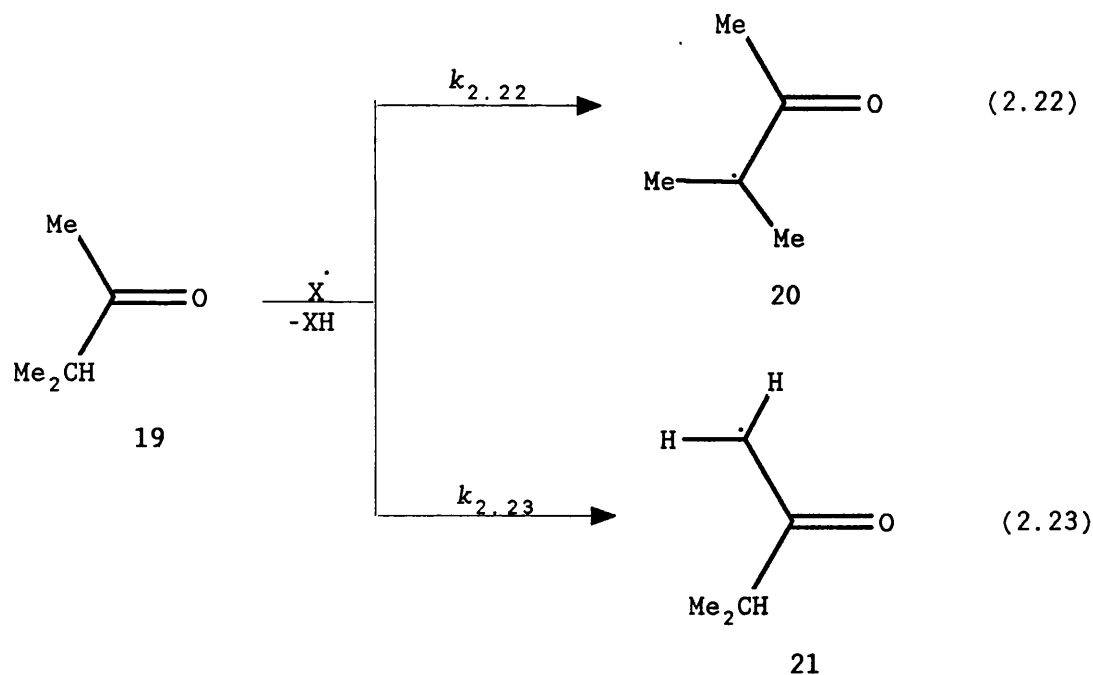
The spectrum of the radical **20** appears at first glance to consist of a septet (with further fine structure), but it is actually a quartet of quartets with second-order effects, because the two methyl groups attached to the radical centre are non-equivalent. Delocalisation of the unpaired electron from $C\alpha$ onto the carbonyl group induces partial double bond character between the carbon atoms

a)

b)

c)

10 G

Figure 2.1

39
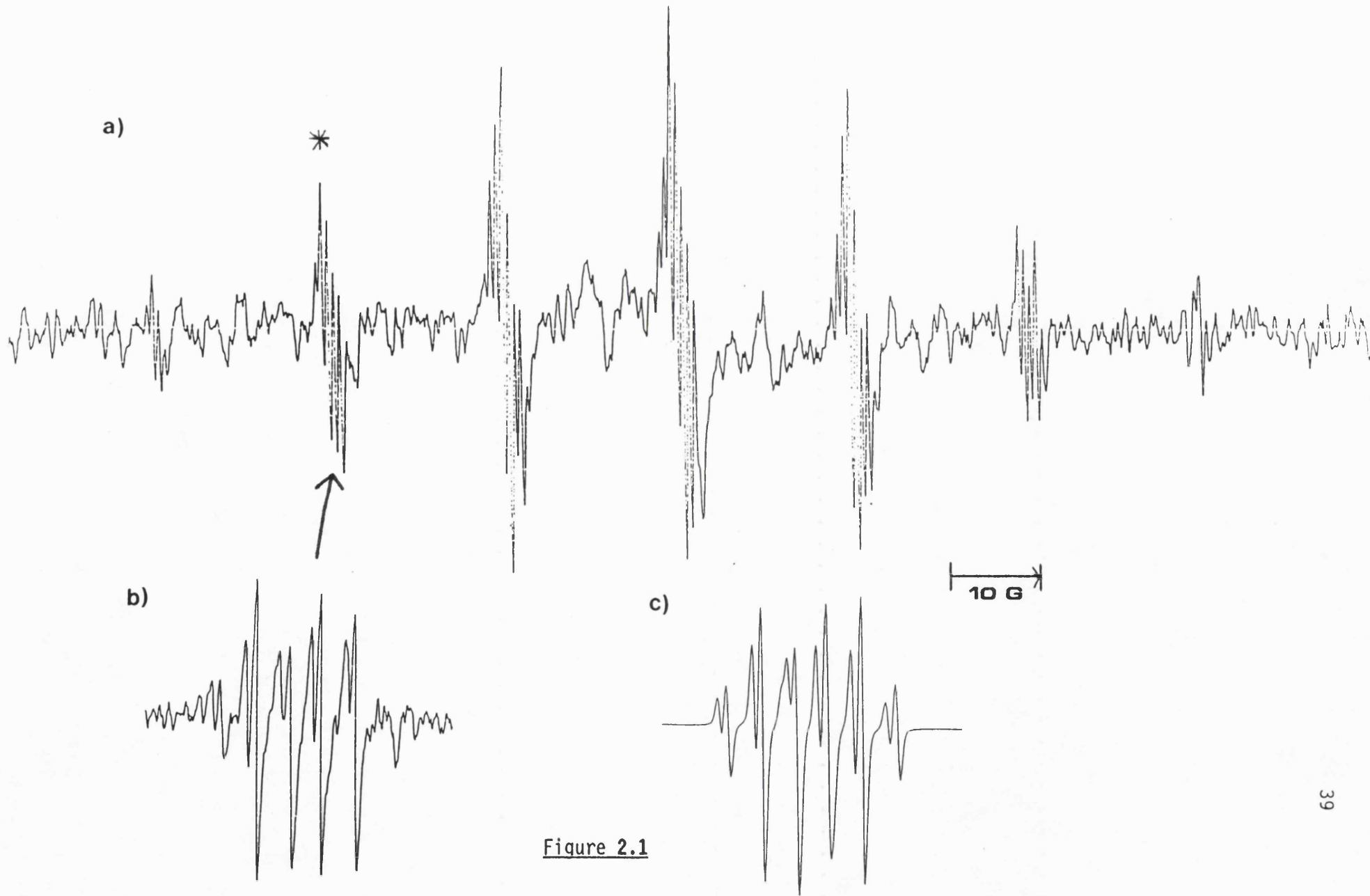
Figure Captions

Figure **2.1** (a) ESR spectrum of $CH_3C(O)\dot{C}Me_2$ **20** generated in the presence of methyl isopropyl ketone and DTBP in cyclopropane at 190 K. (b) Expansion of lines marked with _an asterisk_ (c) Computer simulation of (b) using the parameters given in the text.

[structures **22a** and **22b**] and gives rise to an appreciable barrier to

22a   22b
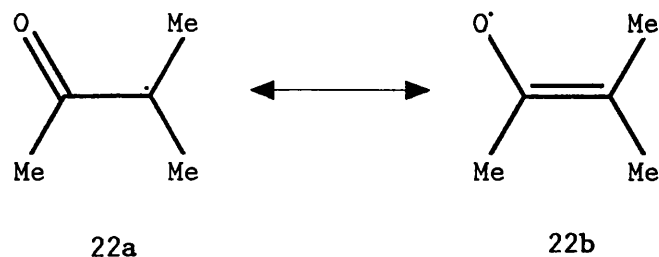
rotation about the Ċ-C(O) bond, as described previously. Rotation about C_α-C_β is slow on the ESR timescale for such radicals below room temperature and different splittings are observed for groups attached to C_α which are *cis-* or *trans-* to the carbonyl group.

While Bu^{t}O· preferentially abstracts the more weakly bound and less electron deficient α-hydrogen, the amine-alkylboryl radical Me$_3$N→ḂHThx **23** abstracts more rapidly a more strongly bound, but more electron-deficient, hydrogen from the MeC(O) group. Although polar effects are clearly important in determining the regioselectivities of Bu^{t}O· and **23**, the bulky amine-alkylboryl radical would also prefer to abstract from the MeC(O) group for steric reasons. In fact, steric factors appear to be predominant, since when the experiment was repeated with **24** as the catalyst, which yields the less bulky amine-alkylboryl radical **25**, hydrogen was abstracted mainly from the isopropyl group.

24   25

Quantitative selectivities for hydrogen-atom abstraction from the ketone **19** by various amine-alkylboryl radicals were determined

using ESR spectroscopy. Relative concentrations of the radicals **20** and **21** were determined by computer simulation of spectra obtained at 190 K during UV irradiation of cyclopropane or oxirane* solutions containing DTBP (35% v/v), **19** (0.85 M), and the amine-alkylborane (0.23 M). The value of [21]/[20] is taken[13] to be equal to ($k_{2.23}/k_{2.22}$) and was unchanged when the amine-alkylborane concentration was increased to 0.44 M, showing that all the t-butoxyl radicals are being trapped and converted to amine-alkylboryl radicals, which are responsible for hydrogen abstraction. The selectivity of $Bu^tO\cdot$ was determined from experiments in the absence of amine-alkylborane; the results are given in Table **2.1**. Figure **2.2a** shows the second [$M_I(6H_\beta)$ = +1] and third [$M_I(6H_\beta)$ = +2] groups of lines in the spectrum of the radical **20**, which is the only radical detected when $Bu^tO\cdot$ reacts with the ketone **19**, and Figures **2.2c** and **2.2d** show the same regions of the spectra obtained when abstraction is brought about by $Me_3N\text{-}\dot{B}HThx$ and by $Me_3N\text{-}\dot{B}HBu^n$, respectively.

As congestion at the boron-radical centre decreases, so the tendency to abstract the more weakly bound of the two types of α-hydrogens in **19** becomes more pronounced. The ratios of ([21]/[20]) increase with the increasing steric demands of R in $Me_3N\text{-}\dot{B}HR$ along the series R = $Bu^n<Bu^i<Bu^s<Thx$. Although the B-alkyl groups in $Me_3N\text{-}\dot{B}HBu^s$ and **26** are both secondary, the isopinocampheyl group is appreciably the more sterically demanding. The amine-boryl radical

---

*In oxirane at 190 K, **20** shows splittings of 20.44 ($3H_\beta$), 19.02 ($3H'_\beta$), and 0.83 G ($3H_\gamma$). The radical **21** shows 19.94 (H_α), 19.60 (H'_α), 0.72 (H_γ), and 0.34 G ($6H_\delta$).
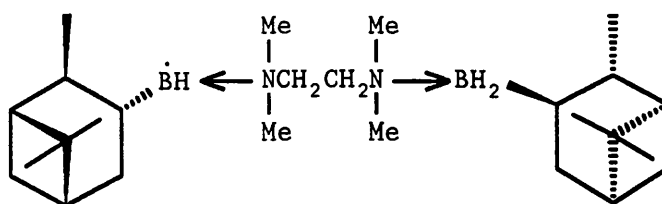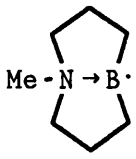
26

26 therefore shows a greater preference than $Me_3N{\rightarrow}\dot{B}HBu^s$ for abstraction from the less hindered α-C-H group.

Table **2.1**

Relative rates of α-hydrogen-atom abstraction $(k_{2.23}/k_{2.22})$ from methyl isopropyl ketone at 189 K.

Abstracting Radical	Solvent[a]	$(k_{2.23}/k_{2.22})$[b]
$Bu^{t}\overset{\cdot}{O}$ [c]	A	≤ 0.1
$Me_3N{\rightarrow}\overset{\cdot}{B}HBu^{n}$	A	0.60
	B	0.56
$Me_3N{\rightarrow}\overset{\cdot}{B}HBu^{i}$	A	0.75
$Me_3N{\rightarrow}\overset{\cdot}{B}HBu^{s}$	A	0.92
$Me_3N{\rightarrow}\overset{\cdot}{B}HThx$	A	7.6
25	A	0.7^{d}
Me–N→B[•] (ring)	A	0.45
26	B	4.0

a A = cyclopropane, B = oxirane. *b* Independent of the amine-borane concentration in the range 0.23-0.44 *M*; the ketone concentration was generally 0.85 *M*. *c* No amine-borane present. *d* Weak spectra.

a)

b)

c)

d)

e)

10 G
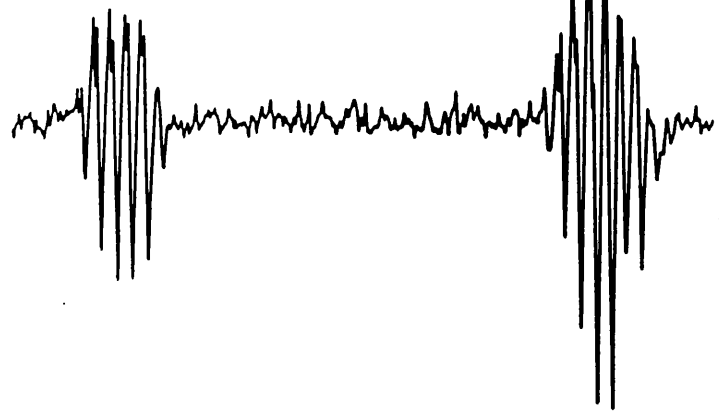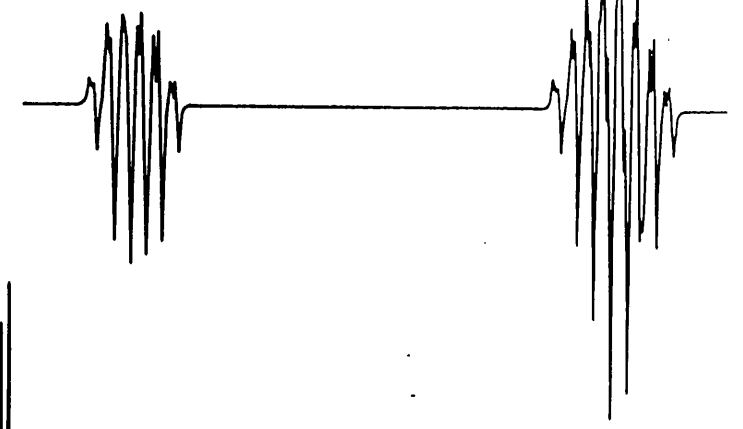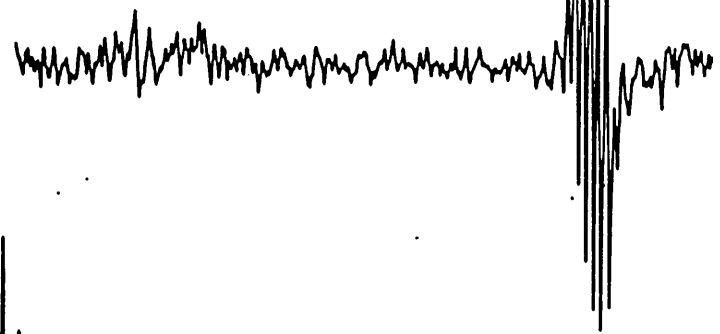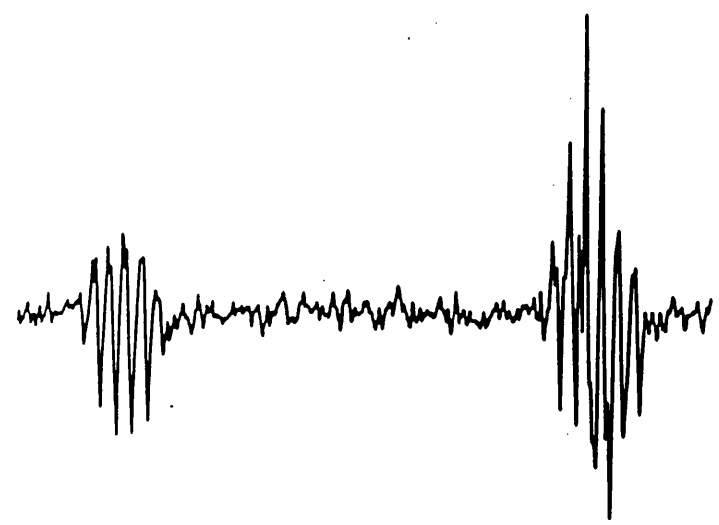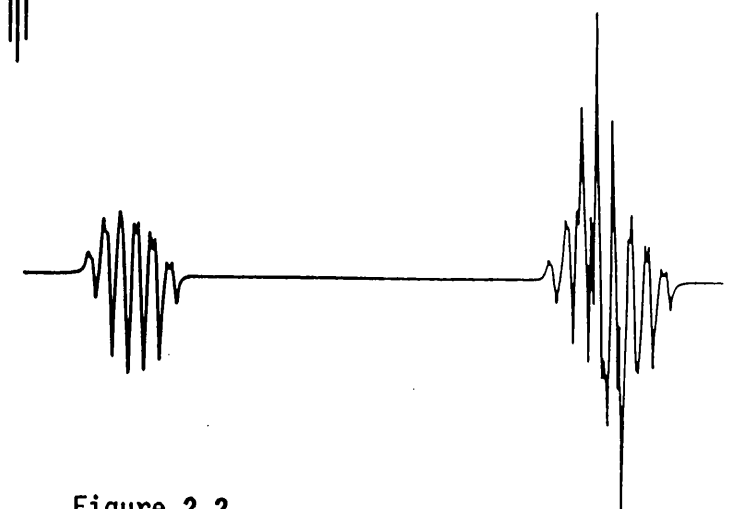
Figure 2.2

Figure Captions

Figure 2.2 Low field regions from the ESR spectra of **20** and **21** in cyclopropane at 190 K. The $M_I(2H_\alpha)$ = -1 lines for **21** and the $M_I(6H_\beta)$ = +1 and +2 lines for **20** are shown; computer simulations (including second-order effects) were obtained using the parameters given in the text. (a) Hydrogen abstraction by $Bu^tO\cdot$, only **20** is detected. (b) Simulation of (a). (c) Hydrogen abstraction by $Me_3N{\to}\overset{\bullet}{B}HThx$; [21]/[20] = 7.8. (d) Hydrogen abstraction by $Me_3N{\to}\overset{\bullet}{B}HBu^n$. (e) Simulation of (d), [21]/[20] = 0.56.

2.2.3 From Cyclobutanone

Photolysis of a mixture of cyclobutanone (1.2 M) and DTBP (36% v/v) in cyclopropane at 199 K gave mainly the 2-oxocyclobutyl radical **27** with a trace of **28** . When the experiment was repeated in the presence of **1** (0.19 M), only the radical **27** [$a(H_\alpha)$ 18.73, $a(2H_\beta)$ 35.32, $a(2H_\gamma)$ 0.63 G, and g 2.0044 at 199 K] was observed.
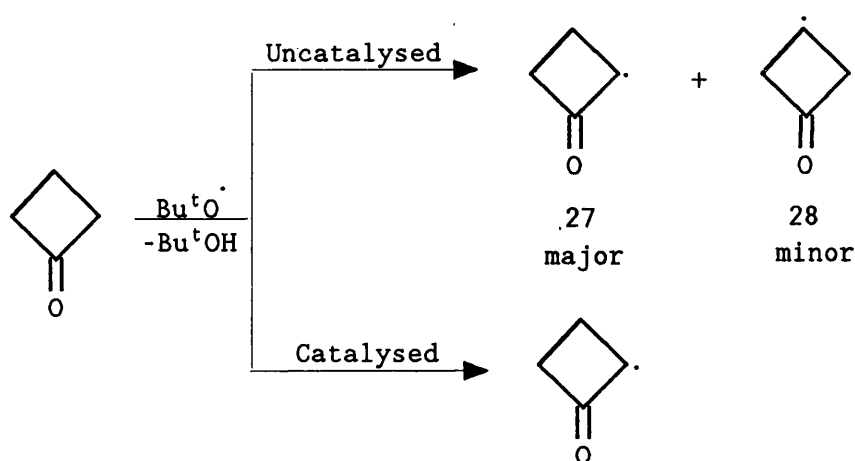
Figure **2.3** shows the ESR spectrum of **27**. It consists of a triplet of doublets due to coupling to two β-hydrogens and to one α-hydrogen, respectively. The fine structure on the wing line shows a further triplet due to coupling with two γ-hydrogens. However, the fine structure on the line corresponding to $M_I(2H_\beta)$ = 0 shows a 1:3:3:1 quartet. This results from overlapping of two triplets due to second-order effects.[14] The second-order splitting $[a(2H_\beta)]^2/B_0$ (= 0.39 G) is quite close in magnitude to $a(2H_\gamma)$.
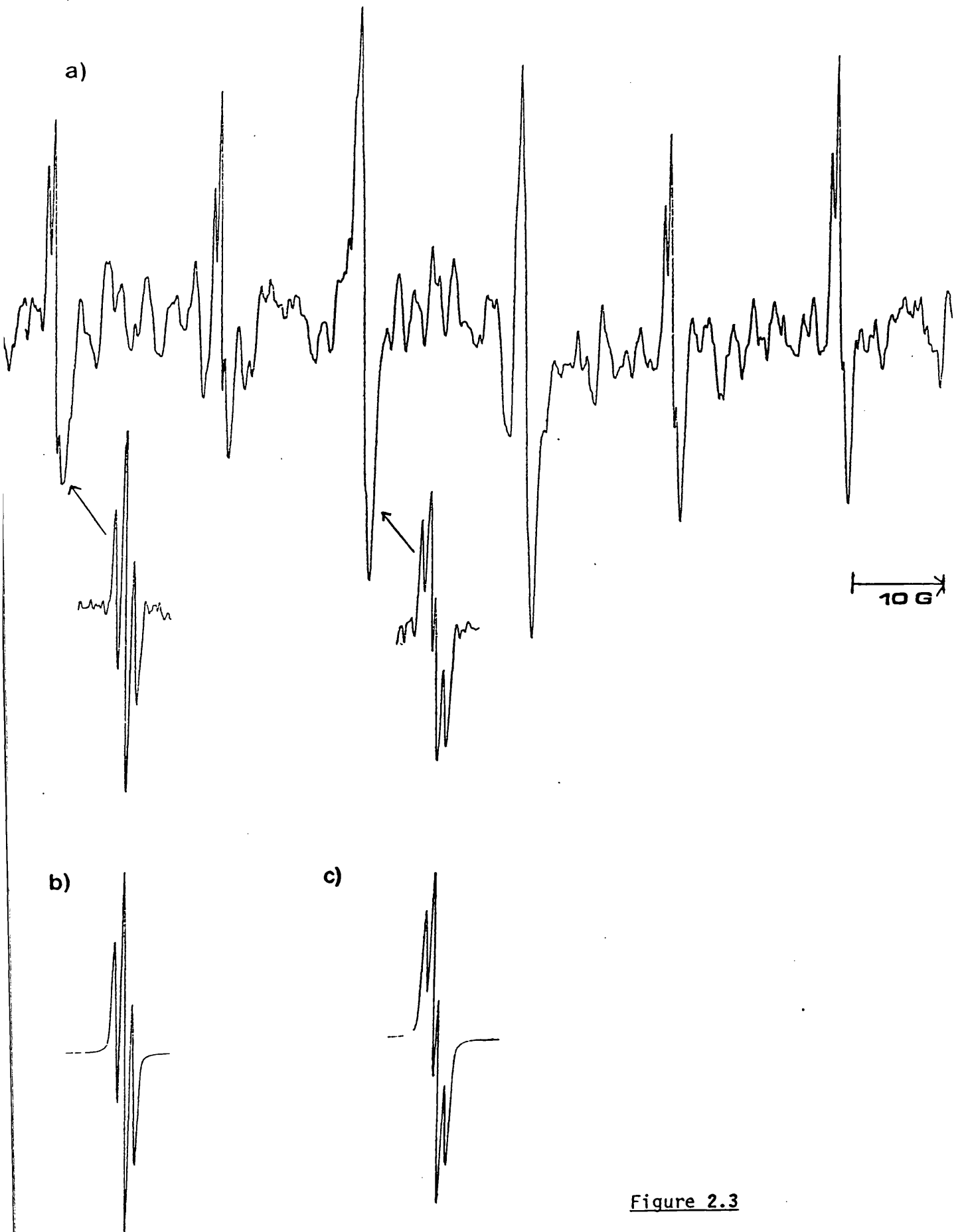
Figure 2.3

Figure Captions

Figure 2.3 (a) ESR spectrum of 2-oxocyclobutyl radical **27** generated by photolysis of DTBP in the presence of cyclobutanone (1.2 M) and $Me_3N{\rightarrow}BH_2Thx$ (0.19 M) in cyclopropane at 199 K. (b) Computer simulation of the fine structure on the lines corresponding to $M_I(2H_\beta)$ = +1. (c) Computer simulation of fine structures on the lines corresponding to $M_I(2H_\beta)$ = 0.

2.2.4 From Cyclopentanone

When DTBP (36% v/v) was photolysed in the presence of cyclopentanone (1.0 M) in cyclopropane, the planar 2-oxocyclopentyl radical **29** is the major product, because of the resonance effect which causes **29** to be stabilized by delocalisation of the unpaired electron onto the oxygen atom [structures **30a** and **30b**]. However, the

30a   30b
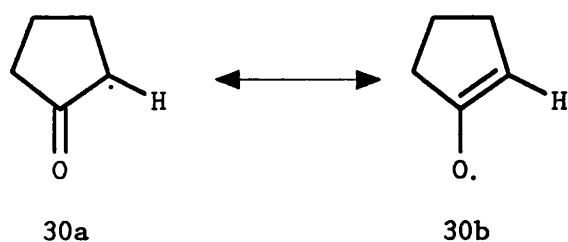
reaction must be quite slow as evidenced by the weak spectra obtained. In contrast, when **1** (0.19 M) is present, only **29** [$a(H_\alpha)$ 18.33, $a(2H_\beta)$ 36.45, $a(2H_\gamma)$ 2.78, $a(2H_\delta)$ 0.37 G, and g 2.0045 at 154 K] was detected and a strong ESR spectrum was observed (Figure **2.4**).
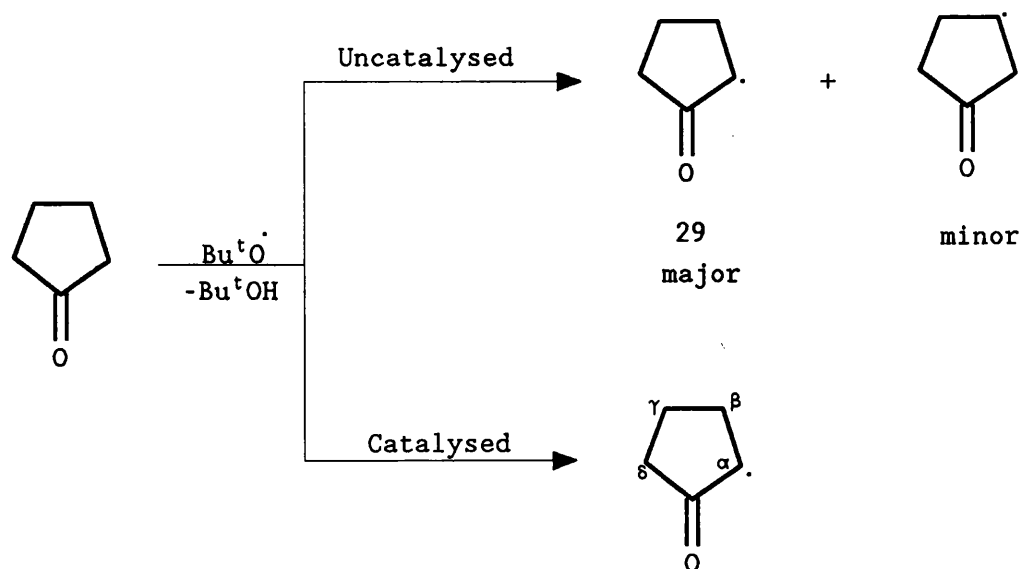
The spectrum of **29** shows a triplet of doublets which results from coupling of the unpaired electron with two β-protons and one

10 G
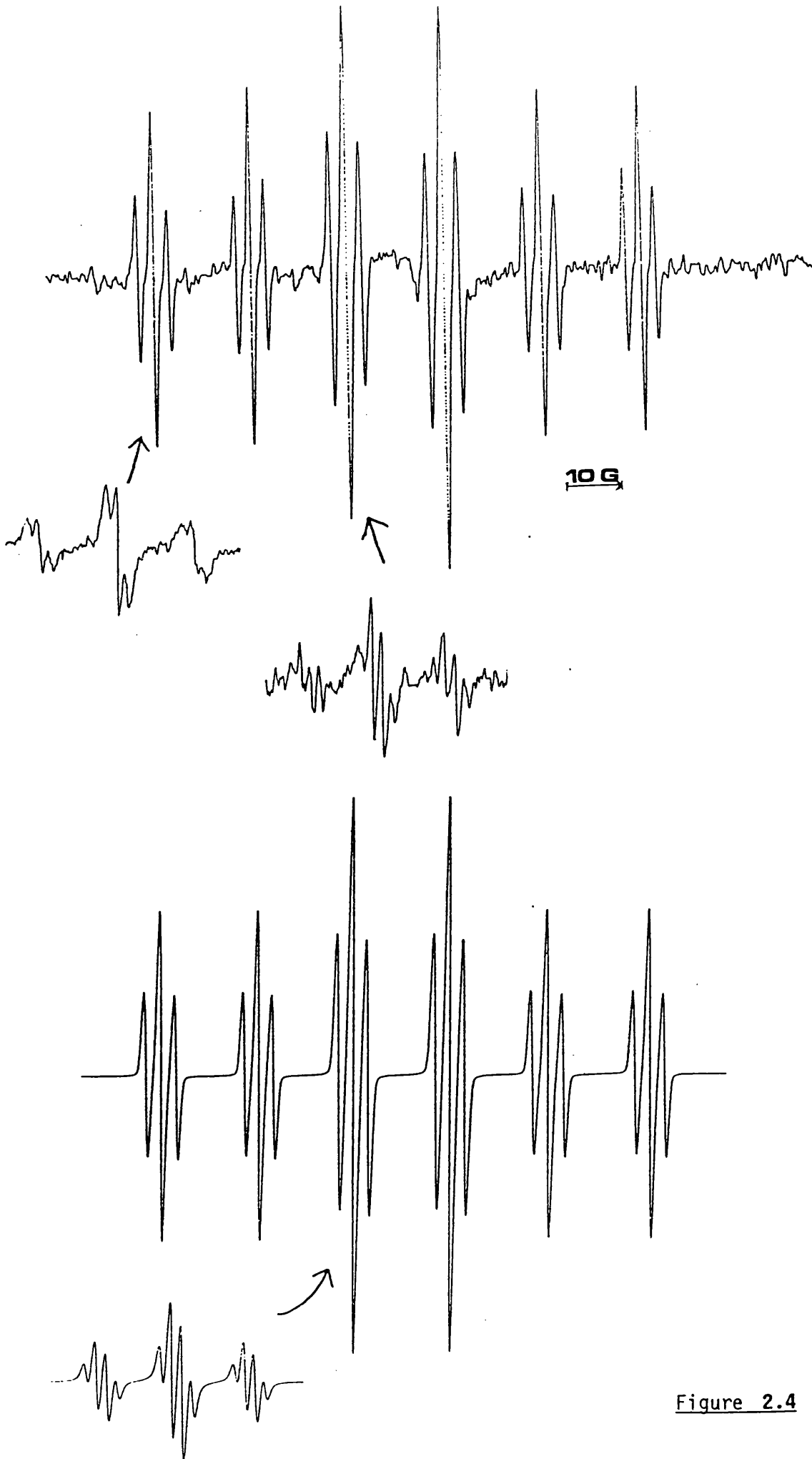
Figure 2.4

Figure Captions

Figure 2.4 (a) ESR spectrum of the 2-oxocyclopentyl radical **29** generated by photolysis of cyclopentanone (1.0 *M*), DTBP, and **1** (0.19 *M*) in cyclopropane at 154 K. (b) Computer simulation of (a), using the parameters given in the text.

α-proton. Each of these lines is then further split into a triplet by coupling with two γ-protons. Under still higher resolution, each line of the first triplet $[M_I(2H_\beta) = +1]$ of the spectrum of **29** shows a further triplet splitting due to coupling with two δ-protons. However, resolving the third triplet $[M_I(2H_\beta) = 0]$ did not give triplets but approximate 1:3:3:1 quartets. Again, this is due to a second-order effect as in the case of the radical from cyclobutanone. To first-order, we have a 1:2:1 triplet due to coupling with two equivalent β-hydrogens, but the intensity two component splits into a 1:1 doublet spaced by $[a(2H_\beta)]^2/B_0$ at second order. The 1:3:3:1 quartets resolvable on the lines corresponding to $[M_I(2H_\beta) = 0]$ result from overlapping of two triplets because of the near equality of $a(2H_\delta)$ and $[a(2H_\beta)]^2/B_0$ (=0.41 G) (Figure **2.5**).

A competition experiment was carried out to determine the relative reactivities of cyclopentanone and t-butyl methyl ether towards hydrogen atom abstraction by Bu^{t}O· and by Me$_3$N–$\overset{\bullet}{B}$HThx. When a 1:2 molar mixture of cyclopentanone and t-butyl methyl ether was photolysed with DTBP (32% v/v) in cyclopropane in the presence of **1** (0.18 *M*) at 154 K, a spectrum attributed to **29** <u>alone</u> was observed, and there was no sign of abstraction from the ether. Cyclopentanone must thus be at least 20 times as reactive as Bu^{t}OMe towards Me$_3$N–$\overset{\bullet}{B}$HThx. When the experiment was repeated in the absence of the catalyst, a mixture of **29** and **31** were obtained [equations (2.24) and (2.25); Figure **2.6**].

By computer simulation, it was found that $(k_{2.24}/k_{2.25})$ is *ca.* 1.3, *i.e.* cyclopentanone is *ca.* 1.3 times more reactive than Bu^{t}OMe towards hydrogen-atom abstraction by Bu^{t}O·. Although polar effects favour hydrogen abstraction from Bu^{t}OMe, the α-C-H bond weakening

1st order

$\underline{a}(2H_\beta)$

$[a(2H_\beta)]^2/B_0 = 0.41$ G

2nd order

$\underline{a}(H_\alpha)$

$\underline{a}(2H_\gamma)$

← overlapping of two triplets

$\underline{a}(2H_\delta)$

← fine structure on line $M_I(2H_\beta) = 0$

Three 1:3:3:1 quartets
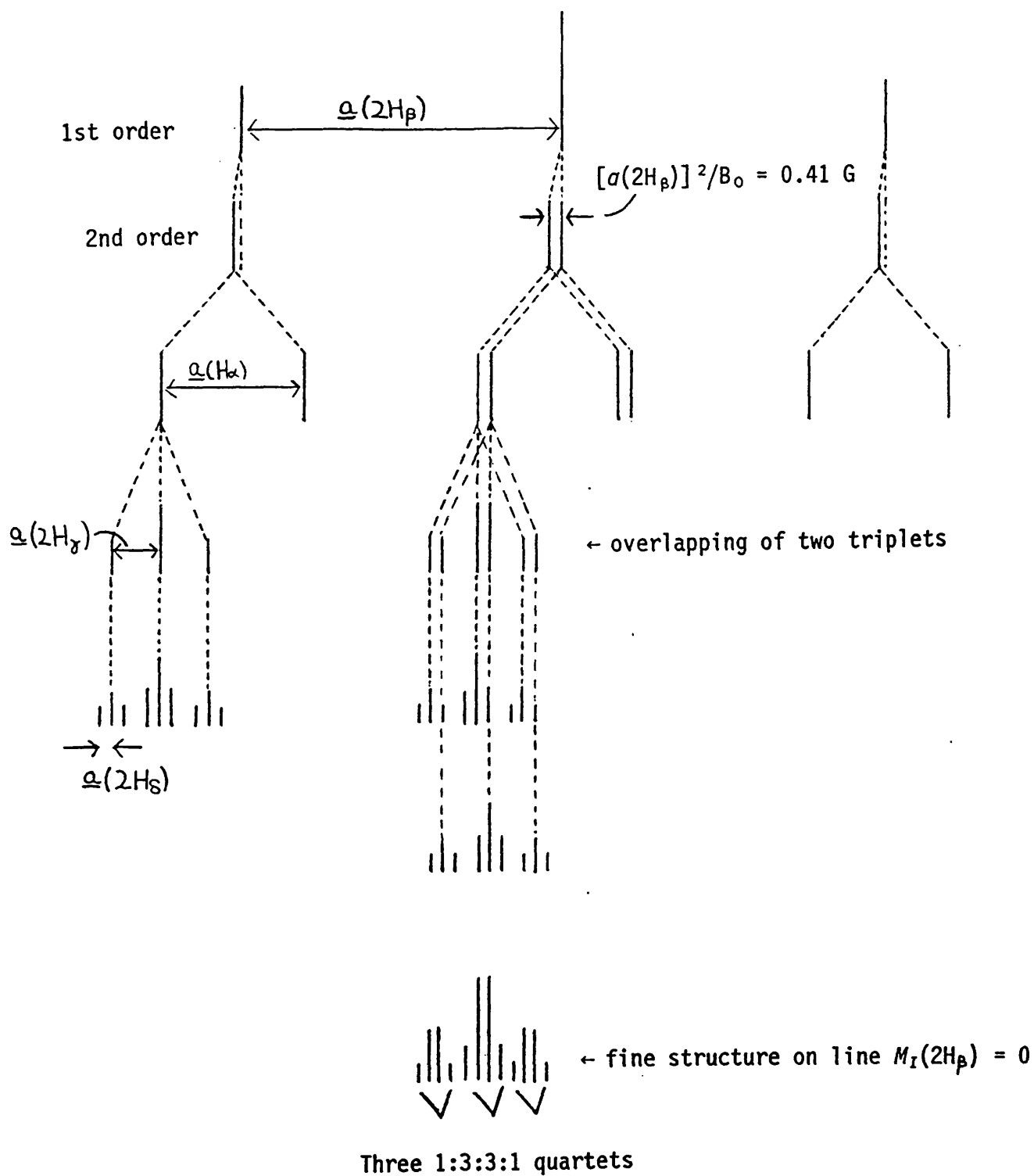
Figure 2.5 Stick diagram showing the analysis of the ESR spectrum of the radical **29**.

Figure 2.6 ESR spectrum of the mixture of radicals derived from a 1:2 molar mixture of cyclopentanone and t-butyl methyl ether in the absence of polarity reversal catalyst at 154 K. The lines marked with an asterisk arise from $Bu^tO\dot{C}H_2$.

$$\text{Bu}^t\text{O}^\bullet \quad + \quad \text{(cyclopentanone)} \quad \xrightarrow{k_{2.24}} \quad \text{(cyclopentanone radical)}^\bullet \quad + \quad \text{Bu}^t\text{OH} \qquad (2.24)$$

29

$$\text{Bu}^t\text{O}^\bullet \quad + \quad \text{Bu}^t\text{OCH}_3 \quad \xrightarrow{k_{2.25}} \quad \text{Bu}^t\text{O}\dot{\text{C}}\text{H}_2 \quad + \quad \text{Bu}^t\text{OH} \qquad (2.25)$$

31
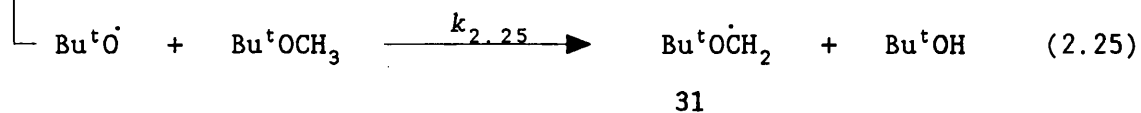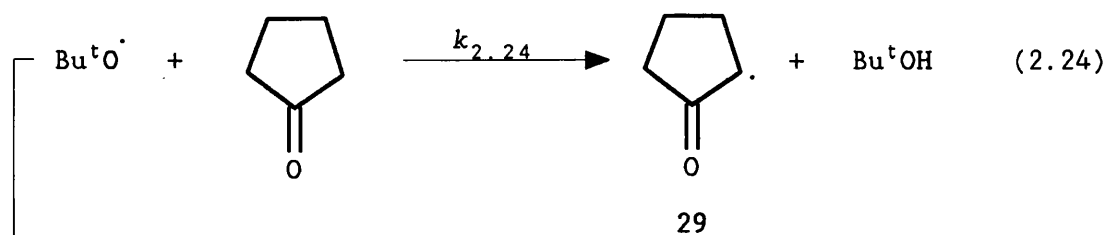
$$\frac{k_{2.24}}{k_{2.25}} = \frac{[29]}{[\text{Bu}^t\text{O}\dot{\text{C}}\text{H}_2]} \quad \text{X} \quad \frac{[\text{Bu}^t\text{OCH}_3]}{[\text{cyclopentanone}]}$$

effect of the adjacent carbonyl group is evidently considerable and outweighs the polar effects.

2.2.5 From Cyclohexanone

Photolysis of a solution containing cyclohexanone (0.88 M) and DTBP (36% v/v) in cyclopropane gives mainly the 2-oxocyclohexyl radical **32**. However, in the presence of **1** (0.19 M), all lines other than those attributed to the radical **32** were absent and the spectrum of **32** was very strong [$a(H_\alpha)$ 17.84, $a(H_\beta{}^{ax})$ 43.38, $a(H_\beta{}^{eq})$ 23.62, $a(H_\gamma)$ 1.31 G, and g 2.0046 at 147 K].
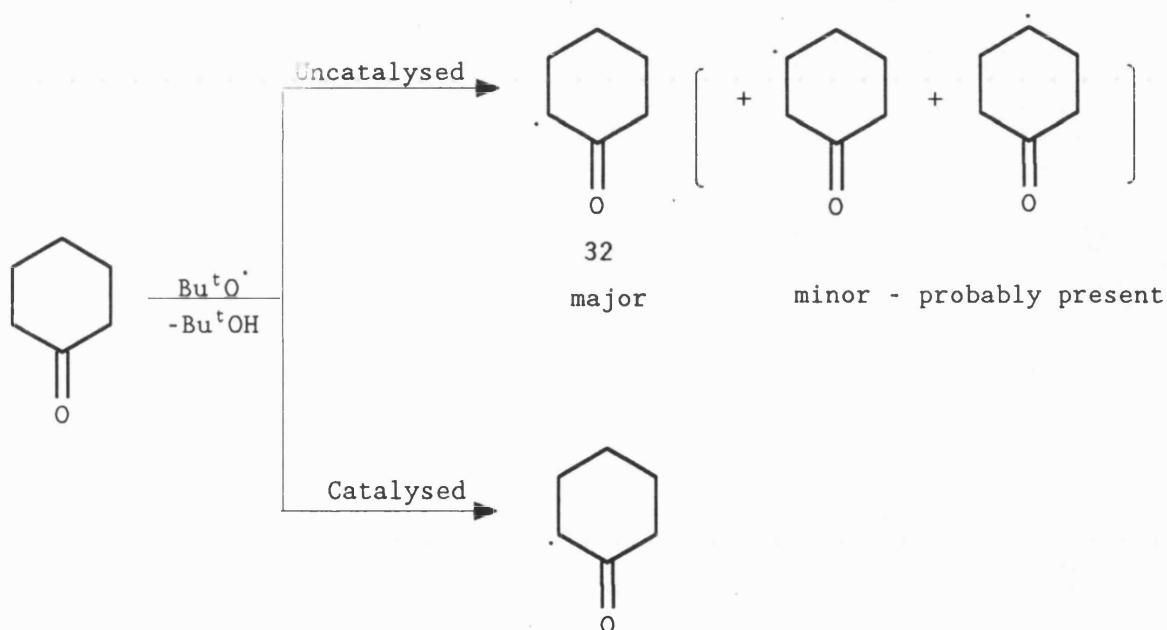
Figure **2.7** shows spectra of **32** obtained at different temperatures. The 2-oxocyclohexyl radical is thought to exist in the half-chair conformation shown in structures **33a** and **33b**.[15] At low temperatures such as 147 K, exchange between $H_\beta{}^{ax}$ and $H_\beta{}^{eq}$ (as a result of ring inversion) is slow on the ESR time scale, so the two are non-equivalent.

The mechanism of hyperfine coupling with a β-proton is hyperconjugation and the value of $a(H_\beta)$ depends on the dihedral angle (θ) between the semi-occupied orbital on C_α and the β-C-H bond [see

58

Temperature

147 K

10 G

168 K

184 K

210 K

259 K

284 K
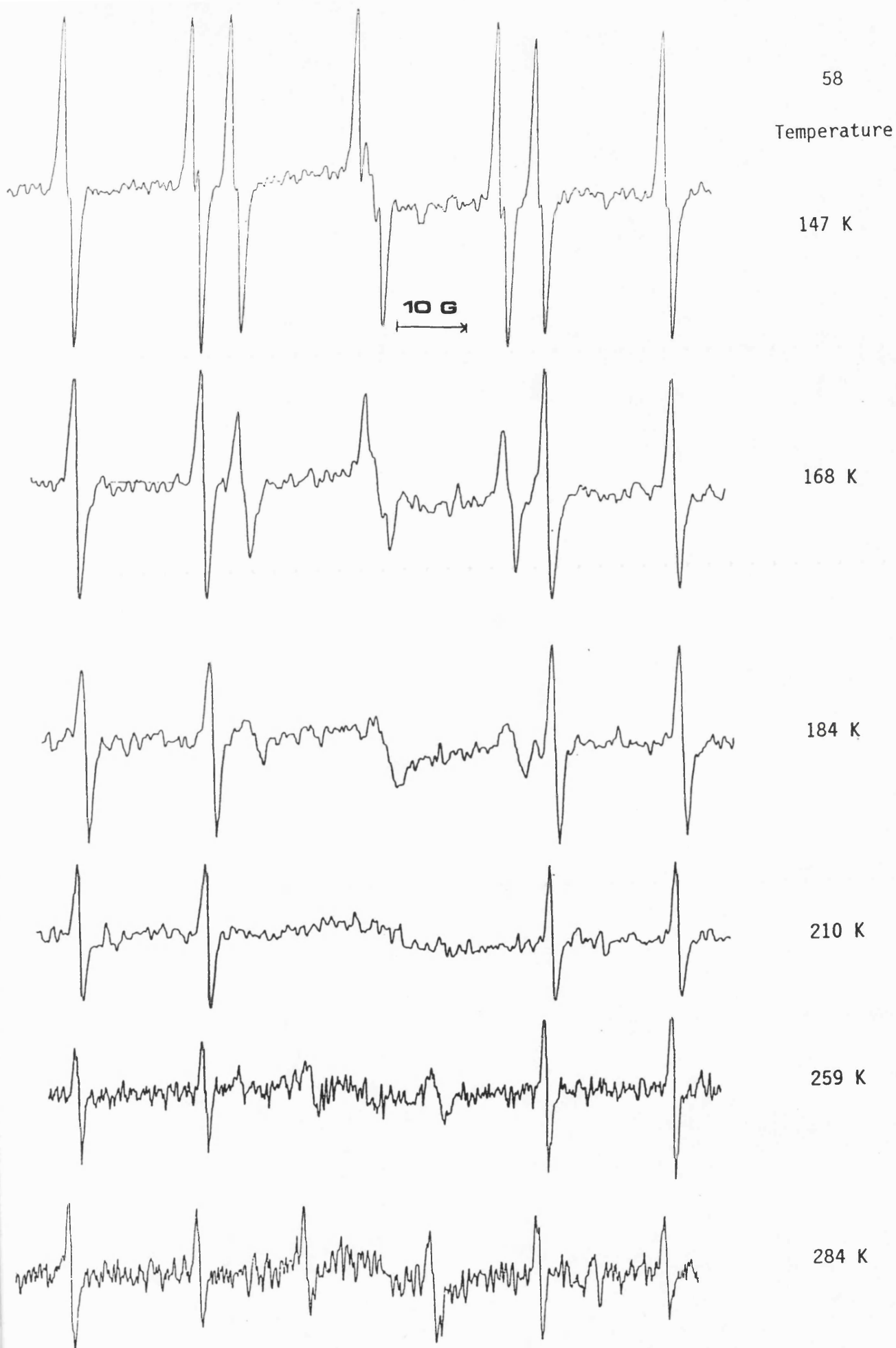
Figure 2.7   ESR spectrum of 32 obtained at different temperatures in cyclopropane solvent.

33a   33b
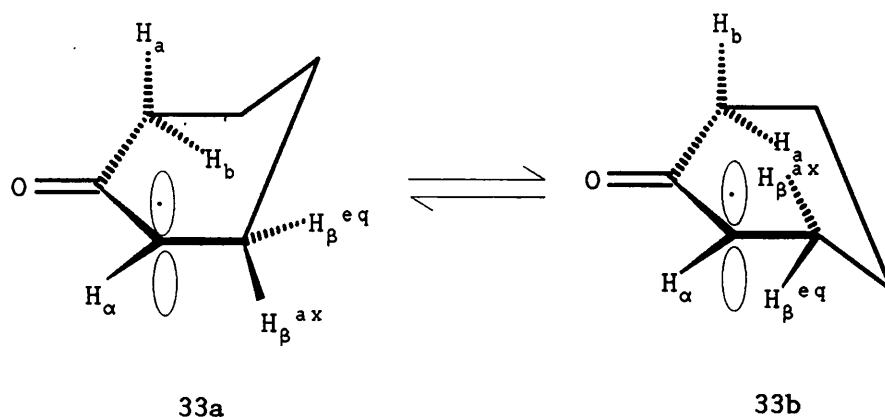
34] according to the Heller-McConnell equation (2.26),[16,17] in which
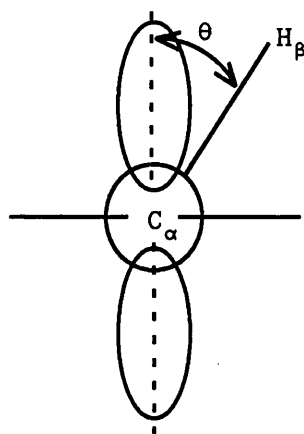
34

$$a(H_\beta) = (A + B\cos^2\theta)\rho^\pi_{C\alpha} \qquad (2.26)$$

A (*ca.* 1 G) and B (*ca.* 58.5 G) are constants and $\rho^\pi_{C\alpha}$ is the π spin population on C_α. Maximum hyperconjugation arises when the dihedral angle is equal to zero. Therefore, at low temperatures when the two β-hydrogens are non-equivalent, the value of $a(H_\beta^{ax})$ is much greater than $a(H_\beta^{eq})$ and the spectrum obtained at 147 K is interpreted as a doublet of doublets due to coupling to these two non-equivalent β-hydrogens. Each of the lines is then further split by coupling to the α-hydrogen into a doublet, and a long-range doublet splitting, probably H_a (as in **33a**), is also present.

As the temperature increases, interconversion between the two half-chair conformations and exchange of the β-hydrogens becomes

faster. When the inversion occurs at an "intermediate" rate, the central lines associated with $M_I(2H_\beta) = 0$ are broadened beyond detectability [Figure 2.8]. As temperature increases still further, the two β-hydrogens are no longer distinguishable, and the spectrum appears as a triplet of doublets [Figure 2.8].
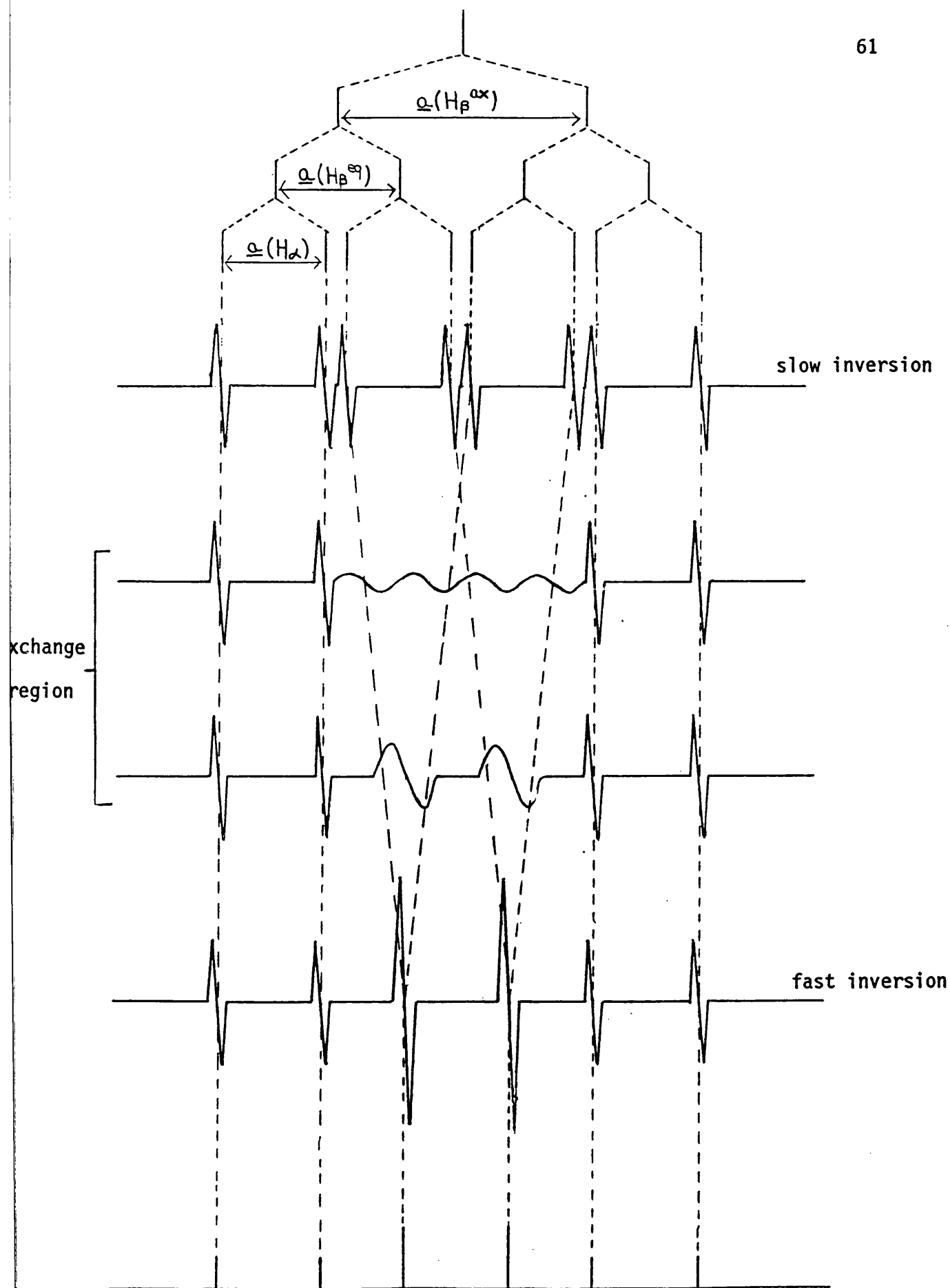
Figure 2.8 Change in splitting pattern in 32 as a function of rate of ring-inversion.

2.3 Halogen Abstraction from Alkyl Chlorides

During UV irradiation of a sample containing DTBP (16% v/v), $Me_3N{\to}BH_2Bu^n$ (1 M), and methyl chloride (1 M) in cyclopropane at 190 K, a strong ESR spectrum of the methyl radical was observed [equation (2.27)]. This suggests that $Me_3N{\to}BH_2Bu^n$ could usefully replace

$$Me_3N{\to}\overset{\bullet}{B}HBu^n \; + \; MeCl \; \longrightarrow \; Me_3N{\to}BHClBu^n \; + \; Me^{\bullet} \qquad (2.27)$$
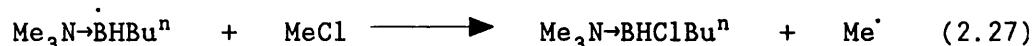
triethylsilane as a source of halogen-abstracting radicals for the production of alkyl radicals from alkyl halides for ESR studies.

Halogen abstraction from alkyl bromides using photochemically generated triethylsilyl radicals is a very useful general method for the production of specific alkyl radicals for ESR studies in solution.[18] However, this method is less suitable for alkyl chlorides, especially at low temperature, because silyl radicals abstract chlorine more slowly than they abstract bromine; ESR spectra are weaker and persistent radicals tend to build up in static samples. UV irradiation of solutions containing DTBP, $Me_3N{\to}BH_2Bu^n$, and an alkyl chloride provides a general route to alkyl radicals which complements the "triethylsilane method"[18] for alkyl bromides.

ESR spectra of the corresponding alkyl radicals were also obtained from similar samples containing Pr^nCl, Bu^nCl, Pr^iCl, Bu^tCl, 2-chloronorbornane,[19] 1-chloroadamantane,[20] or benzyl chloride[21] in place of MeCl (the papers cited display spectra of quality similar to those obtained in the present work). Figure **2.9a** shows the ESR spectrum of the n-butyl radical generated by halogen abstraction from Bu^nCl by $Me_3N{\to}\overset{\bullet}{B}HBu^n$ at 190 K in cyclopropane. For comparison, Figure **2.9b** shows the spectrum obtained from a similar sample in which the

amine-alkylborane has been replaced by an equal concentration of triethylsilane. The spectrum of $Et_3Si\cdot$ is still apparent, that of $Bu^n\cdot$ is much weaker than in Figure **2.9a** and spectra of persistent radicals are evident.

The high reactivity of $Me_3N\overset{\cdot}{\rightarrow}BHBu^n$ towards alkyl chlorides is probably a result of polar effects. The transition state for dechlorination of an alkyl chloride by an amine-boryl radical is likely to be significantly stabilised by a large degree of charge transfer from $Me_3N\overset{\cdot}{\rightarrow}BHBu^n$ to the chlorine [see structures **35a** and **35b**]. Alkyl bromides appear to react even faster than alkyl

$$[Me_3N\overset{\cdot}{\rightarrow}BHBu^n \quad R\text{-}Cl] \longleftrightarrow [Me_3N\overset{+}{\rightarrow}BHBu^n \quad \overset{\cdot}{R} \quad Cl^-]$$

$$\textbf{35a} \hspace{5cm} \textbf{35b}$$
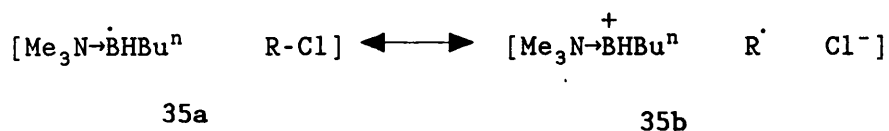
chlorides with $Me_3N\overset{\cdot}{\rightarrow}BHBu^n$, presumably because of more favourable enthalpic factors.[18]

Ingold and co-workers have shown that photolysis of *N*-hydroxypyridine-2-thione esters can provide a source of alkyl radicals for ESR spectroscopic and mechanistic studies.[21] However, the esters would need to be synthesised. The above method from $Me_3N\rightarrow BH_2Bu^n$ and an alkyl chloride would be more convenient.

(a)

(b)

20 G
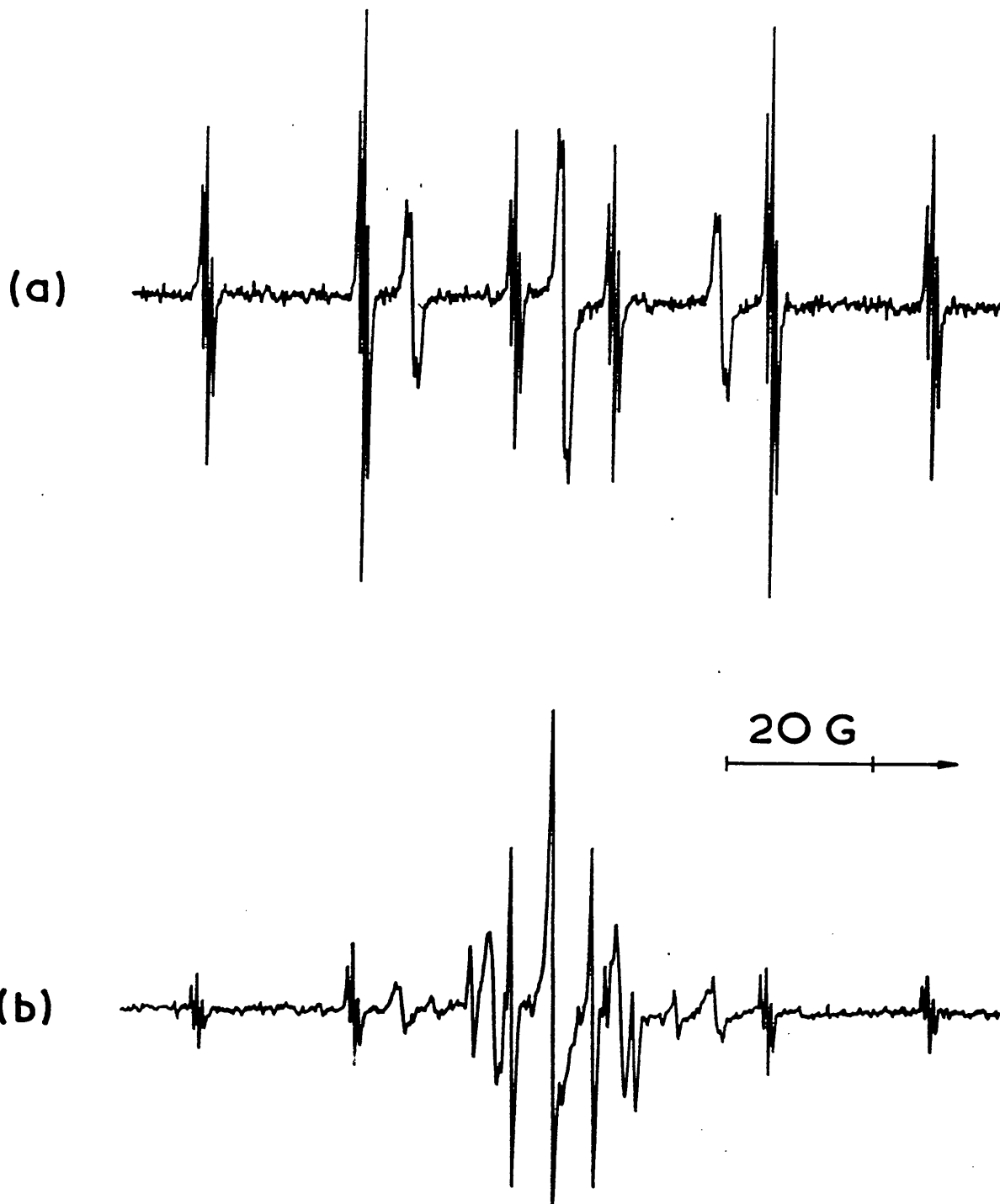
Figure 2.9 ESR spectra recorded during UV irradiation at 190 K. (a) The butyl radical obtained from $Me_3N\rightarrow BH_2Bu^n$ (1 M), Bu^nCl (1 M), and DTBP (17% v/v) in cyclopropane. (b) The mixture of radicals obtained from Et_3SiH (1 M), Bu^nCl (1 M), and DTBP (17% v/v). The gain is slightly lower than for (a), otherwise the instrumental conditions are the same.

References to Chapter 2

1. H. C. Brown and G. J. Klender, *Inorg. Chem.*, 1962, **1**, 204.

2. V. Paul and B. P. Roberts, *J. Chem. Soc., Perkin Trans. 2*, 1988, 1183.

3. M. F. Hawthorne, *J. Am. Chem. Soc.*, 1961, **83**, 831.

4. V. Paul and B. P. Roberts, *J. Chem. Soc., Chem. Commun.*, 1987, 1322.

5. V. Paul, B. P. Roberts and C. A. S. Robinson, *J. Chem. Res. (S)*, 1988, 264.

6. P. Kaushal, Ph.D. thesis, London, 1990, Ch. 5, p. 114.

7. P. Kaushal, Ph.D. thesis, London, 1990, Ch. 5, p. 109.

8. G. B. Butler, G. L. Statton and W. S. Brey, *J. Org. Chem.*, 1965, **30**, 4194.

9. C. L. McCormick and G. B. Butler, *J. Org. Chem.*, 1976, **41**, 2803.

10. N. E. Miller, *Inorg. Chem.*, 1974, **13**, 1459.

11. H. Paul and H. Fischer, *Chem. Commun.*, 1971, 1038.

12. V. Paul, B. P. Roberts and C. R. Willis, *J. Chem. Soc., Perkin Trans. 2*, 1989, 1953.

13. A. G. Davies, D. Griller and B. P. Roberts, *J. Chem. Soc. B*, 1971, 1823.

14. R. W. Fessenden, *J. Chem. Phys.*, 1962, **37**, 747.

15. B. C. Gilbert and M. Trenwith, *J. Chem. Soc., Perkin Trans. 2*, 1975, 1083.

16. C. Heller and H. M. McConnell, *J. Chem. Phys.*, 1960, **32**, 1535.

17. J. K. Kochi, *Adv. Free Radical Chem.*, 1975, **5**, 189.

18. A. Hudson and R. A. Jackson, *Chem. Commun.*, 1969, 1323.

19. T. Kawamura, Y. Sugiyama and T. Yonezawa, *Mol. Phys.*, 1977, **33**, 1499.

20. P. J. Krusic, T. A. Rettig and P. v. R. Schleyer, *J. Am. Chem. Soc.*, 1972, **94**, 995.

21. K. U. Ingold, J. Lusztyk, B. Maillard and J. C. Walton, *Tetrahedron Lett.*, 1988, **29**, 917.

CHAPTER 3

EXPERIMENTAL

3.1 ESR Spectroscopy

The details of this technique, including the methods for measuring hyperfine coupling constants and g-values are described in Chapter 9. Liquid samples were flame-sealed in evacuated Suprasil quartz tubes (either 3 mm i.d., 4 mm o.d. or 2.0 mm i.d., 3.0 mm o.d., the latter for samples which had a high dielectric constant).

Spectra were obtained using Varian E-109 or Bruker ESP-300 instruments operating at 9.1-9.4 GHz. Computer simulations of spectra were obtained using a modified version of Krusic's program ESRSPEC2,[1] extended to handle composite spectra from up to four radicals with different centres, second-order shifts for coupling to single nuclei with $I > 1/2$, and lineshapes continuously variable between 100% Gaussian and 100% Lorentzian.

3.2 NMR Spectroscopy

^{11}B and ^{1}H NMR spectra were recorded using Varian XL-200 or VXR-400 instruments, with $BF_3.OEt_2$ (^{11}B) external or tetramethyl-silane (^{1}H) internal standards. J-values are quoted in Hz.

3.3 Materials

Cyclopropane (Union Carbide) and oxirane (Fluka) were used as received. DTBP (98% pure, Aldrich) was purified by passage down a column of basic alumina (activity 1) followed by distillation under

reduced pressure (b.p. 31-32 °C at 30 Torr). The ketones and t-butyl methyl ether, were freshly distilled under argon before use. The alkyl halides were obtained from commercial sources and, if liquids, were distilled before use. Trimethylamine-thexylborane[2,3] **1** (compound numbers as in Chapter 2), and 1,1,-dimethyl-1,2-azaborolidine[4,5] **24**, were prepared by Dr. Vikram Paul. Trimethylamine-s-butylborane[6] and -n-butylborane[6] complexes were prepared by Dr. Parveen Kaushal. Trimethylamine-isobutylborane was prepared from tri-isobutylboroxine by the method of Hawthorne.[6] The tetramethylethylenediamine complex of isopinocampheylborane [prepared from (1R)-(+)-α-pinene and sold as R-Alpine-Boramine by the Aldrich Chemical Company] was purified by recrystallisation from diethyl ether.

For competition experiments, a stock mixture of the two reactants was made up accurately by weight and portions of this were used for sample preparation.

3.3.1 1-Methyl-cis-1-azonia-5-boratabicyclo[3.3.0]octane 6

A solution of N-methyldiallylamine (16.4 g, 148 mmol) and triethylamine-borane (16.5 g, 143 mmol) in benzene (400 cm^3) was stirred and heated in a sealed pressure vessel (Berghof, capacity 750 cm^3) at ca. 190 °C for 3.5 h. The solution was allowed to cool to room temperature. Benzene and triethylamine were removed using a rotary evaporator, and the residual liquid was distilled under reduced pressure to give 1-methyl-cis-1-azonia-5-borata-bicyclo[3.3.0]octane (2.4 g, 13%), b.p. 58-60 °C/3.0 Torr (lit.[7] b.p. 53-54 °C/1.8 Torr). δ(^{1}H)(C$_6$D$_6$) 0.70 (m, 2H, CH^{A}B), 1.27 (m, 2H, CH^{B}B), 1.58 (m, 4H, C$\underline{H}_2$CH$_2$B), 2.01 (s, 3H, MeN), 2.09 (m, 4H, CH$_2$N),

and 2.84 (q, 1H, $^1J_{BH}$ 99, BH). $\delta(^{11}B)(C_6H_6)$ 4.1 (d, $^1J_{BH}$ 103).

3.3.2 *N,N*-Dimethylglycinatoborane 10[8]

A solution of trimethylamine-iodoborane[9] (5.01 g, 25.2 mmol) in chloroform (36 cm^3) was added with stirring to a suspension of *N,N*-dimethylglycine (2.60 g, 25.2 mmol) in chloroform (28 cm^3). The mixture was stirred at room temperature for 0.5 h, after which time the heavy crystalline precipitate [(CH$_3$)$_3$NH$^+$I$^-$] was separated by filtration. Evaporation of the chloroform from the filtrate under vacuum left a residue which was subsequently taken up in methanol and transferred to a sublimation apparatus. The methanol was then removed by evaporation under reduced pressure and the residue was sublimed twice at 120 °C (bath)/0.1 Torr to give 1.03 g (35%) of *N,N*-dimethylglycinatoborane, m.p. 113 °C (lit.[8] m.p. 119-121 °C). (Found: C, 42.25; H, 8.81; N, 12.30. C$_4$H$_{10}$BO$_2$N requires C, 41.80; H, 8.77; N, 12.19%). $\delta(^1H)(CDCl_3)$ 2.81 (s, 6H, Me$_2$N), 3.45 (s, 2H, CH$_2$). $\delta(^{11}B)(C_6H_6)$ 5.12 (t, $^1J_{BH}$ *ca.* 118).

References to Chapter 3

1. P. J. Krusic, Quantum Chemistry Program Exchange, Program no. 210.

2. H. C. Brown and G. J. Klender, *Inorg. Chem.*, 1962, **1**, 204.

3. V. Paul and B. P. Roberts, *J. Chem. Soc., Perkin Trans. 2*, 1988, 1183.

4. R. M. Adams and F. D. Poholsky, *Inorg. Chem.*, 1963, **2**, 640.

5. M. Ferles and Z. Polivka, *Coll. Czech. Chem. Commun.*, 1968, **34**, 3009.

6. M. F. Hawthorne, *J. Am. Chem. Soc.*, 1961, **83**, 831.

7. P. Kaushal, Ph.D. thesis, London, 1990, Ch. 6, p. 188.

8. N. E. Miller, *Inorg. Chem.*, 1974, **13**, 1459.

9. G. E. Ryschkewitsch and J. W. Wiggins, *Inorg. Synth.*, 1970, Vol. 12, p. 120.

SECTION B : <u>POLARITY REVERSAL CATALYSIS OF ENANTIOSELECTIVE</u>

<u>HYDROGEN-ATOM ABSTRACTION</u>

CHAPTER 4

INTRODUCTION

The transition state energies for the reaction of an optically active molecule with a racemic mixture are different for each enantiomer. If a racemic mixture [50% (R)-enantiomer + 50% (S)-enantiomer] reacts with an optically active reagent, say the (R)-enantiomer, the two transition states **1** and **2** will be

$$[R_{substrate} \cdots \cdots R_{reagent}]^{\neq} \qquad [S_{substrate} \cdots \cdots R_{reagent}]^{\neq}$$

$$\textbf{1} \qquad\qquad\qquad \textbf{2}$$
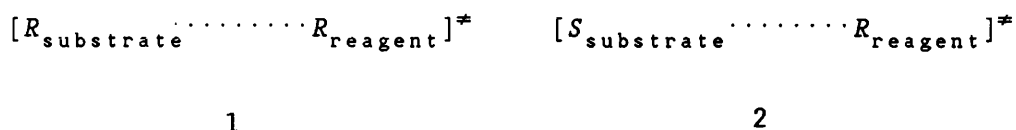
diastereomeric and thus the two enantiomers will react at different rates. Hence, the reaction will be enantioselective and one enantiomer will be removed more rapidly. If the reactivity difference is sufficiently large, this would ultimately lead to the resolution of the racemic mixture.

An application of this technique (kinetic resolution[1]) is provided by the resolution of racemic 1,3-dimethylallene with the optically active hydroborating agent (+)-tetra-isopinocampheyl-diborane [Scheme 4.1].[2] The recovered allene was enriched in the (R)-enantiomer with an enantiomer excess (ee) of 12.6%

The ee resulting from a kinetic resolution can, in principle, be tuned to any required value by adjusting the degree of conversion. Sharpless and co-workers[3,4] have shown that relatively small enantioselectivities can give rise to products of very high ee after only moderate conversions. For example, if one enantiomer reacts 10 times faster than the other, the material remaining after *ca.* 70% total consumption will show an ee of *ca.* 99%. Even a small rate

Me$\diagdown$
　　C$=$C$=$C$\cdots$Me
H$\diagup$　　　$\diagdown$H

(R) 50%

CH$_3$

BH

2

2

Me$\diagdown$
　　C$=$C$=$C$\cdots$H
H$\diagup$　　　$\diagdown$Me

(S) 50%

Me$\diagdown$
　　C$=$C$=$C$\cdots$Me
H$\diagup$　　　$\diagdown$H

(R) 12.6% ee

Scheme 4.1
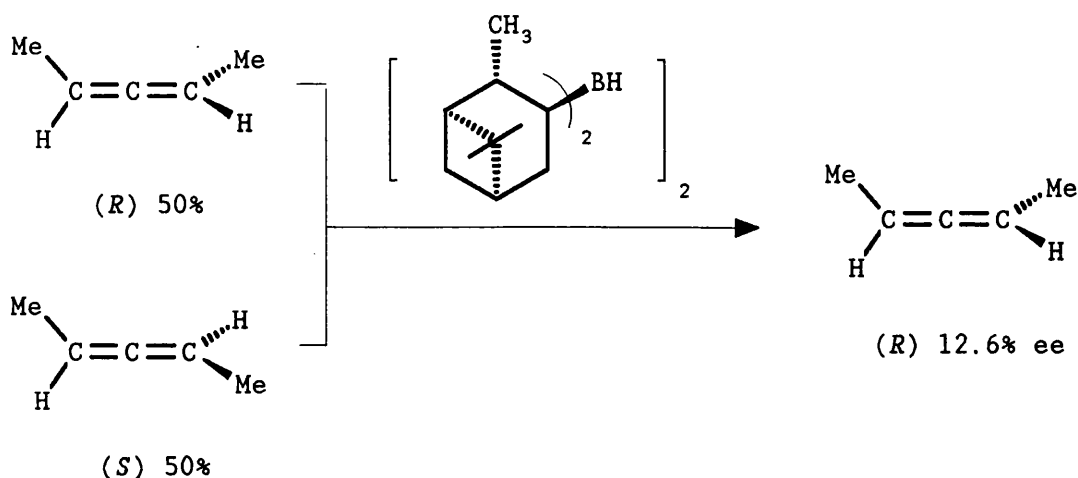
ratio of *ca.* 5 can still provide useful amounts of substance with a very high ee (see Figure **4.1**).

It has been shown[5-7] that α-hydrogen-atom abstraction from esters by $Bu^tO\cdot$ is, like that from ketones, subject to PRC by amine-alkylborane complexes. An aim of this section of the Project was to discover whether α-hydrogen-atom abstraction from esters of the type $R^1R^2CHCO_2R^3$ by optically active donor polarity reversal catalysts is significantly enantioselective and, if so, to make use of this property to bring about the kinetic resolution of such esters using PRC.

Although numerous stereoselective radical reactions are known, only a few enantioselective homolytic processes have been identified. The first example of an enantioselective hydrogen-atom abstraction process to be reported[8] was the kinetic resolution of racemic 2-phenylbutane by its reaction with the optically active 2-phenyl-2-butoxyl radical **3** [equation (4.1)]. When **3** was 86.2% optically pure, after 50% consumption of 2-phenylbutane, the unreacted alkane recovered was found to be enriched with 15.4% of the
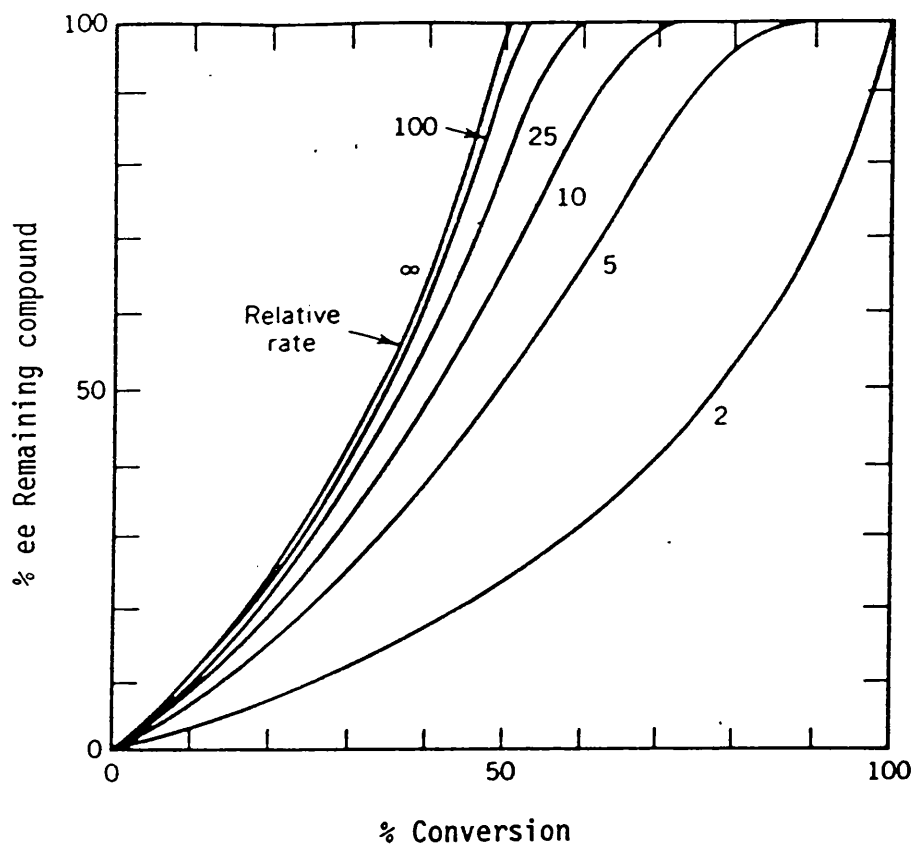
Figure 4.1[3] Dependence of enantiomeric excess (ee) on relative rates of reaction of two enantiomers.

$$(+)\text{-}Ph\overset{\displaystyle Me}{\underset{\displaystyle Et}{\overset{|}{\underset{|}{C}}}}\!\!-\!O^{\cdot} \quad + \quad (\pm)\text{-}Ph\overset{\displaystyle Me}{\underset{\displaystyle Et}{\overset{|}{\underset{|}{C}}}}\!\!-\!H \quad\longrightarrow\quad (+)\text{-}Ph\overset{\displaystyle Me}{\underset{\displaystyle Et}{\overset{|}{\underset{|}{C}}}}\!\!-\!OH \quad + \quad Ph\overset{\displaystyle Me}{\underset{\displaystyle Et}{\overset{|}{\underset{|}{C}}}}\!\!^{\cdot} \qquad (4.1)$$

3
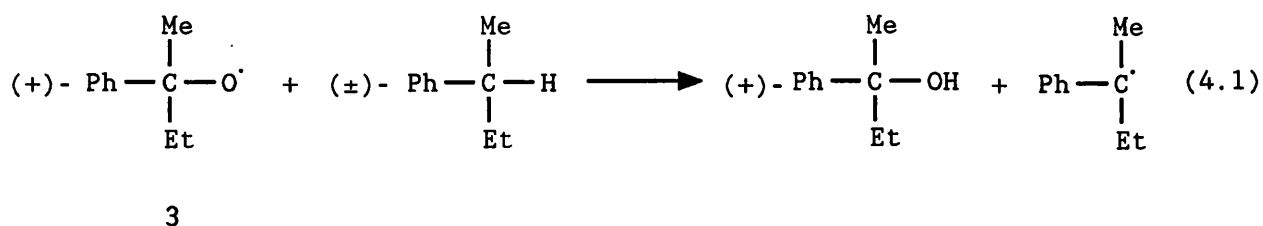
(+)-enantiomer, which corresponds to a value of 1.42 for (k_-/k_+) at 293 K, where (k_-/k_+) is the ratio of the rates of reaction of the (-)- and (+)- enantiomers.

The second example is provided by the enantioselective oxidation of benzoin **4** by the chiral acylaminyl oxide **5*** [equation (4.2)].[9] After 60% consumption of **4** at room temperature, the

$$(4.2)$$

4
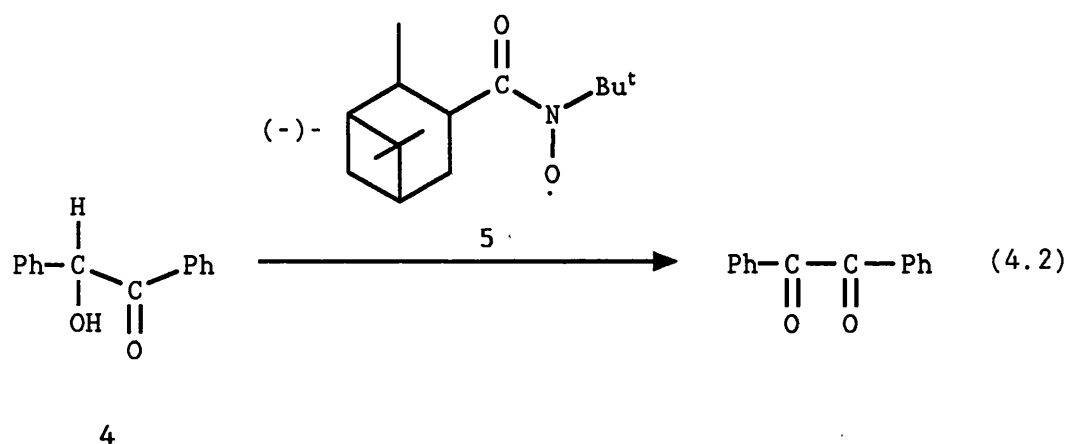
unreacted benzoin recovered showed $[\alpha]_D^{25}$ (CHCl$_3$) = +14°, corresponding to an ee of 7%. This implies that, hydrogen is abstracted from the (-)-enantiomer by the (-)-nitroxide 1.17 times faster than from the (+)-enantiomer.[3]

*The nitroxide **5** was prepared by oxidation of the corresponding (-)-hydroxamic acid. The sign of rotation of **5** is assumed to be (-) also.

The third example of an enantioselective hydrogen-atom transfer reaction is that which takes place from the 4-position of the optically active dihydronicotinamides **6** to the radical anion **7** derived from the prochiral phenyl trifluoromethyl ketone [equation (4.3)].[10] The radical anion **7** reacts with (**6**; R = H) or (**6**; R = Me)

$$R \overset{H}{\underset{5}{\overset{}{\bigvee}}} \quad \overset{O}{\underset{3}{\overset{\|}{C}}} \quad \overset{Me}{\underset{}{\overset{|}{C}}}_{\text{Ph}} \quad + \quad \overset{O^-}{\underset{Ph}{\overset{|}{\underset{CF_3}{C}}}} \quad \longrightarrow$$

6   **7**

$$R \overset{O}{\underset{}{\overset{\|}{C}}} \overset{Me^{\cdot}}{\underset{}{\overset{|}{C}}}_{Ph} \quad + \quad \overset{CF_3}{\underset{Ph}{\overset{|}{\underset{H}{C}}}} O^- \qquad (4.3)$$

8
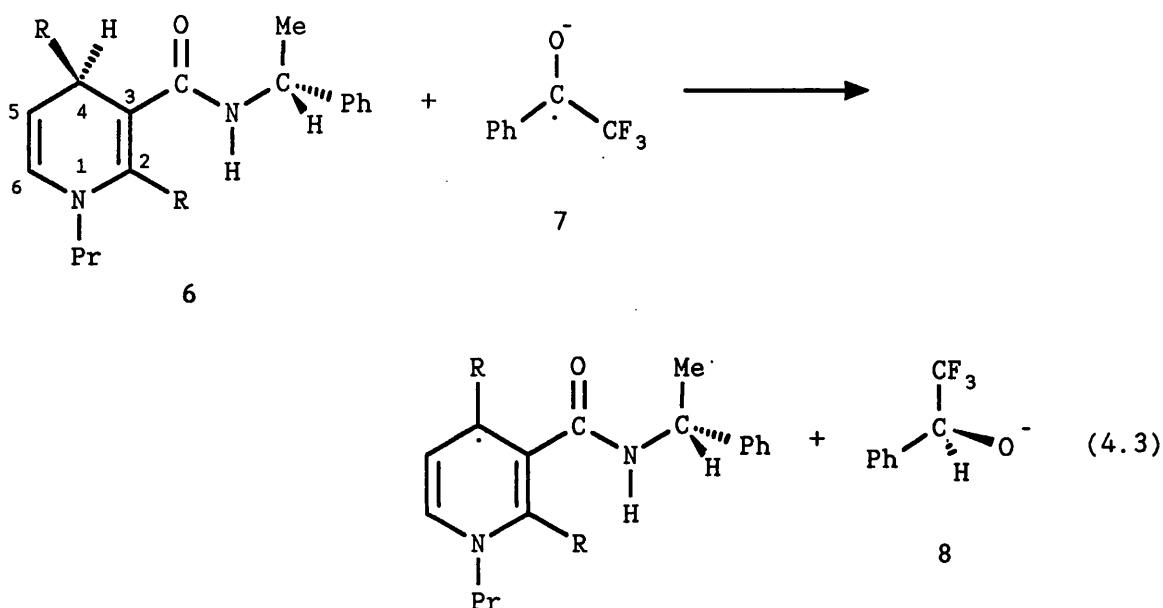
to give predominantly the (S)-alkoxide **8** with an ee of *ca.* 22% and *ca.* 67%, respectively.

In this section of the thesis, the catalytic kinetic resolutions of racemic esters by optically active amine-alkylboryl radicals are described.

In general, the nature of either the amine ligand or the B-alkyl group of an amine-alkylborane may be optically active and may be tailored to optimise enantioselectivity. However, it would be expected that the closer the chiral auxiliary is to the boron radical centre, the higher will be the enantioselectivity. Hence, it seemed likely that having an optically active B-alkyl group in the amine-alkylborane complex would be the better choice. Moreover,

these complexes can be prepared relatively easily by hydroboration of optically active alkenes. Although there are many naturally-occurring optically active amines available, *e.g.* brucine, quinine and strychnine, it would be expected that the bulkiness of these ligands would result in them forming unstable complexes with the alkylboranes.

The optically active amine-alkylborane complexes **9-13** have been

$$R \quad \overset{Me}{\underset{Me}{\overset{|}{N}}}CH_2CH_2\overset{Me}{\underset{Me}{\overset{|}{N}}} \quad R$$

BH$_2$ ⟵ NCH$_2$CH$_2$N ⟶ BH$_2$

BH$_2$

9;   R = H   13
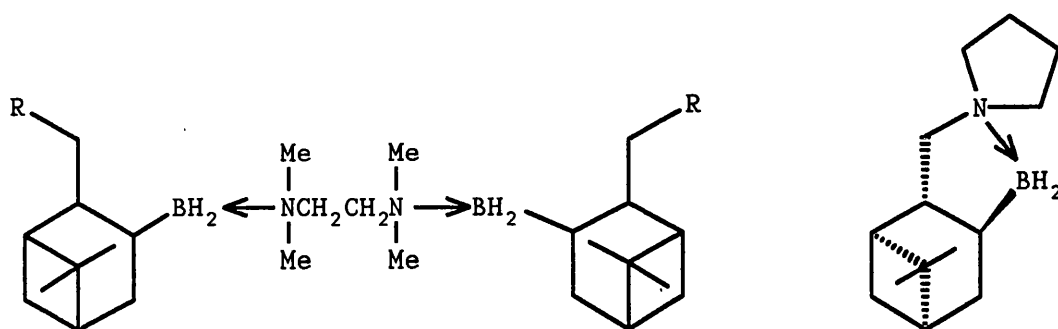
10;   R = Me

11;   R = CH$_2$OMe

12;   R = CH$_2$OCH$_2$Ph

prepared and their abilities to catalyse enantioselective hydrogen-atom abstraction from the substrates **14-24** [the (4*S*, 5*S*) enantiomer is shown for **24**] have been investigated, using the results of kinetic resolutions to determine the enantioselectivitiess.

In addition, ESR spectroscopy has been used, for the first time, to measure the relative rates of the elementary enantioselective hydrogen-atom abstraction reactions of optically active amine-boryl radicals derived from **9-12**.

$$Ph-\underset{\underset{R}{|}}{\overset{\overset{H}{|}}{C}}-CO_2R'$$
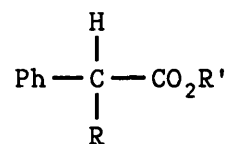
14; R = Me , R' = Me

15; R = Me , R' = Et

16; R = Me , R' = Bu^t

17; R = Et , R' = Me

18; R = Bu^t, R' = Me

$$Ph-\underset{\underset{Me}{|}}{\overset{\overset{H}{|}}{C}}-CH_2-CO_2Me$$

19

$$Bu^i-\!\!\!\!\text{<benzene>}\!\!\!\!-\underset{\underset{Me}{|}}{\overset{\overset{H}{|}}{C}}-CO_2Me$$

20

21

22

CO_2Me
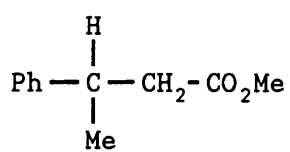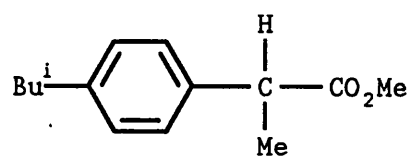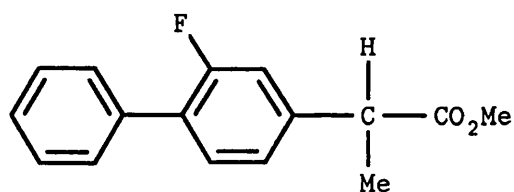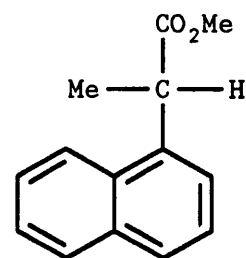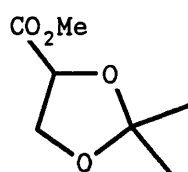
23
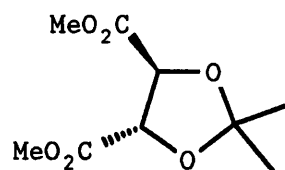
24

References to Chapter 4

1. P. H. Boyle, *Q. Rev. Chem. Soc.*, 1971, **25**, 323.

2. W. L. Waters, W. S. Lim and M. C. Caserio, *J. Am. Chem. Soc.*, 1968, **90**, 6741.   W. R. Moore, H. W. Anderson and S. D. Clark, *J. Am. Chem. Soc.*, 1973, **95**, 835.

3. V. S. Martin, S. S. Woodard, T. Katsuki, Y. Yamada, M. Ikeda and K. B. Sharpless, *J. Am. Chem. Soc.*, 1981, **103**, 6237.

4. H. B. Kagan and J. C. Fiaud, *Topics Stereochem.*, 1988, **18**, 249.

5. V. Paul and B. P. Roberts, *J. Chem. Soc., Chem. Commun.*, 1987, 1322;   *J. Chem. Soc., Perkin Trans. 2*, 1988, 1183.

6. V. Paul, B. P. Roberts and C. R. Willis, *J. Chem. Soc., Perkin Trans. 2*, 1989, 1953.

7. P. Kaushal, P. L. H. Mok and B. P. Roberts, *J. Chem. Soc., Perkin Trans. 2*, 1990, 1663.

8. J. H. Hargis and H. H. Hsu, *J. Am. Chem. Soc.*, 1977, **99**, 8114.

9. C. Berti and M. J. Perkins, *Angew. Chem., Int. Ed. Engl.*, 1979, **18**, 864.

10. D. D. Tanner and A. Kharrat, *J. Am. Chem. Soc.*, 1988, **110**, 2968.

CHAPTER 5

RESULTS AND DISCUSSION

5.1 Syntheses of Catalysts

The 1:2 complex **2** of TMEDA with (+)-isopinocampheylborane[1-4] is commercially available (Aldrich, R-Alpine-Boramine), or can be prepared from the hydroboration of optically active (1R)-(+)-α-pinene **1** with borane-methyl sulphide complex (BMS), followed by the addition of TMEDA (see Scheme 5.1).
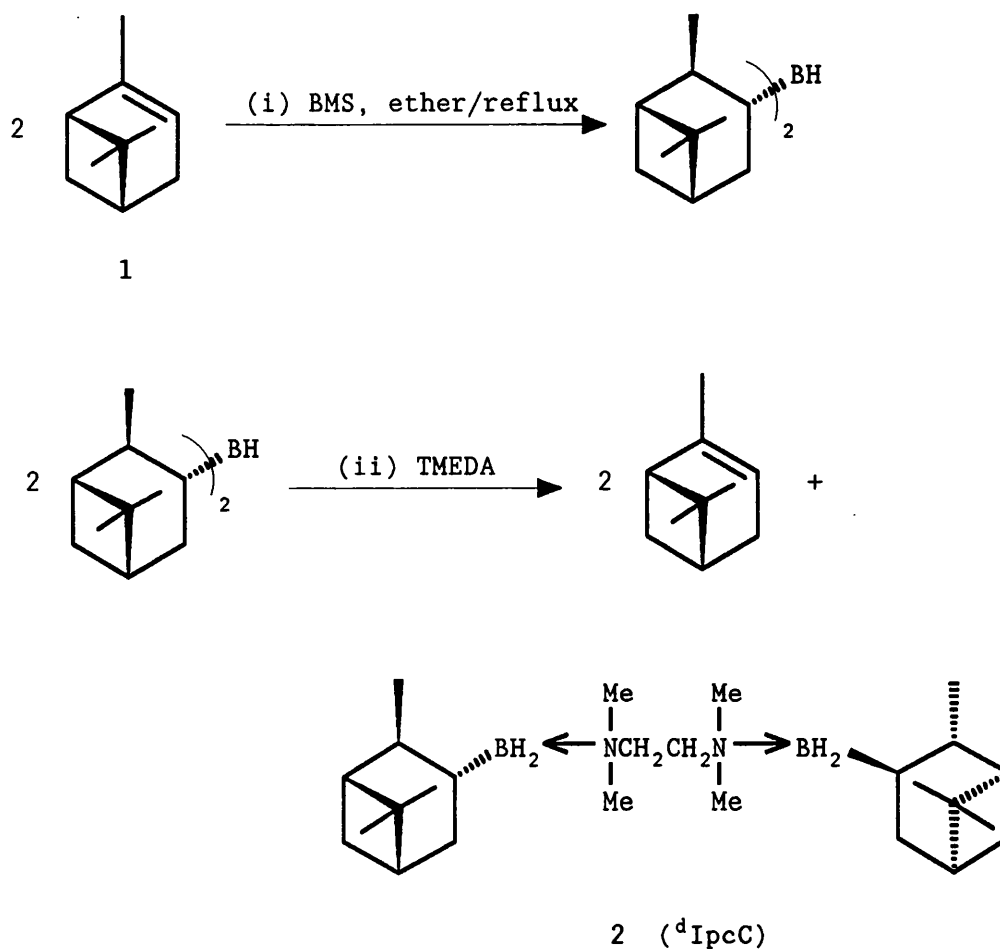
Scheme 5.1

Treatment of **1** (or its enantiomer **3**) with BMS in refluxing

diethyl ether gives di-isopinocampheylborane. Subsequent addition of 0.5 molar equivalent of TMEDA gives the complex **2** (or its enantiomer **8**) by displacement of α-pinene, as described by Brown and his co-workers.[1-4] Corresponding alkylborane-TMEDA complexes **9-11** were prepared similarly from the 2-substituted apopinenes **4-6** which are readily available from natural sources.[5-11] The use of chiral
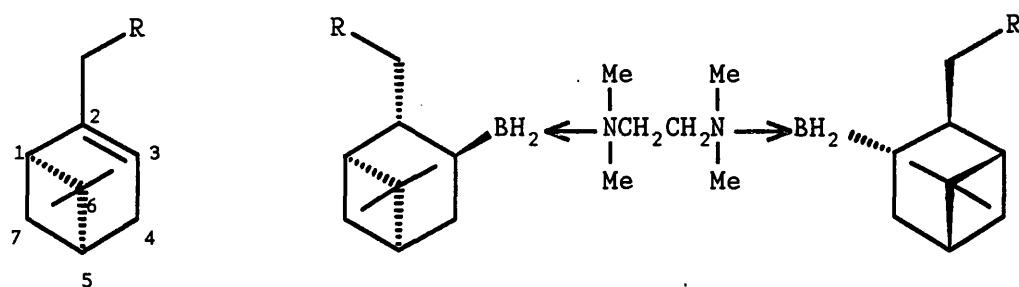
3; R = H

4; R = Me

5; R = CH$_2$OMe

6; R = CH$_2$OCH$_2$Ph

7; R = CH$_2$OH

8; R = H (^{1}IpcC)

9; R = Me (^{1}EapC)

10; R = CH$_2$OMe (^{1}MeapC)

11; R = CH$_2$OCH$_2$Ph (^{1}BeapC)

organoboranes of this type for asymmetric synthesis, based on heterolytic reactions, is well established.[12,13]

The acronyms, given in parentheses after the structures (**2**, and **8-11**) indicate that the complex contains the isopinocampheyl (Ipc), iso-2-ethylapopinocampheyl (Eap), iso-2-(2-methoxyethyl)-apopinocampheyl (Meap) or iso-2-(2-benzyloxyethyl)apopinocampheyl (Beap) group attached to boron, and the superscript d or l indicates whether the starting pinene was *dextro-* or *laevo*-rotatory, following the conventions adopted by Brown *et al.*[5,7,10,14] *Syn*-hydroboration takes place from the less hindered face of the pinene (opposite from the 6,6-dimethyl bridge) to give a product of defined

stereochemistry.[10,12]

Pure crystalline IpcC was unchanged after exposure to the atmosphere for more than 12 h at room temperature. Contrary to reports in the literature,[1-4] it was found that dIpcC did not melt cleanly at 140-141 °C and, in either a sealed or open tube, the behaviour of this compound depended on the rate of heating. Even when the complex was transferred to the preheated apparatus at 110 °C and then heated at 2 °C min^{-1}, the crystals began to melt at ca. 120 °C; solid was still present until ca. 145 °C and melting was accompanied by slow evolution of a gas (presumably hydrogen). We conclude that dIpcC is thermally unstable at or below its melting point; the other complexes 8-11 behaved in a qualitatively similar way on heating.

The samples of (1R)-(+)- and (1S)-(-)-α-pinene used were each almost enantiomerically-pure (>99% ee). However, it has been reported that when dIpcC is prepared from (+)-α-pinene of lower enantiomeric purity (91% ee), the complex may be upgraded to an ee of ca. 100% by crystallisation from diethyl ether.[1] The structure of dIpcC has been determined by X-ray crystallography.[15]

The pinenes 9-11 were prepared from (1R)-(-)-nopol 7, which is available commercially with an ee of ca. 90%. The complex lEapC is upgraded to 99-100% ee by crystallisation from ether.[5] The complexes lMeapC and lBeapC have not been described previously and their enantiomeric purities were determined by oxidation with alkaline hydrogen peroxide,[1,5,11,16,17] followed by reaction of the derived alcohol with (S)-(+)-2-methoxy-2-phenyl-3,3,3- trifluoropropanoyl chloride (Mosher's acid chloride)[18,19] 12 and determination by ^{1}H and ^{19}F NMR spectroscopy of the diastereomeric composition of the ester

13 or 14 (see Scheme 5.2 in which only the major enantiomer of the pinanol is shown). Complete conversion to the esters is important for accurate measurement of ee of the alcohols, since the esterifications can be enantioselective. By using an excess of the acid chloride, the final step shown in Scheme 5.2 was ≥98% completed.

^{1}MeapC   or ^{1}BeapC $\xrightarrow{\text{(i)}}$

10   11

(ii)

13;   X = CH$_2$OMe

14;   X = CH$_2$OCH$_2$Ph
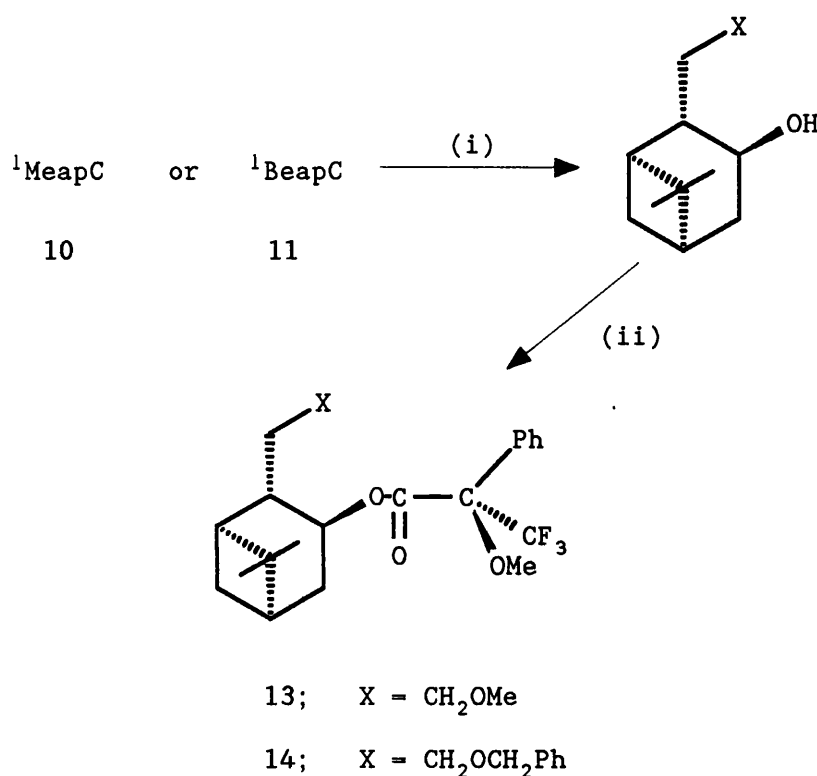
Reagents :   (i) H$_2$O$_2$ / HO$^-$

(ii) (S)-(+)-PhC(OMe)(CF$_3$)COCl 12 / Et$_3$N

Scheme 5.2

The diastereomeric chemical shift differences observed for α-substituents at the acid moiety were generally too small to be useful, except for the ^{19}F NMR signals of the trifluoromethyl group. However, the diastereomeric ratios can be determined by examination of the CHO signals in the ^{1}H NMR spectra. Direct hydroboration/oxidation of the pinenes 5 and 6 provided ca. 95:5

diastereomeric mixtures of the Mosher esters for comparative purposes. After two recrystallisations from hexane/diethyl ether (1:1), ^{1}BeapC prepared from 6 (89% ee) was upgraded to ≥98.5% ee, while ^{1}MeapC was upgraded much more slowly by recrystallisation from hexane/diethyl ether (2.5:1) and the ee of the complex used as a catalyst in this work was 91%.

The spirocyclic amine-alkylborane complex 15 was thought to be a potentially good chiral catalyst due to the steric bulkiness of the substituents and the rigid stereochemistry. It was prepared from (1R)-(-)-myrtenol 16 as outlined in Scheme 5.3.
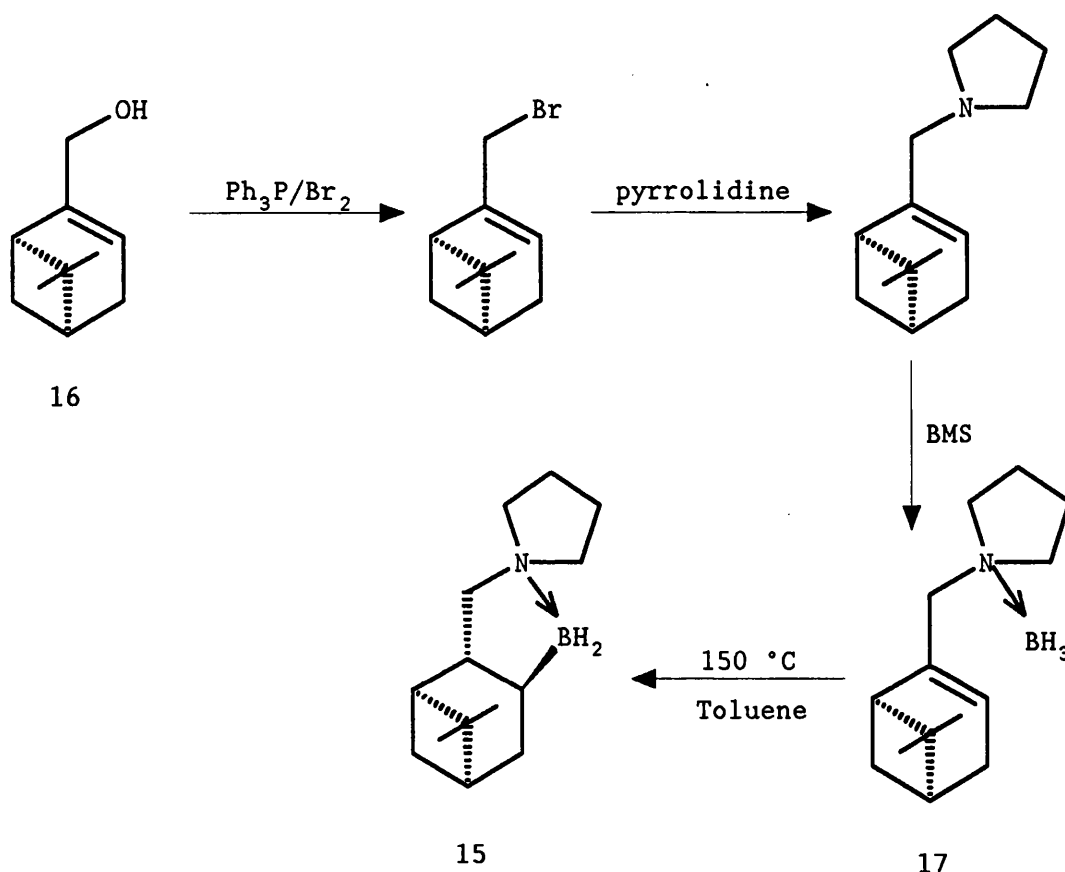
Scheme 5.3

Cyclisation of the amine-alkylborane 17 has been studied using differential scanning calorimetry (DSC), in which the uncyclised

amine-alkylborane and a reference substance were both subjected to a continuously increasing temperature. When the thermocouples indicated a temperature difference, heat was added to the cooler of the two until temperature equality was restored. The added heat therefore compensates for that lost or gained as a consequence of endothermic or exothermic reactions occurring in the sample. The rate of heating required to keep the temperatures equal was recorded as a function of sample temperatures. Figure **5.1 curve A** shows the DSC thermogram of the amine-borane **17**. The graph first shows an endothermic change which corresponds to the melting point of the amine-borane (*ca.* 80 °C). As the temperature was increased further, an exothermic reaction began at *ca.* 150 °C and it proceeded with an endothermic effect. The exothermic reaction was likely to be the intramolecular hydroboration of the CC double bond in the amine-borane to give **15**.

Cyclisation of the amine-borane **17** was thus carried out at 150 °C in toluene solvent in a sealed-tube. ^{11}B NMR spectroscopic examination of the toluene solution after heating showed a main triplet at δ_B -0.97 ppm (J_{BH} 105 Hz) (*ca.* 90%) which presumably corresponds to the cyclic amine-borane **15**. There was also a small amount of the uncyclised amine-borane **17** and other unidentified impurities. Compound **15** was stable at 5 °C in toluene solution in the absence of air for > 2 months. However, upon removal of the solvent, the complex gradually changed into what appeared to be a mixture of its oligomers. In the absence of solvent, oligomerisation may be favoured because monomer units are held in close proximity and appropriately orientated by dipole-dipole attraction (see Scheme 5.4). Compound **15** was therefore stored and used as a stock solution
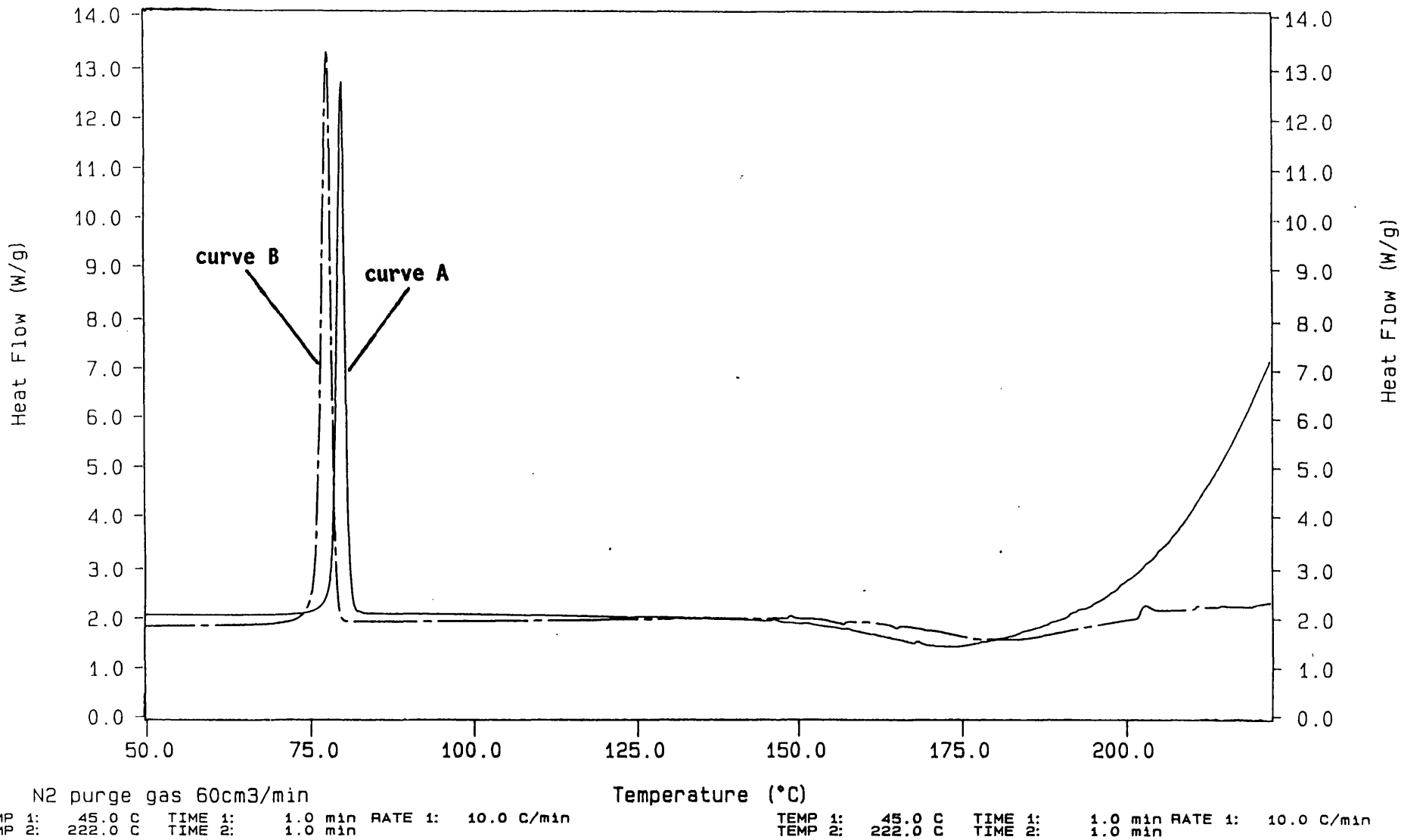
Figure **5.1**   DSC thermograms of the amine-boranes **17** (**curve A**) and **21**

(**curve B**).

Scheme 5.4

cyclodimer
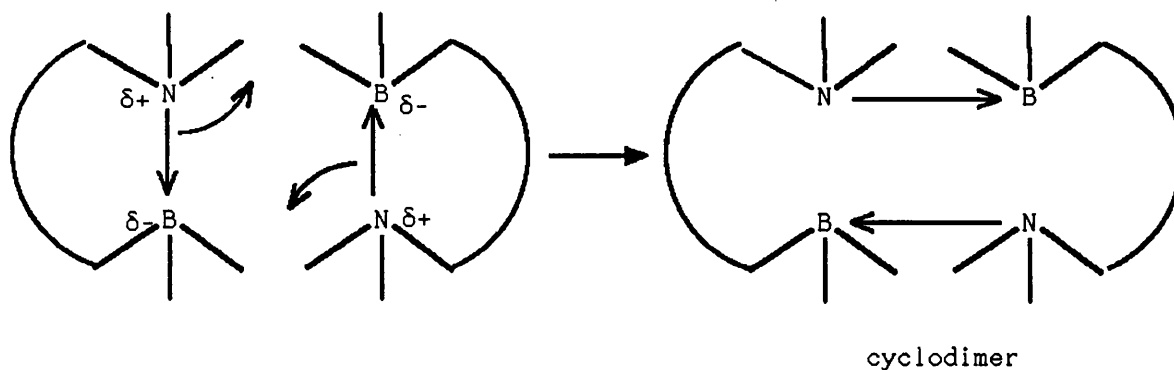
in toluene.

ESR experiments were carried out to test the efficiency of this solution as a polarity reversal catalyst. When a solution of ethyl acetate (1.0 M) and DTBP (22% v/v) in a mixture of toluene and cyclopropane solvents (1.2:1) was UV irradiated in the cavity of an ESR spectrometer at 183 K, only the benzyl radical, produced from H-atom abstraction from the toluene solvent by $Bu^tO\cdot$, was detected. When the experiment was repeated with an equal volume of the stock solution of 15 in place of the toluene, only the radical 18 was detected. Abstraction must now be brought about by the nucleophilic radical 19, which reacts regioselectively at an electron-deficient C-H bond of the ethyl acetate. The stock solution of 15 in toluene

18   19
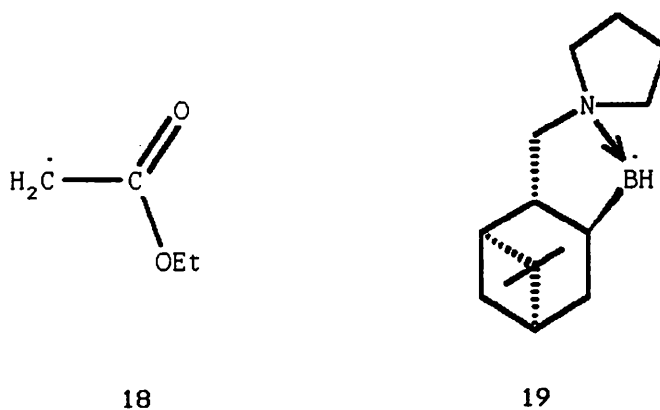
can therefore act as a good polarity reversal catalyst.

The cyclic amine-borane **20** was to be prepared similarly from dimethylamine, *via* the amine-borane **21**. Cyclisation of the

20   21
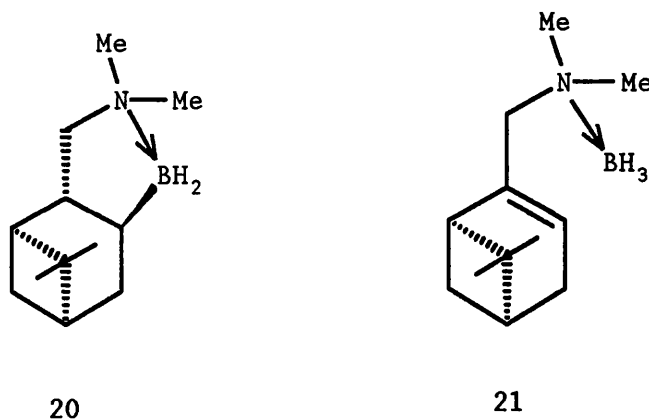
amine-borane **21** was carried out at 150 °C in toluene as before. ^{11}B NMR spectroscopic examination of the toluene solution after heating showed a triplet (δ_B +1.45 ppm, J_{BH} 116 Hz) which presumably corresponds to the cyclic amine-borane **20**. However, a large amount of the uncyclised amine-borane **21** (δ_B -7.41 ppm, J_{BH} 97 Hz) and other unidentified impurities were also present. This result is in accord with DSC experiments which were carried out later. Figure **5.1 curve B** shows the DSC thermogram of the amine-borane **21**. The endothermic change at *ca.* 78 °C corresponds to the melting point of the amine-borane. The exothermic reaction occurs at a higher temperature, accounting for the fact that more of the amine-borane **21** remained after heating under the same conditions as used for **17**.

5.2 Kinetic Resolution of Esters

When an oxirane solution containing DTBP (20% v/v) and t-butyl 2-phenylpropanoate **22** (0.96 M) was irradiated with UV light at 199 K while the sample was in the microwave cavity of the ESR spectrometer, only the spectrum of the oxiranyl radical was observed [equation (5.1)]. However, when the experiment was repeated in the presence of

$$Bu^tO^. + \triangle\!\!\!\!\!\!O \longrightarrow \triangle\!\!\!\!\!\!O + Bu^tOH \qquad (5.1)$$

either amine-borane **23** (0.23 M) in oxirane or cyclopropane, or amine-borane **2** (0.15 M) in oxirane, an ESR spectrum ascribed to the radical **26** [$a(3H_\beta)$ 16.53, $a(1H_p)$ 4.61, $a(2H_o)$ 4.11, $a(2H_m)$ 1.40 G, and g 2.0031 in cyclopropane at 190 K] was detected in place of that of the oxiranyl radical [Figures **5.2** and **5.3**]. The t-butoxyl radical

$$XNMe_2 \rightarrow BH_2R \xrightarrow[-Bu^tOH]{Bu^tO^.} XNMe_2 \rightarrow \overset{.}{B}HR \qquad (5.2)$$

23	X = Me, R = Bu^n	**24**
2	X = CH$_2$CH$_2$NMe$_2$→BH$_2$R	**25**

R =

$$XNMe_2 \rightarrow \overset{.}{B}HR + PhMeC(H)CO_2Bu^t \longrightarrow PhMe\overset{.}{C}CO_2Bu^t$$
$$\qquad\qquad\qquad\quad \mathbf{22} \qquad\qquad\qquad\qquad \mathbf{26}$$
$$+ \quad XNMe_2 \rightarrow BH_2R \qquad (5.3)$$
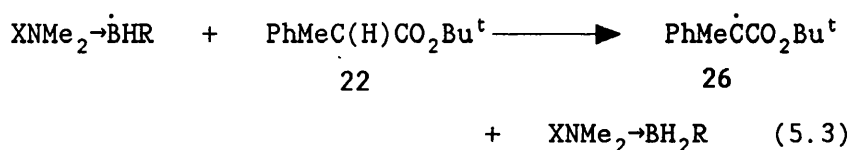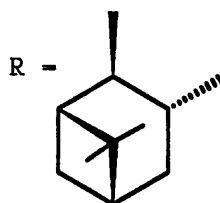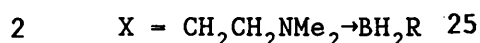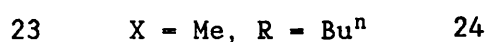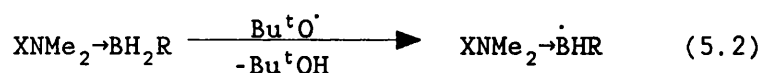
now abstracts hydrogen from the amine-borane in preference to oxirane and hydrogen abstraction from the ester is brought about by the

a)

10 G
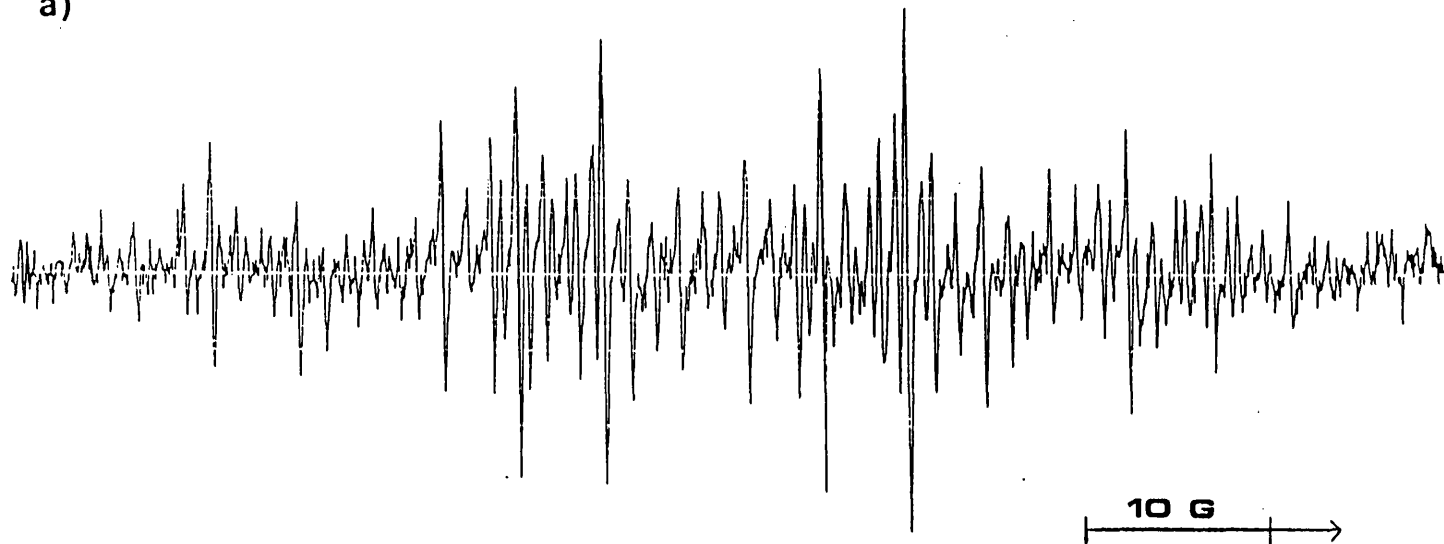
b)
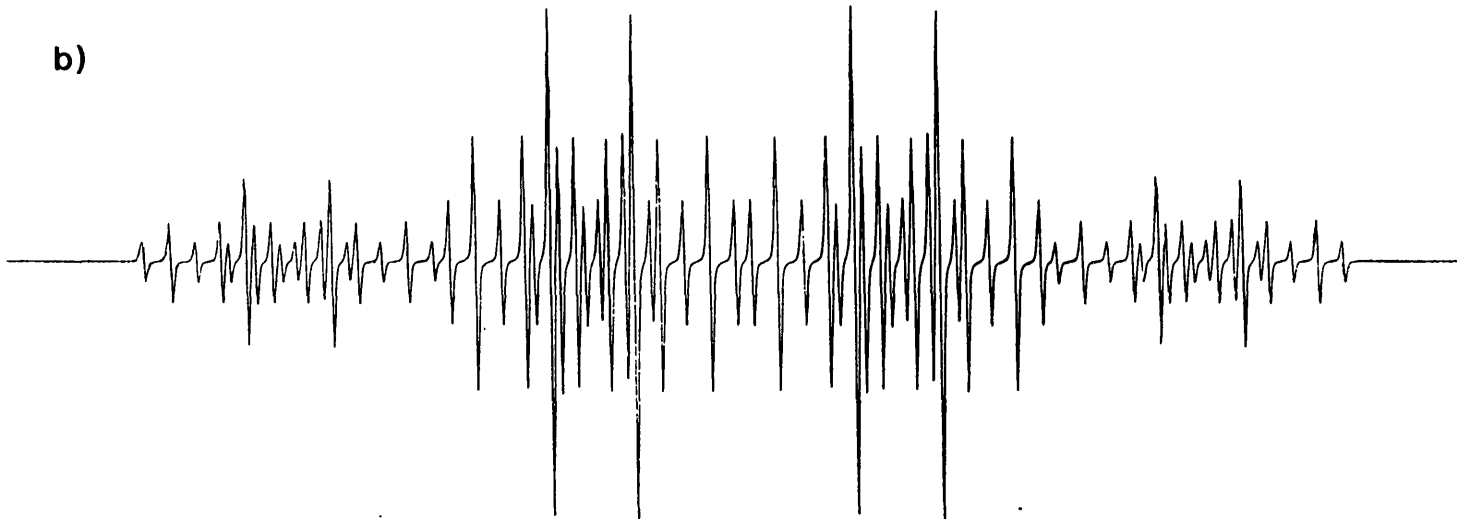
Figure 5.2

Figure Caption

Figure **5.2**

(a) ESR spectrum of the radical PhMeĊCO$_2$Bu^t **26** generated in the presence of **23** as polarity reversal catalyst in cyclopropane at 190 K. (b) Computer simulation of (a) using the parameters given in the text.

a)

10 G

b)
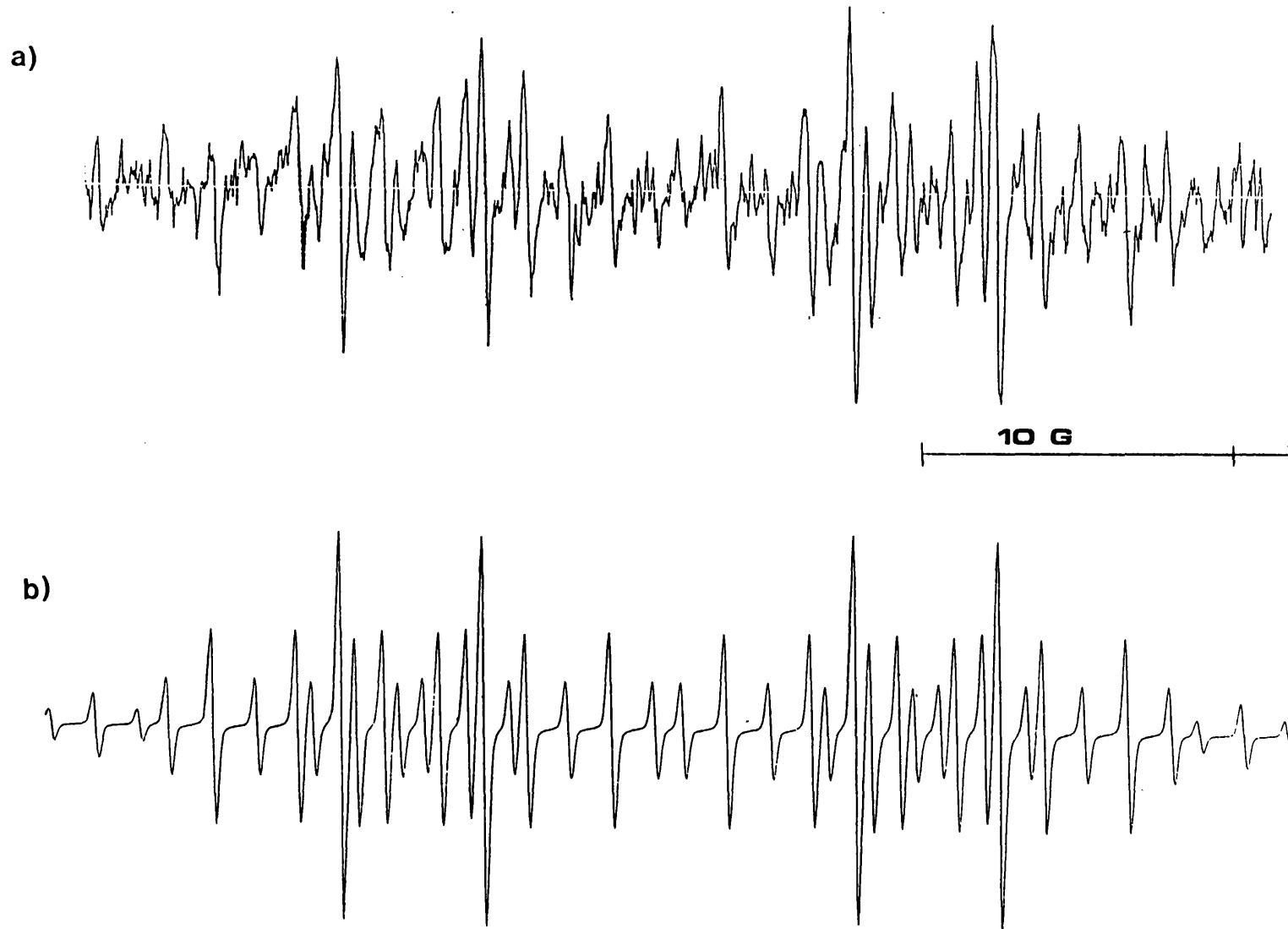
Figure 5.3 (a) Central region of the spectrum of $PhMe\dot{C}CO_2Bu^t$ 26.

(b) Computer simulation of (a).

derived amine-boryl radical [equations (5.2) and (5.3)]. In principle, two rotational isomers of **26** which differ in geometry about the $\dot{C}$-C(O) bond [see structures **27** and **28**], could be present.

27   28
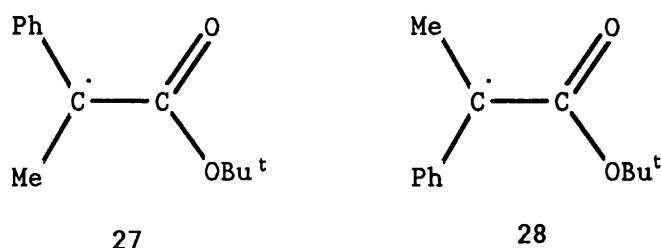
A few weak lines which might be associated with a minor isomer were detected alongside the main spectrum.

Similar results were obtained with the methyl ester **29**. When an oxirane solution containing DTBP (21% v/v) and the ester (0.98 M) was UV irradiated at 189 K, only the spectrum of the oxiranyl radical was observed [equation (5.1)]. However, when the experiment was repeated in the presence of either **23** (0.25 M) or **2** (0.17 M), a spectrum attributed to the radical **30** was detected instead [equations (5.2) and (5.4)]. The ESR spectrum of **30** was more complex and

$$\text{XNMe}_2{\rightarrow}\dot{\text{B}}\text{HR} \quad + \quad \text{PhMeC(H)CO}_2\text{Me} \xrightarrow{\hspace{1cm}} \text{PhMe}\dot{\text{C}}\text{CO}_2\text{Me} \quad + \quad \text{XNMe}_2{\rightarrow}\text{BH}_2\text{R} \qquad (5.4)$$
$$\text{29} \qquad\qquad\qquad\qquad \text{30}$$
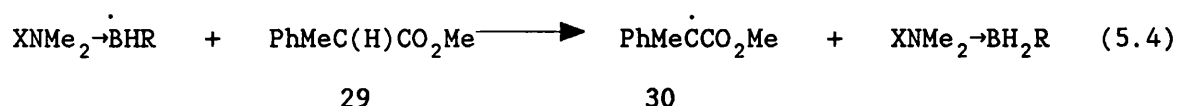
consequently weaker than that of its O-t-butyl counterpart.

A probe experiment was also carried out with n-propyl bromide. When an oxirane solution containing n-propyl bromide (1 M) and DTBP (23% v/v) was irradiated at 191 K, only the oxiranyl radical was detected, indicating that oxirane is more reactive than the alkyl bromide towards Bu^{t}O· under these conditions. When the experiment was repeated in the presence of **29** (1 M) and **2** (0.17 M), only the spectrum of the n-propyl radical was detected. This confirms that in the presence of **2**, Bu^{t}O· reacts with the amine-borane in preference

to oxirane and produces the radical **25**, which then goes on to abstract the halogen atom from n-propyl bromide.[20] The bromide is thus more reactive than the ester under these conditions. Since no oxiranyl radical was detected, it shows that all the t-butoxyl radicals generated were trapped by the amine-borane **2**.

The next stage was to investigate whether α-hydrogen-atom abstraction from **29** by the optically active amine-boryl radical **25** is enantioselective. Preliminary experiments were carried out using 0.2 mmol of ester.

An oxirane solution containing racemic **29** (0.8 M), DTBP (18% v/v), and t-butylbenzene (0.32 M) as an internal concentration standard was UV irradiated in the microwave cavity of the ESR spectrometer at 191 K for 3 h. Oxirane was allowed to evaporate from the sample at room temperature, after which GLC analysis showed that 96% of the ester still remained. This result is in accord with the earlier observations made by ESR spectroscopy, since $Bu^tO\cdot$ should react almost exclusively with oxirane under these conditions. However, when the experiment was repeated in the presence of ^dIpcC **2** (0.15 M), 26% of the ester was consumed. Examination of the residual ester by 400 MHz ^1H NMR spectroscopy in the presence of the optically active shift reagent europium tris(D-3-heptafluorobutylcamphorate) [Eu(hfc)$_3$], showed it to be enriched in one enantiomer with an ee of 14%.*

---

* In the absence of DTBP, with or without added t-butyl alcohol (0.16 M) (which would be formed as a photo-product from the peroxide), no ester was consumed.

Clearly hydrogen-atom abstraction by the optically active amine-boryl radical **25** from the ester **29** is an enantioselective process. Comparison with the NMR spectrum obtained from ester of known ee prepared from authentic (*R*)-**29** and racemic ester, showed that the radical **25** derived from ^{d}IpcC abstracts hydrogen more rapidly from the (*R*)-ester.

As an important control for the experimental methods used , it was shown that racemic ester remained after 49% consumption of **29** in the presence of the achiral trimethylamine-butylborane **23**.

It was hoped that by increasing the ester consumption, the ee would also increase. However, photolysing the sample for 5 h increased the ester consumption to only 31%. One possible way to increase the ester consumption is to use a higher concentration of the catalyst **2**. However, a 0.15 *M* solution of **2** at 190 K in oxirane is already saturated. Diethyl ether, 1,2-dimethoxyethane, toluene, and a mixture of DTBP and benzene (5:2), were tried as solvents, but all were less good than oxirane. Tetrahydrofuran (THF) is a very good solvent for **2**. However, when a solution containing methyl 2-phenylpropanoate (0.8 *M*), DTBP (18% v/v), t-butylbenzene (*ca*. 0.3 *M*), and **2** (0.15 *M*) in THF was UV irradiated at 191 K, the radical **31** (produced by H-atom abstraction from the THF by Bu^{t}O·) was detected.
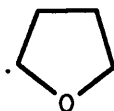
31

Oxirane is therefore the most suitable solvent for use with **2**.

Increasing the reaction temperature should increase the solubility of **2**. However, it is generally true that the lower the reaction temperature, the greater will be the difference in rates of

reaction of the two enantiomers, and thus the higher the enantioselectivity. The kinetic resolutions studied here were therefore carried out at low temperatures (ca. 196 K).

It might be possible to increase the consumption of ester by increasing the concentration of DTBP so that more light is absorbed by the peroxide. An oxirane solution containing the ester 29 (0.18 M), 2 (0.15 M), t-butylbenzene (0.5 M) and DTBP (28% v/v, cf. 18% v/v previously) was photolysed for 5 h at 191 K, after which GLC analysis showed that consumption of the ester had increased to 41%. The residual ester was shown by ^{1}H NMR analysis to contain a 22% ee of the (S)-ester. However, a further increase in concentration of DTBP is not possible because it drastically reduces the solubility of 2.

If none of the α-carbonylalkyl radicals 30 produced in reaction (5.4) go on to abstract hydrogen and regenerate racemic substrate, the enantioselectivity factor s will be given by equation (5.5).[21,22] Here k_A and k_B are the rate constants for abstraction of hydrogen from the faster- and slower-reacting enantiomer, respectively, C is the fraction of substrate consumed, and EE is the fractional ee of the ester which remains. According to this equation, an ee of 22%

$$s = (k_A/k_B) = \ln[(1-C)(1-EE)]/\ln[(1-C)(1+EE)] \qquad (5.5)$$

after 41% consumption of the ester implies that the (R)-ester is ca. 2.4 times more reactive than the (S)-ester towards 25 at 190 K.

The experiment could be carried out on a larger scale with 0.8 mmol of ester using the apparatus shown in Figure 5.4. The UV source was a Mazda 250 W high-pressure mercury arc lamp and unfiltered light from this was focused onto the sample by a pair of quartz lenses (focal length 10 cm, diameter 10 cm). The temperature of the
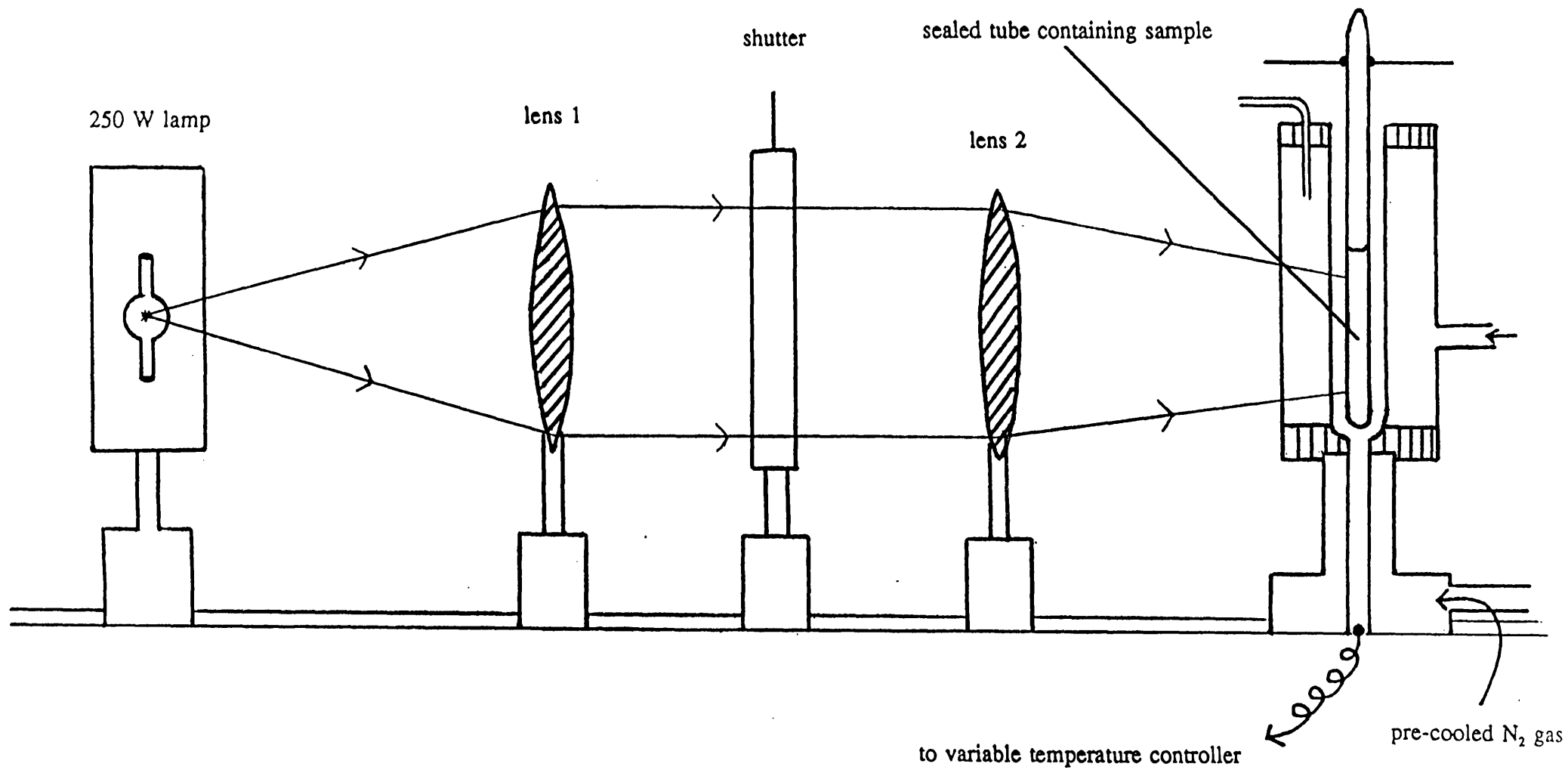
Figure 5.4 Apparatus used for kinetic resolution of the esters

reaction mixture was controlled by passing a stream of pre-cooled nitrogen gas over the sample tube, using a Varian ESR spectrometer temperature unit. The temperature of the sample was monitored by a thermocouple placed in the gas stream alongside the sample tube.

After 5 h of UV irradiation at 206 K, 55% of the ester **29** was consumed, and the residual substrate had 30% ee of the (S)-ester. This corresponds to an s value of 2.2, according to equation (5.5). Repetition of the experiment using the antipode of **2**, ^{1}IpcC **8**, gave rise to 53% consumption of the ester. The recovered substrate showed an ee of 29% in favour of the (R)-ester. Now, the (S)-enantiomer reacts faster than the (R)-enantiomer, and k_S/k_R is 2.2. Figure **5.5** shows the 400 MHz ^{1}H NMR spectra in the C-methyl region obtained from the ester **29** in the presence of Eu(hfc)$_3$.

The radical **30** would be expected to be removed mainly *via* coupling[23] to produce the dimers **32** and **33** [equation (5.6)].[23-25] However, a small portion might undergo disproportionation which would produce **34** and regenerate the racemic ester [equation (5.7)]. The

$$
\text{dimerisation} \quad \begin{array}{cc} \overset{\text{Ph}}{|} & \overset{\text{Ph}}{|} \\ \text{Me-C} & \text{-C-Me} \\ | & | \\ \text{MeO}_2\text{C} & \text{CO}_2\text{Me} \end{array} + \begin{array}{cc} \overset{\text{Ph}}{|} & \overset{\text{Me}}{|} \\ \text{Me-C} & \text{-C-Ph} \\ | & | \\ \text{MeO}_2\text{C} & \text{CO}_2\text{Me} \end{array} \quad (5.6)
$$

32   33

$$
\begin{array}{c} \overset{\text{Ph}}{|} \\ \text{C} \cdot \\ \text{Me} \quad \text{CO}_2\text{Me} \end{array}
$$

$$
\text{disproportionation} \quad \begin{array}{c} \text{H} \quad \text{Ph} \\ \text{C} = \text{C} \\ \text{H} \quad \text{CO}_2\text{Me} \end{array} + \text{PhMeC(H)CO}_2\text{Me} \quad (5.7)
$$

34
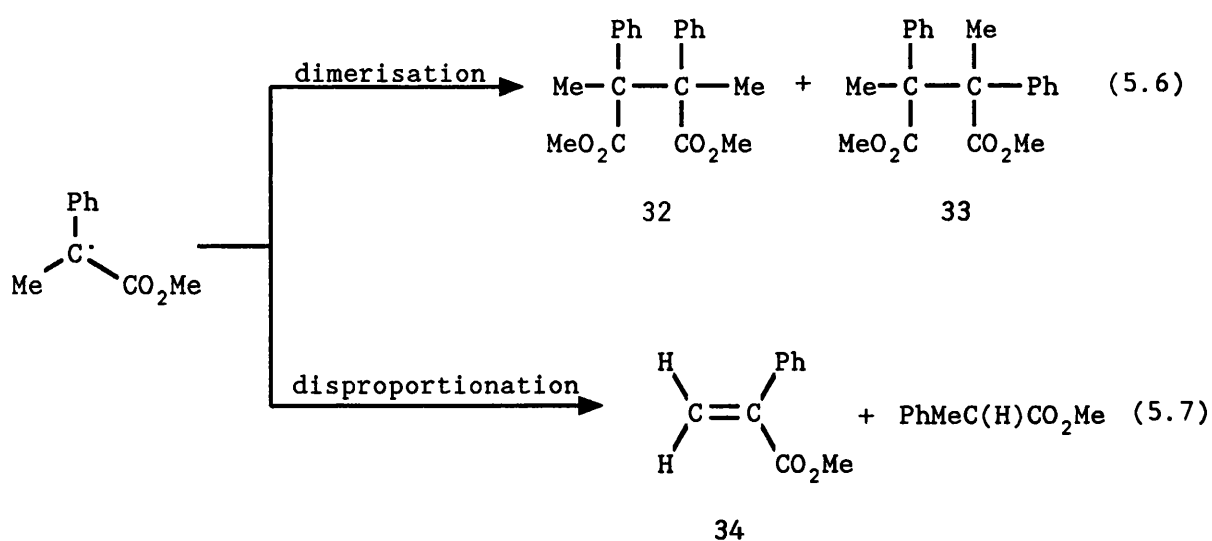
fate of the α-carbonylalkyl radical **30** is important since, if efficient kinetic resolution is to be achieved, the major route for its

(S)-ester   (R)-ester

2.9   2.7 ppm

30 % e.e.

3.6   3.3 ppm

29 % e.e.

3.1   2.9 ppm

$$(\pm)- \quad Ph—\overset{\overset{\displaystyle H}{|}}{\underset{\underset{\displaystyle Me}{|}}{C}}—CO_2Me$$

29
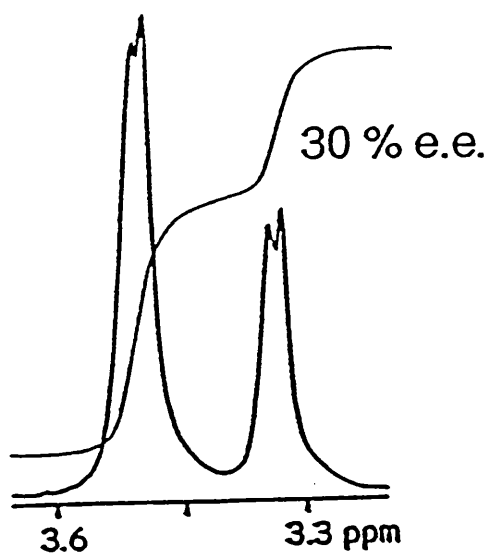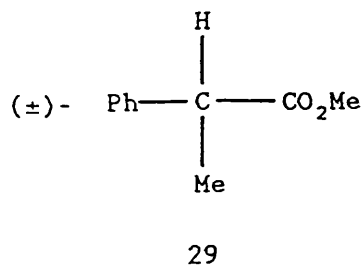
[d]IpcC catalyst, 190 K

55% ester consumed

$k_R/k_S = 2.2$
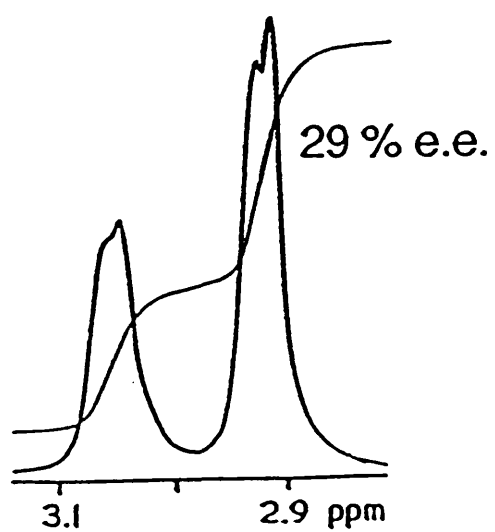
[l]IpcC catalyst, 190 K

53% ester consumed

$k_S/k_R = 2.2$

Figure 5.5

Figure Caption

Figure 5.5

400 MHz ^{1}H NMR spectra in the C-methyl region obtained from methyl 2-phenylpropanoate **29** in CDCl$_3$ in the presence of Eu(hfc)$_3$ (*ca.* 0.2 molar equivalents). (a) From racemic ester. (b) From residual ester after UV irradiation with DTBP and ^{d}IpcC **2** prepared from (1R)-(+)-α-pinene. (c) As (b), but ^{l}IpcC **8** prepared from (1S)-(-)-α-pinene was used in place of **2**.

decay must not be by abstraction of hydrogen to regenerate racemic ester.

A control experiment using authentic (R)-29, which is 97% enantiomerically pure as judged by ^{1}H NMR in the presence of Eu(hfc)$_3$, was carried out to ascertain the fate of the radical 30. Using the same experimental conditions as for the kinetic resolution of racemic 29 with ^{d}IpcC catalyst, 60% of the ester was consumed and the residual ester contained 15% of the (S)-enantiomer. Since the (S)-ester is the slower reacting enantiomer towards the radical 25 derived from ^{d}IpcC, this experiment has the best chance of detecting enantiomer interconversion under the conditions of kinetic resolution. Clearly some racemisation does take place and hence, the value of s obtained using equation (5.5) will be a lower limit. H-atom transfer to the α-carbonylalkyl radical would not cause a problem if this radical were to be trapped rapidly in another type of reaction, for example by addition to a CC double bond.[26]

The temperature dependence of s should be described by the Arrhenius equation (5.8), in which E is the activation energy, A is the pre-exponential factor and T is the absolute temperature. The

$$s = (k_A/k_B) = (A_A/A_B) \exp(E_B-E_A)/RT \qquad (5.8)$$

value of s would be expected to increase with decreasing temperature and the activation energy difference (E_B-E_A) can be determined from the temperature dependence of s. However, more accurate measurements of s over a wider range of temperatures and using a more quantitative technique[27] (see Chapter 7) than that employed here would be required to determine (A_A/A_B) and (E_B-E_A) separately. If (A_A/A_B) is taken to be unity, then s values of 2-20 at 198 K correspond to activation energy differences (E_B-E_A) of 1.1-4.9 kJmol^{-1}.

If a kinetic resolution is to yield useful quantities of substrate with a high ee, the value of s must be $ca.$ 5 or greater.[21,22] When optically active isopinocampheylborane or its derivatives hydroborate prochiral alkenes, the extent of asymmetric induction is sensitive to the steric requirement of the substituent at the 2-position of the apopinocampheyl group, although the effects are not large.[12] For example,[5] hydroboration of a series of trans and trisubstituted alkenes with $EapBH_2$, followed by oxidation of the intermediate organoborane, produces the corresponding alcohols with significantly improved enantiomeric purities over those realised with $IpcBH_2$ under the same conditions. Similarly, reductions of prochiral ketones by lithium B-alkyl-9-borabicyclo[3.3.1]nonyl hydrides 35 or by the chiral dialkyl(chloro)-boranes 36 and 37 generally proceed

35   R = Me
     R = $CH_2CH_2OCH_2Ph$
     R = Et

36

37
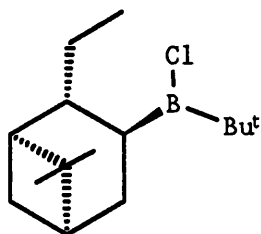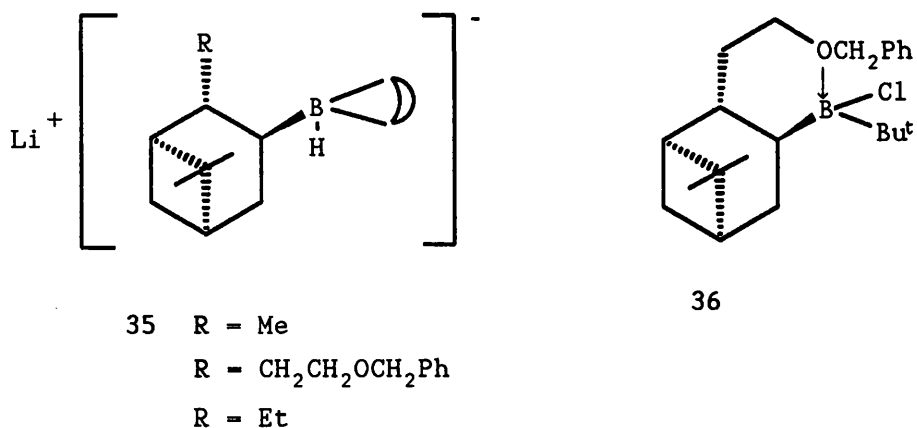
with a greater degree of asymmetric induction when the B-alkyl group is Eap (35, R = Et) or Beap (35, R = $CH_2CH_2OCH_2Ph$) than when it is

Ipc (**35**, R = Me). The next stage of the project was, therefore, to investigate the effect of replacing the Me group at the 2-position of the pinene moiety with more bulky substituents. It was found that, using the amine-boranes **9-11** in place of IpcC as catalyst has an effect on the enantioselectivity of H-atom abstraction similar to that found for the non-radical processes discussed above (Table **5.1**, entries 2-6).

Other esters **38-46** [the (4*S*,5*S*) enantiomer is shown for **46**]

Ph—C—CO$_2$R with H above and Me below

29; R = Me
38; R = Et
39; R = Bu^t

Bu^i—(ring)—C—CO$_2$Me with H above and Me below

40

41 (F-biphenyl)—C—CO$_2$Me with H above and Me below

CO$_2$Me
Me—C—H
(naphthyl)

42

Ph—C—CO$_2$Me with H above and Et below

43

Ph—C—CO$_2$Me with H above and Bu^t below

44

Ph—C—CH$_2$-CO$_2$Me with H above and Me below

45

MeO$_2$C / MeO$_2$C dioxolane ring
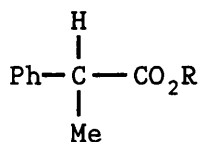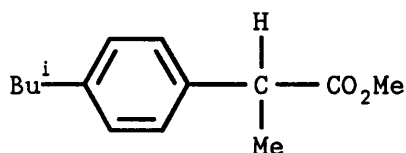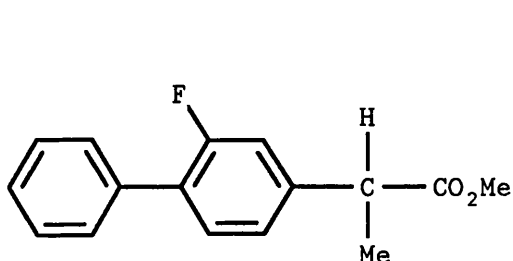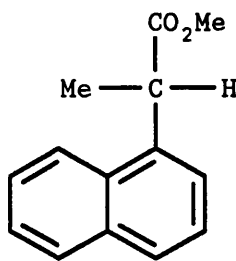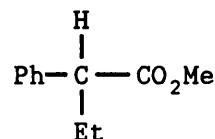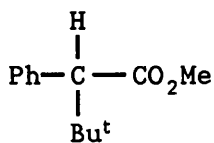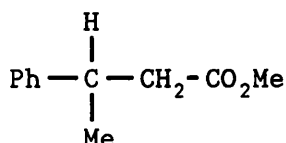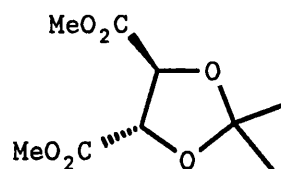
46

were then examined in an initial attempt to identify some of the factors which influence the enantioselectivity of α-H-atom abstraction by chiral amine-boryl radicals. Typically, samples consisted of the racemic substrate (*ca.* 0.8 *M*), DTBP (*ca.* 28% v/v),

Table **5.1**: Results from representative kinetic resolutions of racemic esters in oxirane

Entry	Substrate	Catalyst	Temp/K	Irradiation time[a]	Substrate consumption (%)	More reactive enantiomer	Ee of residual substrate (%)[b]	s[c]
1	29	^{d}IpcC	190	5 h	41.0	R	22.0 (S)	2.4
2	29	^{d}IpcC	206	5 h	54.5	R	30.2 (S)	2.2
3	29	^{l}IpcC	206	5 h	52.9	S	28.5 (R)	2.2
4	29	^{l}EapC	196	5 h	14.7	S	10.4 (R)	4.5
5	29	^{l}MeapC	196	5 h	41.3	S	22.0 (R)	2.3
6.	29	^{l}BeapC	196	5 h	25.4	S	17.8 (R)	3.8
7	38	^{d}IpcC	196	5 h	49.3	d	27.4	2.3
8	39	^{d}IpcC	196	5 h	29.1	d	22.5	4.2
9	40	^{d}IpcC	201	5 h	46.5	R	23.2 (S)	2.1
10	40	^{l}IpcC	201	5 h	48.9	S	27.7 (R)	2.3
11	40	^{l}BeapC	196	5 h	21.9	S	8.8 (R)	2.1
12	41	^{d}IpcC	201	5 h	48.6	R	17.8 (S)	1.7
13	41	^{l}BeapC	201	5 h	33.5	S	17.2 (R)	2.4
14	42	^{d}IpcC	196	5 h	14.7	d	4.0	1.7
15	43	^{d}IpcC	196	5 h	10.5	R	7.0 (S)	4.2
16	43	^{l}IpcC	196	5 h	18.2	S	14.3 (R)	5.3
17	45	^{d}IpcC	201	5 h	48.4	S	12.7 (R)	1.5
18	45	^{l}IpcC	196	5 h	50.8	R	10.5 (S)	1.3
19	46	^{d}IpcC	183	15 min	42.8	S,S	58.4 (R,R)	14.6
20	46	^{l}IpcC	183	15 min	47.0	R,R	64.5 (S,S)	12.0
21	46	^{d}IpcC	183	25 min	75.0	S,S	96.6 (R,R)	(6.7)[e]

a With the aromatic substrates **29** and **38-45**, the sample developed a pronounced yellow colouration during irradiation; this resulted in unproductive light absorption and necessitated the long irradiation times.
b Enantiomer present in excess shown in parentheses.
c Calculated using equation (5.5).
d Not determined.
e Under these experimental conditions, the value of s calculated from C and EE will be a gross underestimate.

amine-borane catalyst (*ca.* 0.15 *M*) and t-butylbenzene (0.5 *M*) in oxirane solvent. The results of representative kinetic resolutions are summarised in Table **5.1**.

With IpcC catalyst, increasing the bulk of the *O*-alkyl group in the 2-phenylpropanoate esters from Me in **29** to Bu^t in **39** causes *s* to increase from 2.2 to 4.2, approaching the critical value 5 required for efficient kinetic resolution.

2-(4-Isobutylphenyl)propanoic acid is the well-known anti-inflammatory drug Ibuprofen[28] and its methyl ester **40** showed a value of *s* similar to that obtained for the unsubstituted compound. With ^{d}IpcC catalyst, the methyl ester of Flurobiprofen™ **41** showed a lower value of *s* than **29**, but the enantioselectivity was increased when ^{l}BeapC was used. Exchanging the phenyl group in **29** for a 1-naphthyl group (compound **42**) caused a small decrease in *s*. Increasing the bulk of the α-alkyl group from Me in **29** to Et in **38** resulted in a significant increase in *s*, but the photochemical reaction became very sluggish and only a low conversion was achieved. This could be because H-atom abstraction is retarded by the more bulky ethyl group and/or because the α-carbonylalkyl radicals produced undergo predominant disproportionation,[23] rather than combination as in the case of the α-methyl analogue.[23-25] In addition to regenerating racemic substrate, disproportionation would give the unsaturated ester **34**, to which amine-boryl radicals would add very readily because of favourable polar effects.[29] The α-t-butyl analogue **44** did not react under the normal conditions and this must be the result of steric hindrance to H-atom abstraction by the amine-boryl radical; disproportionation of the derived α-carbonylalkyl radical is not now possible.

Amine-boryl radicals abstract hydrogen only from the α-carbon atom of methyl 3-phenylbutanoate **45** as judged by ESR spectroscopy.* The α-hydrogen atoms are diastereotopic and non-equivalent in **45**; the asymmetric centre is retained in the derived radical **47** and its

$$Ph-\underset{\underset{Me}{|}}{\overset{\overset{H}{|}}{C}}-\overset{\overset{H}{\diagup}}{\underset{\diagdown}{C}}{\diagdown\atop CO_2Me}$$
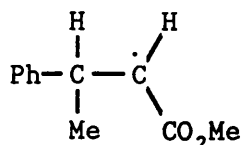
47

reaction products will be optically active if the initial H-atom abstraction is enantioselective. Considering that abstraction takes place from the carbon   adjacent to the asymmetric centre, the value of *s* is encouragingly large.

α-Hydrogen-atom abstraction from the isopropylidene tartrate **46** takes place with high enantioselectivity (entries 19 and 20) and in an experiment when 75% of the tartrate was consumed (entry 21), the ee of the residual ester was 97%. The lower value of *s* obtained from the latter data is not surprising considering the sensitivity of *s* to *C* and *EE* when *s* is relatively large and the fact that *C* and *EE* provide only an indirect measure of *s* using equation (5.5).

A control experiment was carried out to assess the extent of racemisation of **46** under the reaction conditions. Using (4*S*,5*S*)-**46**, which is more reactive than the (4*R*,5*R*)-enantiomer towards the

* The ESR spectrum of **47** shows $a(1H_{\alpha})$ 20.4, $a(1H_{\beta})$ 9.8 G and *g* 2.0034 at 208 K in cyclopropane; further splittings arising from long-range hyperfine coupling were observed and distortions indicated the probable presence of two rotameric forms.

amine-boryl radical **25** derived from ^{d}IpcC, after 20 min irradiation at 183 K under the usual conditions, 51% of the ester had been consumed. The residual ester contained a barely-detectable amount (<0.3%) of the (4R,5R)-enantiomer; its absence is understandable since its formation requires inversion at both asymmetric centres, which would have to take place *via* the intermediacy of the *cis*-(*meso*)-isomer.[27]

Although the spirocyclic amine-borane **15** is a good polarity reversal catalyst (as mentioned previously), its ability to induce enantioselective H-atom abstraction is poor (see Table **5.2**). As with IpcC catalyst, increasing the bulk of the *O*-alkyl in the 2-phenylpropanoate esters from Me in **29** to Et in **43** causes *s* to increase, although the effect is not as large.

Table **5.2**

Kinetic resolutions of racemic esters using the spirocyclic amine-borane **15** in toluene.[a]

Entry	Substrate	Substrate consumption (%)	More reactive enantiomer	Ee of residual substrate (%)[b]	s^c
1	29	64.1	R	4.6 (S)	1.1
2	40	61.7	R	7.9 (S)	1.2
3	43	34.6	R	8.1 (S)	1.5
4	45	59.4	S	18.0 (R)	1.5

a Concentration of catalyst is *ca.* 0.3 *M*. All samples were irradiated at 196 K for 5 h. *b* Enantiomer present in excess shown in parentheses. *c* Calculated using equation (5.5).

5.3 Model for Enantioselective Hydrogen-atom Abstraction

It is clearly important to develop a transition state model which will account for the absolute stereochemical course of enantioselective H-atom transfer. For steric and electronic reasons, it is likely that abstraction of hydrogen from four coordinate carbon by an amine-boryl radical will proceed through a transition state in which the preferred geometry of the B···H···C fragment is near-to linear, although distortion from the optimum angle would not be expected to result in a large increase in activation energy.[30]

If long-range torsional/steric interactions between the substituents on the boron and carbon atoms are dominant in determining the preferred transition state conformation, the latter should be of the staggered type **48**, in which the symbols L, M and S refer to substituents of large, medium and small effective bulk.
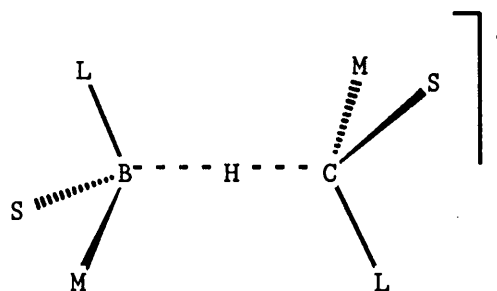
48

If we define *steric chirality*, by analogy with the Cahn-Ingold-Prelog[31] conventions for describing absolute stereochemistry, using the priority sequence L > M > S, then a boron centre of steric chirality **49a** (ρ) will give a lower-energy transition state when associated with a carbon-centre of steric chirality **49b** (σ) than with a centre of steric chirality ρ (E = B or C).
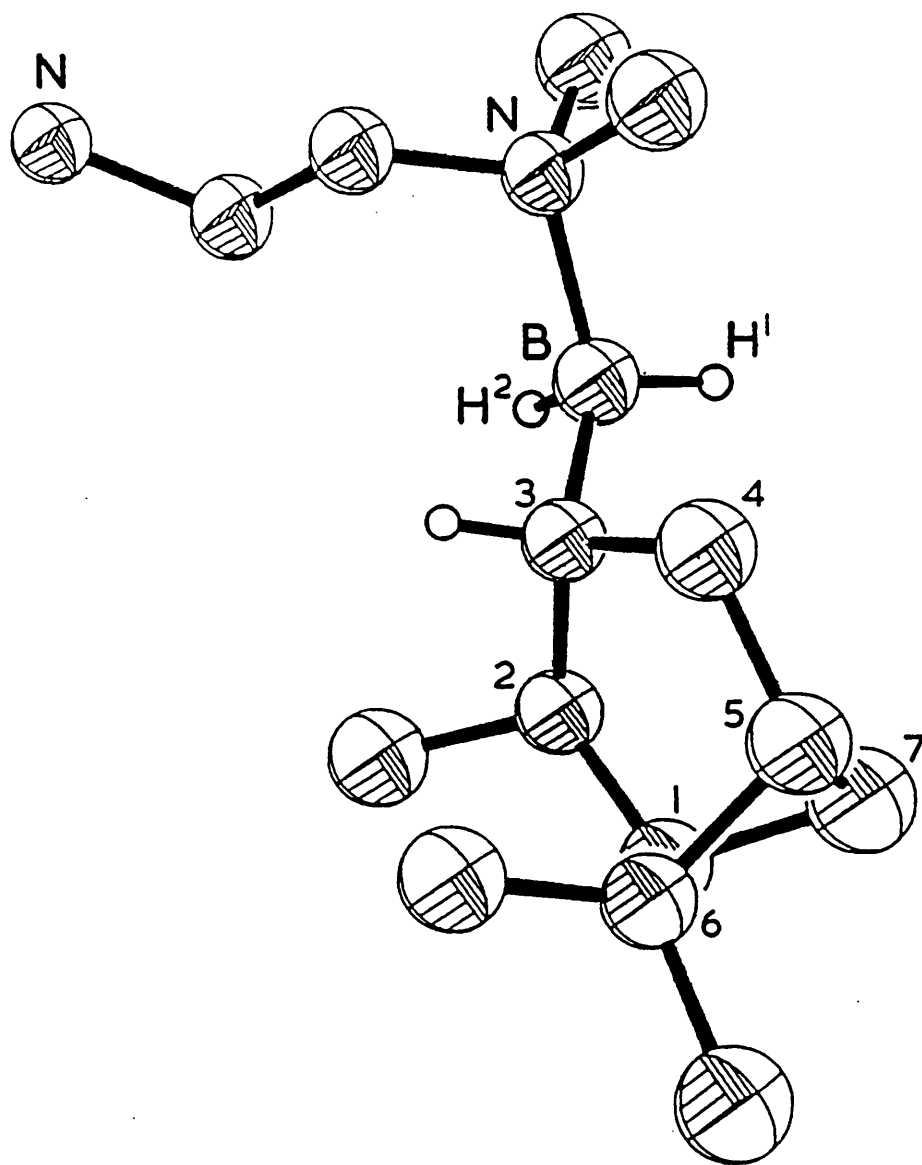
Figure 5.6 Partial structure of ^{d}IpcC in the crystal, drawn using the coordinates given in ref. 15.

Inspection of the crystal structure determined for [d]IpcC by Soderquist. et al.[15] and shown partially in Figure **5.6**, suggests that the hydrogen atom being transferred from C to B will be in a position similar to that occupied by H[1], rather than that occupied by the more sterically encumbered H[2]. Thus, the configuration at the

49a (ρ)   49b (σ)
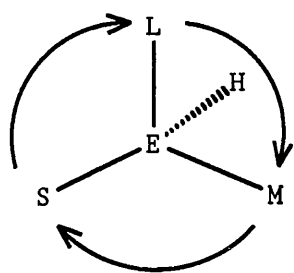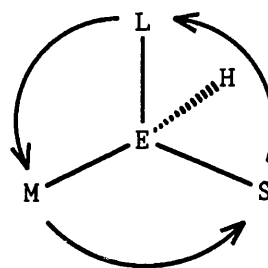
boron-centre in the transition state for abstraction catalysed by this enantiomer of the amine-borane will be σ, as shown in **50**. The preferred steric chirality at the carbo-centre will thus be ρ, as shown.
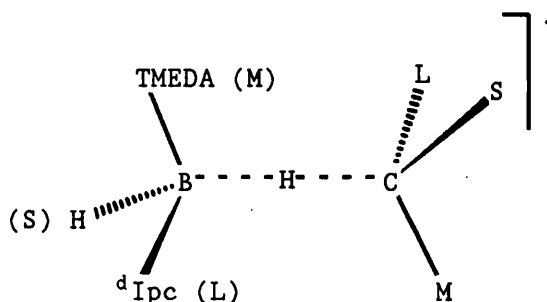
50

When assessing the effective bulk of substituents attached to carbon, stereoelectronic effects must be considered, since in the transition state carbonyl groups, alkoxy groups and aromatic rings will presumably adopt conformations in which overlap is optimised between their π systems and the nascent semi-occupied orbital on C_α.

For the rigid tartrate **46**, molecular models indicate that the (4S,5S) enantiomer possesses ρ steric chirality at C_α and thus this

Table **5.3**: Steric chiralities of substrate enantiomers which are the
more reactive towards the amine-boryl radical derived from ^{d}IpcC

Substrate	More reactive enantiomer	Steric chirality
29	R	ρ [a]
40	R	ρ [a]
43	R	ρ [a]
45	S	ρ [b]
46	S,S	ρ [c]

a Assuming substituent size CO_2Me > Ph, p-Bu^{i}C$_6$H$_4$ > Me, Et.

b See text.

c Assuming substituent size $C(H)(O-)CO_2Me$ > CO_2Me > $OC(O-)Me_2$.

enantiomer should react more rapidly than its antipode with the amine-boryl radical derived from ^{d}IpcC, in accord with experiment (see Table 5.3).

For many of the substrates resolved in this work it is not straightforward to decide on the steric chirality at C_α. If the assumptions are made that the effective C_α-substituent sizes in the transition state are CO_2Me > Ph, p-Bu^{i}C$_6$H$_4$ > Me, Et for the acyclic esters **29**, **40** and **43**, then the steric chiralities of the enantiomers which are found to react more rapidly with the amine-boryl radical derived from ^{d}IpcC will be those shown in Table **5.3**. These steric chiralities are all ρ, in accord with the predictions of the torsional-strain model.

For the ester **45** the preferred conformation about the C_α-C_β bond should be that shown in **51** for the (S)-enantiomer and this

51
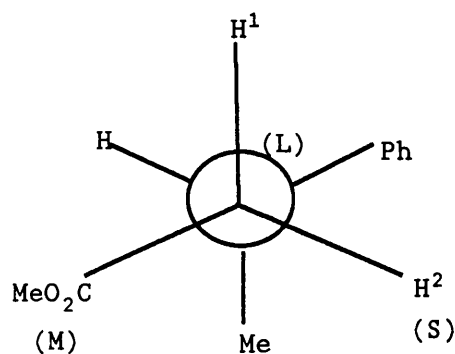
conclusion is consistent with the experimental values of $^3J_{HH}$ (8.3 and 6.9 Hz), although the conformational preference is evidently not large. On steric grounds, the more accessible H^1 should be abstracted more readily than H^2 and, assuming that the substituent sizes in the transition state are PhC(H)Me = L, MeO$_2$C = M and H = S, the steric chirality of **51** is ρ. Thus, the prediction of the torsional-strain model is that the (S)-enantiomer of **45** should react

more rapidly when ^{d}IpcC is the catalyst, as is observed by experiment (see Table 5.3).

The low enantioselectivities observed with the catalyst **15** is probably due to the small difference in sizes of the pinene and pyrrolidine substituents attached to the radical centre in **19**, which reduces the preference for a particular transition state conformation.

References to Chapter 5

1. H. C. Brown, J. R. Schwier and B. Singaram, *J. Org. Chem.*, 1978, **43**, 4395.

2. B. Singaram and J. R. Schwier, *J. Organomet. Chem.*, 1978, **156**, C1.

3. H. C. Brown, B. Singaram and J. R. Schwier, *Inorg. Chem.*, 1979, **18**, 51.

4. A. K. Mandal, P. K. Jadhav and H. C. Brown, *J. Org. Chem.*, 1980, **45**, 3543.

5. H. C. Brown, R. S. Randad, K. S. Bhat, M, Zaidlewicz, S. A. Weissman, P. K. Jadhav and P. T. Perumal, *J. Org. Chem.*, 1988, **53**, 5513.

6. P. V. Ramachandran, H. C. Brown and S. Swaminathan, *Tetrahedron Asymmetry*, 1990, **1**, 433.

7. H. C. Brown, P. V. Ramachandran, S. A. Weissman and S. Swaminathan, *J. Org. Chem.*, 1990, **55**, 6328.

8. M. M. Midland and A. Kazubski, *J. Org. Chem.*, 1982, **47**, 2495.

9. M. M. Midland and A. Kazubski, *J. Org. Chem.*, 1982, **47**, 2814.

10. H. C. Brown and P. V. Ramachandran, *J. Org. Chem.*, 1989, **54**, 4504.

11. C. S. Shiner, C. M. Garner and R. C. Haltiwanger, *J. Am. Chem. Soc.*, 1985, **107**, 7167.

12. H. C. Brown and B. Singaram, *Acc. Chem. Res.*, 1988, **21**, 287.

13. H. C. Brown and P. V. Ramachandran, *Acc. Chem. Res.*, 1992, **25**, 16.

14. N. N. Joshi, M. Srebnik and H. C. Brown, *J. Am. Chem. Soc.*, 1988, **110**, 6246.

15. J. A. Soderquist, S.-J. Hwang-Lee and C. L. Barnes, *Tetrahedron Lett.*, 1988, **29**, 3385.

16. H. C. Brown, W. S. Park and B. T. Cho, *Bull. Korean Chem. Soc.*, 1987, **8**, 276.

17. C. F. Lane, *J. Org. Chem.*, 1974, **39**, 1437.

18. J. A. Dale, D. L. Dull and H. S. Mosher, *J. Org. Chem.*, 1969, **34**, 2543.   J. A. Dale and H. S. Mosher, *J. Am. Chem. Soc.*, 1973, **95**, 512.

19. D. E. Ward and C. K. Rhee, *Tetrahedron Lett.*, 1991, **32**, 7165.

20. P. Kaushal, P. L. H. Mok and B. P. Roberts, *J. Chem. Soc., Perkin Trans 2*, 1990, 1663.

21. V. S. Martin, S. S. Woodard, T. Katsuki, Y. Yamada, M. Ikeda and K. B. Sharpless, *J. Am. Chem. Soc.*, 1981, **103**, 6237.

22. H. B. Kagan and J. C. Fiaud, *Topics Stereochem.*, 1988 **18**, 249.

23. C. T. Ng, X. Wang and T. -Y. Luh, *J. Org. Chem.*, 1988, **53**, 2536.

24. C. deLuca, A. Inesi and L. Rampazzo, *J. Chem. Soc., Perkin Trans. 2*, 1982, 1403.

25. F. Xi, P. Lillya, W. Bassett jr. and O. Vogl, *Monatsh Chem.*, 1985, **116**, 401.

26. H. -S. Dang and B. P. Roberts, *Tetrahedron Lett.*, 1992, **33**, 4621 and 6169.

27. P. L. H. Mok and B. P. Roberts, *Tetrahedron Lett.*, 1992, in the press.

28 C. Giordano, G. Castaldi and F. Uggeri, *Angew. Chem., Int. Ed. Engl.*, 1984, **23**, 413.

29. V. Diart and B. P. Roberts, *J. Chem. Soc., Perkin Trans. 2*, 1992, 1761.

30. G. L. Fox and H. B. Schlegel, *J. Phys. Chem.*, 1992, **96**, 298.   L.

Pardo, J. R. Banfelder and R. Osman, *J. Am. Chem. Soc.*, 1992, **114**, 2382. X. L. Huang and J. J. Danenberg, *J. Org. Chem.*, 1991, **56**, 5421. A. Dorigo and K. N. Houk, *J. Org. Chem.*, 1988, **53**, 1650.

31. R. S. Cahn, C. K. Ingold and V. Prelog, *Angew. Chem.*, *Int. Ed. Engl.*, 1966, **5**, 385.

CHAPTER 6

EXPERIMENTAL

6.1 ESR Spectroscopy

The techniques used to obtain ESR spectra from samples in fluid solution were those described in Chapter 3. The experimental details, including the method for measuring hyperfine coupling constants and g-values are described in Chapter 9.

6.2 NMR Spectroscopy

^{1}H, ^{11}B, and ^{19}F NMR spectra were recorded using Varian XL-200 or VXR-400 instruments, with $BF_3.OEt_2$ (^{11}B), trifluoroacetic acid (^{19}F) external or tetramethylsilane (^{1}H) internal standards; J-values are quoted in Hz. Spectra of ^{d}IpcC, ^{1}IpcC, ^{1}EapC, ^{1}MeapC and ^{1}BeapC were recorded immediately after preparation of the solutions.

6.3 Gas Liquid Chromatography Analyses

GLC analyses were carried out using a Pye-Unicam 204 chromatograph equipped with a flame-ionisation detector and a Pye-Unicam model DP 88 integrator. A glass column (2 m x 1/8 in) packed with 10% OV-101 on Chromosorb WHP 80-100 mesh with nitrogen carrier gas.

6.4 High-Performance Liquid Chromatography

HPLC analyses were carried out using a Gilson 305 instrument in conjunction with a UV (254 nm) detector. The achiral stationary phase was Nucleosil 5 μm silica gel (analytical and preparative) and Chiralcel OD (Daicel Chemical Industries) was used to effect analytical separation of enantiomers. Peaks were integrated using a Hewlett-Packard 3390A integrator. The mobile phases were hexane-ethyl acetate mixtures (achiral) or hexane-isopropyl alcohol mixtures (Chiralcel OD).

6.5 Column Chromatography and TLC

Column chromatography and TLC were carried out using Merck Kieselgel 60 (230-400 mesh) and Kieselgel 60 F_{254} aluminium-backed pre-coated plates, respectively. Light petroleum refers to petroleum ether b.p. 60-80 °C.

6.6 Optical Rotation Measurements

Optical rotations were determined at 589 nm (sodium D line) with an Optical Activity AA-10 automatic digital polarimeter using a 1 dm pathlength cell.

6.7 Differential Scanning Calorimetry

DSC analyses were carried out using a Perkin-Elmer DSC-7 instrument. Samples were heated at 10.0 °C min^{-1}. I am grateful to

Ms. M. Odlyha for carrying out the DSC analyses.

6.8 Materials

All preparations and handling of boron-containing compounds were carried out under an atmosphere of dry argon. All solvents were dried by conventional methods. t-Butylbenzene and TMEDA were distilled from calcium hydride. BMS (10 M solution in excess Me_2S), boron trifluoride-methanol complex (50 wt.% BF_3 in excess methanol), (+)-Eu(hfc)$_3$, (R)-(+)-2-methoxy-2-phenyl-3,3,3-trifluoropropanoic acid (Mosher's acid) (all Aldrich), oxirane (Fluka), and cyclopropane (Union Carbide) were used as received. The sources and enantiomeric compositions of the pinenes used in this project are given in Table 6.1. Nopol methyl ether was prepared by Ms P. T. McKetty. Compound numbers correspond to those in Chapter 5. Racemic and (R)-methyl 2-phenylbutanoate were prepared by Ms. P. T. McKetty from commerically obtained acids (Aldrich) by the method used for the preparation of **29** (see below). The esters **42**[1] and **44** were prepared by Mr. C. J. Cooksey. Compound **44** was obtained by esterification of 3,3-dimethyl-2-phenylbutanoic acid.[2,3] The ester **42** was prepared by treatment of methyl 1-naphthylacetate with lithium di-isopropylamide in THF, followed by quenching of the enolate with methyl iodide. The (4S,5S) enantiomer of the isopropylidene tartrate **46** and its antipode were obtained from Fluka Chemicals. Trimethylamine-n-butylborane **23** was prepared by the method of Hawthorne.[4]

Table **6.1**

Properties of pinenes

Pinene	Source or reference to preparation	B.p./°C (Torr)[a]	$[\alpha]^{20}_D$	$[\alpha]^T_D$ for enantiomerically pure pinene (T/°C)	ee (%)
1	Aldrich	40-41 (10)	+ 51.1° (neat)	+ 51.1° (20)[b] (neat)	> 99
3	Aldrich	40 (10)	- 51.1° (neat)	- 51.3° (20)[b] (neat)	> 99
4	c	48 (5.5)	- 43.8° (neat)	- 46.6° (23)[c] (neat)	94
5	d	60-64 (0.2)	- 32.4° (neat)	- 35.1° (26)[d] (neat)	92
6	Aldrich	105-110 (0.01)	- 26.6° (c=10, CHCl₃)	- 29.8° (20)[e] (c=10, CHCl₃)	89
7	Aldrich	83-84 (1.5)	- 36.4° (neat)	- 40.1° (20)[f] (neat)	91

a   All the pinenes [except (1S)-(-)-nopol **7**] were distilled from calcium hydride.   b   F. H. Thurber and R. C. Thielke, *J. Am. Chem. Soc.*, 1931, **53**, 1030.   c   H. C. Brown, R. S. Randad, K. S. Bhat, M. Zaidlewicz, S. A. Weissman, P. K. Jadhav and P. T. Perumal, *J. Org. Chem.*, 1988, **53**, 5513.   d   C. S. Shiner, C. M. Garner and R. C. Haltiwanger, *J. Am. Chem. Soc.*, 1985, **107**, 7167.   e   H. C. Brown and P. V. Ramachandran, *J. Org. Chem.*, 1989, **54**, 4504.   f   M. M. Midland and A. Kazubski, *J. Org. Chem.*, 1982, **47**, 2814.

6.8.1 Racemic Methyl 2-Phenylpropanoate 29

A solution of racemic 2-phenylpropanoic acid (Aldrich) (9.97g, 66.4 mmol), boron trifluoride-methanol complex (15.0 cm^3, 180.7 mmol),[5] and methanol (70 cm^3) was heated under reflux for 8 h under argon. Methanol was then removed by rotary evaporation. The residue was taken up in diethyl ether (150 cm^3), washed with saturated aqueous sodium hydrogen carbonate (4 x 100 cm^3), saturated aqueous sodium chloride (3 x 80 cm^3) and dried (MgSO$_4$ and K$_2$CO$_3$). Ether was removed under reduced pressure and the residue was distilled to yield 8.3 g (76%) of 29, b.p. 62-65 °C/2.9 Torr (lit.[6] b.p. 98-100 °C/12 Torr). δ(^{1}H)(CDCl$_3$) 1.50 (d, 3H, J 7.1, CMe), 3.66 (s, 3H, CO$_2$Me), 3.73 (q, 1H, J 7.2, HCMe), 7.31 (m, 5H, Ph).

6.8.2 Racemic Methyl 3-Phenylbutanoate 45

This was prepared from racemic 3-phenylbutanoic acid (Fluka) by the method used for 29; b.p. 50 °C/0.1 Torr (lit.[7] b.p. 120-122 °C/15 Torr). δ(^{1}H)(CDCl$_3$) 1.30 (d, 3H, J 6.8, CHMe), 2.55 (dd, 1H, J_{AB} 15.2, J_{AX} 8.3, CH^{A}H^{B}CO$_2$Me), 2.63 (dd, 1H, J_{AB} 15.2, J_{BX} 6.9, CH^{A}H^{B}CO$_2$Me), 3.28 (m, 1H, J 8.0, CHCH$_2$), 3.62 (s, 3H, CO$_2$Me), 7.18-7.32 (m, 5H, Ph).

6.8.3 Racemic Methyl 2-(4-Isobutylphenyl)propanoate 40

This was prepared from racemic 2-(4-isobutylphenyl)propanoic acid (Sigma) by the same method as 29; b.p. 82-86 °C/0.1 Torr (lit.[8] b.p. 110-130 °C/2 Torr). δ(^{1}H)(CDCl$_3$) 0.89 (d, 6H, J 6.8, CHMe$_2$),

1.48 (d, 3H, J 7.2, PhC$\underline{Me}$), 1.84 (m, 1H, J 6.8, C$\underline{H}$Me$_2$), 2.44 (d, 2H, J 6.8, C$\underline{H}_2$CMe$_2$), 3.64 (s, 3H, CO$_2$Me), 3.69 (q, 1H, J 7.2, C$\underline{H}$CO$_2$Me), 7.09, 7.19 (AB quartet, 4H, J_{AB} 8.0).

6.8.4 Racemic Flurbiprofen[TM] Methyl Ester 41

This was prepared from racemic Flurbiprofen, which was a gift from Dr. J. W. Cooper, using the same method as for 29; b.p. 126-130 °C/0.015 Torr, m.p. 46-47 °C. δ(^{1}H)(CDCl$_3$) 1.52 (d, 3H, J 7.2, CH$\underline{Me}$), 3.68 (s, 3H, CO$_2$Me), 3.76 (q, 1H, J 8.0, C$\underline{H}$Me), 7.10-7.54 (m, 8H).

6.8.5 Racemic Ethyl 2-Phenylpropanoate 38

This ester was obtained by esterification of the acid with ethanol in the presence of concentrated sulfuric acid; b.p. 86 °C/4 Torr (lit.[9] b.p. 107-110 °C/13 Torr). δ(^{1}H)(CDCl$_3$) 1.11 (t, 3H, J 6.8, CO$_2$CH$_2$$\underline{Me}$), 1.46 (d, 3H, J 7.9, PhC$\underline{Me}$), 3.67 (q, 1H, J 7.3, PhC$\underline{H}$), 4.06 (q, 2H, J 6.8, CO$_2$CH$_2$), 7.23 (m, Ph).

6.8.6 Racemic t-Butyl 2-Phenylpropanoate 39

Thionyl chloride (9.9 cm^3, 136 mmol) was added dropwise during 25 min to a stirred solution of racemic 2-phenylpropanoic acid (12.87 g, 85.7 mmol) at room temperature. The mixture was further stirred for 0.5 h, heated under reflux for 1 h, and distilled to yield 11.7 g (81%) of 2-phenylpropanoyl chloride, b.p. 55-58 °C/0.95 Torr (lit.[10] 100-101 °C/13 Torr). δ(^{1}H)(CDCl$_3$) 1.59 (d, 3H, J 6.9, CH$\underline{Me}$), 4.11

(q, 1H, J 6.9, C<u>H</u>Me), 7.33 (m, 5H, Ph).

A solution of t-butyl alcohol (4.92 g, 66.3 mmol) and triethylamine (9.8 cm^3, 70 mmol) in diethyl ether (40 cm^3) was heated under gentle reflux and racemic 2-phenylpropanoyl chloride (11.2 g, 66.3 mmol) in diethyl ether (25 cm^3) was added dropwise to the solution. After the addition was complete, the mixture was heated under reflux for a further 2.5 h and then cooled to room temperature. Water (70 cm^3) was added dropwise with stirring and the stirring was continued until all the precipitate had dissolved. The ether layer was separated and washed with cold 10% aqueous sulfuric acid (200 cm^3) until the acid extract did not become cloudy when rendered alkaline with sodium hydroxide solution. It was then washed with saturated aqueous sodium hydrogen carbonate (2 x 50 cm^3) and dried (Na$_2$SO$_4$ and K$_2$CO$_3$). Ether was removed under reduced pressure and the residual oil was distilled to yield 8.0 g (59%) of **39**, b.p. 60-64 °C/0.02 Torr. Found: C, 75.89; H, 8.82. C$_{13}$H$_{18}$O$_2$ requires C, 75.69; H, 8.80%. δ(^{1}H)(CDCl$_3$) 1.39 (s, 9H, CMe$_3$), 1.45 (d, 3H, J 7.1, CH<u>Me</u>), 3.61 (q, 1H, J 7.1, C<u>H</u>Me), 7.30 (m, 5H, Ph).

6.8.7 Optically Active Esters

Authentic samples of optically active esters were prepared from (R)-(-)-2-phenylpropanoic (Aldrich) and (S)-(+)-3-phenylbutanoic (Fluka) acids; (R)-(-)-2-(4-isobutylphenyl)propanoic acid and (S)-(+)-Flurbiprofen were gifts from Dr. J. W. Cooper. The esters were prepared as their racemic counterparts, but on a much smaller scale and were not purified by distillation. The methyl 2-phenylpropanoate so prepared contained a 94% ee of the

(*R*)-enantiomer.

6.8.8 Racemic Dimethyl 2,2-Dimethyl-1,3-dioxolane-*trans*-dicarboxylate 46

This was prepared from racemic tartaric acid and 2, 2-dimethoxypropane using the method of Carmack and Kelley;[11] b.p. 82-84 °C/0.17 Torr (lit.[11] b.p. 82-90 °C/0.02 Torr). $\delta(^1H)$(CDCl$_3$) 1.50 (s, 6H, CMe$_2$), 3.83 (s, 6H, CO$_2$Me), 4.82 (s, 2H, C$\underline{H}$CO$_2$Me). After distillation, the ester was pale yellow but the colour could be removed by column chromatography using light petroleum/diethyl ether (3:1) as eluant.

6.8.9 *R*- and *S*-Alpine-Boramine™ (^{d}IpcC 2 and ^{1}IpcC 8)

The amine-borane ^{d}IpcC$^{12-15}$ was prepared as described in the literature from (1*R*)-(+)-α-pinene; m.p. 120-145 °C dec. (lit.$^{12-15}$ m.p. 140-141 °C). Found: C, 75.07; H, 13.19; N, 6.74. C$_{26}$H$_{54}$B$_2$N$_2$ requires C, 75.01; H, 13.07; N, 6.73%. $\delta(^1H)$(CDCl$_3$) 0.66 (broad m, 2H, C$\underline{H}$B), 0.78 (d, 2H, *J* 9.0), 1.00 (d, 6H, *J* 7.1, C^{2}Me), 1.09 (s, 6H, C$\underline{Me}^A$Me^B), 1.16 (s, 6H, CMe^A$\underline{Me}^B$), 1.56 (m, 2H), 1.73 (m, 2H), 1.83 (m, 4H), 2.08 (m, 2H), 2.20 (m, 2H), 2.60 (s, 6H, NMe^A), 2.63 (s, 6H, NMe^B), 3.20 (m, 4H, CH$_2$N). $\delta(^{13}C)$(CDCl$_3$) 22.7 (C^6$\underline{C}$H$_3{}^A$), 22.8 (C^6$\underline{C}$H$_3{}^B$), 25.2 (broad, $\underline{C}$B), 28.4 (C^2$\underline{C}$H$_3$), 34.1, 38.0, 38.9 (C^6), 42.2, 42.9, 48.6 (C^2), 50.8 (N$\underline{C}$H$_3{}^A$), 51.0 (N$\underline{C}$H$_3{}^B$), 57.2 (N$\underline{C}$H$_2$). $\delta(^{11}B)$(C$_6$H$_6$) 1.11 (broad s).

The complex ^{1}IpcC was prepared from (1*S*)-(-)-α-pinene in the same way as its antipode.

6.8.10 (1*S*)-2-Ethylapopinocampheylborane-TMEDA Complex ([1]EapC) 9

This was prepared using the method of Brown *et. al.*[16] A solution of (1*R*)-(-)-nopol (31.06 g, 187 mmol) in THF (80 cm³) was cooled to -78 °C. n-Butyllithium (122.5 cm³ of a 1.6 *M* solution in hexane, 196 mmol) was added dropwise and then the mixture was stirred for 1 h at -78 °C. *p*-Toluenesulfonyl chloride (35.70 g, 187 mmol) in THF (65 cm³) was added dropwise and the stirring was continued for another hour at -78 °C. The mixture was then warmed to room temperature and stirred for 2 h, during which time a thick paste (LiCl) was formed. The reaction mixture was poured into ice-water (*ca.* 400 cm³) and extracted with pentane (5 x 200 cm³). Removal of the solvent gave a yellow oil, which was redissolved in diethyl ether and dried (MgSO₄). Removal of the ether gave a solid residue which was recrystallised twice from pentane to give 34.0 g (56%) of nopol tosylate; m.p. 49-51 °C (lit.[16] m.p. 50-51 °C).

Lithium aluminium hydride (3.29 g, 86.7 mmol) was dissolved in diethyl ether (130 cm³) by stirring at room temperature. Nopol tosylate (21.4 g, 66.7 mmol) in ether (70 cm³) was added dropwise to the mixture at room temperature. After the addition was complete, the reaction mixture was heated to reflux for 8 h. It was then poured into ice-water (*ca.* 400 cm³) slowly with stirring. Sodium chloride was added and the mixture was filtered through Celite. The filtrate was saturated with more sodium chloride and extracted with ether (3 x 100 cm³). The combined organic layer was washed with 5% sulfuric acid (2 x 200 cm³), aqueous sodium hydrogen carbonate (3 x 200 cm³), brine (2 x 200 cm³), and dried (MgSO₄). After removal of the ether, the residual liquid was distilled from calcium hydride to

give 6.3 g (63%) of 2-ethylapopinene **4**, b.p. 48 °C/5.5 Torr (lit.[16] b.p. 88 °C/40 Torr). $[\alpha]^{20}_D$ -43.8°(neat).

A solution of BMS (1.56 cm^3, 15.6 mmol) in diethyl ether (9 cm^3) was heated to reflux. 2-Ethylapopinene (5.20 g, 34.6 mmol) was added dropwise with stirring and the reaction mixture was refluxed for a further 4 h. TMEDA (1.24 cm^3, 8.22 mmol) was added and the mixture was heated under reflux for another 0.5 h. The cooled reaction mixture was then filtered, the solid was washed on the sinter with cold ether (4 x 1 cm^3) and dried at room temperature under vacuum (0.01 Torr) to give 2.3 g (64%) of ^{1}EapC. The white solid was recrystallised from cyclohexane/toluene (2:1), m.p. 123-140 °C dec. (lit.[16] m.p. 138-141 °C). Found: C, 75.83; H, 12.98; N, 6.26. C$_{28}$H$_{58}$B$_2$N$_2$ requires C, 75.68; H, 13.15; N, 6.30%. $\delta(^1H)(CDCl_3)$ 0.64 (broad m, 2H, CHB), 0.78 (d, 2H, J 8.8), 0.84 (t, 6H, J 7.6, CH$_2$Me), 1.06 (s, 6H, CMe^{A}Me^B), 1.16 (s, 6H, CMe^{A}Me^B), 1.28 (m, 2H, CHEt), 1.40 (m, 4H, CH$_2$CH$_3$), 1.84 (m, 4H), 1.99 (m, 2H), 2.08 (m, 2H), 2.22 (m, 2H), 2.59 (s, 6H, NMe^A), 2.63 (s, 6H, NMe^B), 3.20 (m, 4H, CH$_2$N).

6.8.11 *N, N'*-Bis[(1*S*,2*R*,3*S*,5*S*)-iso-2-(2-methoxyethyl)apopino-campheylborane]-TMEDA Complex (^{1}MeapC) 10

A solution of BMS (2.6 cm^3, 26.0 mmol) in diethyl ether (15 cm^3) was heated to reflux. Nopol methyl ether (9.80 g, 54.4 mmol) was added dropwise and the reaction mixture was heated under reflux for 4 h. TMEDA (2.0 cm^3, 13.3 mmol) was added and the refluxing was continued for a further 1 h. The solution was then allowed to cool to room temperature before half of the volatiles were removed under

reduced pressure. Hexane (15 cm^3) was added and the reaction mixture was left at -20 °C to induce crystallisation. The white solid was then removed by filtration, washed with cold hexane (5 x 5 cm^3) and dried at room temperature under vacuum (0.01 Torr) to give 3.2 g (48%) of ^{1}MeapC. This was recrystallised from hexane/diethyl ether (2.5:1); m.p. 60-85 °C dec. Found: C, 71.25; H, 12.43; N, 5.29. C$_{30}$H$_{62}$B$_2$N$_2$O$_2$ requires C, 71.43; H, 12.39; N, 5.55%. δ(^{1}H)(CDCl$_3$) 0.69 (broad m, 2H, C$\underline{H}$B), 0.78 (d, 2H, J 8.8), 1.10 (s, 6H, C$\underline{Me}^A$Me^B), 1.16 (s, 6H, CMe$^A\underline{Me}^B$), 1.44 (m, 2H), 1.69 (m, 4H), 1.85 (m, 6H), 2.09 (m, 2H), 2.21 (m, 2H), 2.58 (s, 6H, NMe^A), 2.61 (s, 6H, NMe^B), 3.19 (m, 4H, CH$_2$N), 3.32 (s, 6H, OMe), 3.38 (m, 4H, C$\underline{H}_2$OMe).

6.8.12 N, N'-Bis[(1S,2R,3S,5S)-iso-2-(2-benzyloxyethyl)apopino-campheylborane]-TMEDA Complex (^{1}BeapC) 11

A solution of BMS (2.5 cm^3, 25.0 mmol) in diethyl ether (18 cm^3) was heated to reflux. Nopol benzyl ether (14.7 g, 57.5 mmol) was added dropwise as before. The mixture was heated under reflux for 1 h before TMEDA (1.8 cm^3, 11.9 mmol) was added, and the reflux continued for 40 min. The solution was then allowed to cool to room temperature. Ether and dimethyl sulphide were removed under reduced pressure and hexane ($ca.$ 25 cm^3) was added to the residue to induce crystallisation. The solid was removed by filtration, washed with cold hexane and then dried at room temperature under vacuum (0.01 Torr) to give 4.3 g (55%) of ^{1}BeapC. The complex was recrystallised from hexane/diethyl ether (1:1); m.p. 74-89 °C dec.. Found: C, 76.06; H, 10.84; N, 3.91. C$_{42}$H$_{70}$B$_2$N$_2$O$_2$ requires C, 76.82; H, 10.74;

N, 4.27%. $\delta(^1H)(CDCl_3)$ 0.68 (broad m, 2H, CHB), 0.78 (d, 2H, J 8.8), 1.10 (s, 6H, CMe^AMe^B), 1.15 (s, 6H, CMe^AMe^B), 1.46 (m, 2H), 1.7-1.9 (m, 10H), 2.09 (m, 2H), 2.20 (m, 2H), 2.57 (s, 6H, NMe^A), 2.58 (s, 6H, NMe^B), 3.18 (m, 4H, CH_2N), 3.47 (m, 4H, OCH_2CH_2), 4.47, 4.52 (AB quartet, 4H, J_{AB} 12.0, $PhCH_2$), 7.2-7.4 (m, 10H, Ph).

6.8.13 Determination of the Enantiomeric Compositions of [1]MeapC and [1]BeapC

(a) [1]MeapC[17]

A solution of BMS (6.0 cm^3, 60 mmol)[18] in diethyl ether (30 cm^3) was heated to reflux. Nopol methyl ether (11.37 g, 63.1 mmol) was added dropwise to the refluxing solution over a period of 20 min. After the addition, the reaction mixture was refluxed for 4 h. It was then cooled to room temperature. Ethanol (30 cm^3) was added dropwise and the solution was stirred until no more gas (H$_2$) was evolved. Aqueous sodium hydroxide (3 *M*, 21.1 cm^3, 63.6 mmol) was then added and the mixture was cooled in an ice-water bath before 30% aqueous hydrogen peroxide (7.6 cm^3, 67 mmol) was added dropwise with stirring. Following the addition of the peroxide, the cooling bath was removed and the reaction mixture was heated at reflux for 1.25 h. The reaction mixture was allowed to cool to room temperature and was then poured into ice-water (260 cm^3). More ether (100 cm^3) was added and the organic layer was separated and washed with water (2 x 50 cm^3), saturated aqueous sodium chloride (1 x 50 cm^3) and dried (K$_2$CO$_3$). After removal of the ether, the residual oil was distilled to give 8.1 g (68%) of iso-2-(2-methoxyethyl)apopinocampheol, b.p. 83.5-86 °C/0.45 Torr. δ(^{1}H)(CDCl$_3$) 0.91 (s, 3H, C*Me*^{A}Me^B), 1.08 (d, 1H, *J* 9.6), 1.21 (s, 3H, CMe^A*Me*^{B}), 1.59 (m, 1H), 1.76 (m, 1H), 1.81-1.97 (m, 4H), 2.36 (m, 1H), 2.47 (m, 1H), 3.31 (s, 1H, OH), 3.38 (s, 3H, OMe), 3.44-3.61 (m, 2H, C*H*$_2$OMe), 4.15 (m, 1H, *H*COH).

Oxalyl chloride (50 μl, 0.573 mmol) was added to a solution of (*R*)-(+)-Mosher's acid (0.025 g, 0.107 mmol) and *N*,*N*-dimethylformamide (9.5 μl, 0.123 mmol) in hexane (5 cm^3) at room temperature under

argon. A white precipitate formed immediately and the mixture was stirred at room temperature for 1 h. The mixture was then decanted into another flask and hexane was removed by rotary evaporation. A solution of iso-2-(2-methoxyethyl)apopinocampheol (0.0132 g, 0.0664 mmol), triethylamine (40 μl, 0.287 mmol), and 4-dimethylaminopyridine (DMAP) (0.0121 g, 0.0991 mmol) in $CDCl_3$ (1 cm^3) was added to the residue. After standing for 1.5 h at room temperature, ^1H NMR spectroscopic examination of the mixture revealed complete conversion into the diastereomeric Mosher esters **13**.[19] The multiplets arising from the C$\underline{H}$O proton in the ^1H NMR spectrum and from the CF_3 group in the ^{19}F NMR spectrum were used to determine the diastereomeric composition. The major diastereomer (96%) showed δ(^1H) 5.23 (dt, 1H, J 9.5 and 4.1), and δ(^{19}F) 4.17 (s); the minor diastereomer (4%) showed δ(^1H) 5.29 (dt, 1H, J 9.5 and 4.0) and δ(^{19}F) 4.22 (s), confirming that the ee of the starting nopol methyl ether **5** was 92 ± 1% (see Table **6.1**).

Ethanol (5 cm^3) was added dropwise to a solution of ^{1}MeapC (0.549 g, 1.09 mmol) in diethyl ether (5 cm^3), followed by 3 M sodium hydroxide solution (0.8 cm^3, 2.4 mmol). The reaction mixture was then cooled in an ice bath. 30% Aqueous hydrogen peroxide (0.4 cm^3, 3.53 mmol) was added dropwise and the solution was heated to reflux for 1.25 h. The mixture was allowed to cool to room temperature and was poured into ice-water (10 cm^3). More ether (15 cm^3) was added and the organic layer was separated and washed successively with water (2 x 10 cm^3), 2 M sulfuric acid (1 x 10 cm^3), saturated aqueous sodium hydrogen carbonate (1 x 10 cm^3), saturated aqueous sodium chloride (1 x 10 cm^3) and dried (K_2CO_3). After removal of the solvent, the residue was subjected to column chromatography, using

hexane/ethyl acetate (7:3) as eluant, to give 0.32 g (74%) of iso-2-(2-methoxyethyl)apopinocampheol. The alcohol was esterified as before and the diastereomeric composition of the Mosher esters was determined by ^{1}H/^{19}F NMR spectroscopy, showing that the ee of ^{1}MeapC was 91%.

(b) ^{1}BeapC

Nopol benzyl ether was converted to iso-2-(2-benzyloxyethyl)apopinocampheol by the method used for nopol methyl ether; b.p. 120-121 °C/0.01 Torr. δ(^{1}H)(CDCl$_3$) 0.90 (s, 3H, CMe^{A}Me^B), 1.07 (d, 1H, J 10.0), 1.21 (s, 3H, CMe^{A}Me^B), 1.62 (m, 1H), 1.74 (m, 1H), 1.78-1.99 (m, 4H), 2.35 (m, 1H), 2.46 (m, 1H), 3.15 (d, 1H, J 2.8, OH), 3.54-3.72 (m, 2H, CH$_2$OCH$_2$Ph), 4.16 (m, 1H, HCOH), 4.53 (s, 2H, CH$_2$Ph), 7.25-7.40 (m, 5H, Ph).

The alcohol was esterified with Mosher's acid chloride as before. The multiplets arising from the CHO proton in the ^{1}H NMR spectrum and from the CF$_3$ group in the ^{19}F NMR spectrum were used to determine the diastereomeric composition of the esters. The major diastereomer (95%) showed δ(^{1}H) 5.30 (dt, 1H, J 9.8 and 4.2) and δ(^{19}F) 4.02 (s); the minor diastereomer (5%) showed δ(^{1}H) 5.35 (dt, 1H, J 9.7 and 4.2) and δ(^{19}F) 4.10 (s), confirming that the ee of the starting nopol benzyl ether 6 was 90 ± 1%.

Treatment of ^{1}BeapC in a similar way to that derived for ^{1}MeapC, with alkaline hydrogen peroxide gave iso-2-(2-benzyloxyethyl)apopinocampheol, which was purified by column chromatography using hexane/ethyl acetate (7:3) as eluant. The alcohol was then esterified, as before, to give the Mosher ester which showed the ee of ^{1}BeapC to be ≥ 98.5%.

6.8.14 Attempted Synthesis of Cyclic *N*-Myrtenylpyrrolidine-Borane 15

Myrtenyl bromide was prepared from (1*R*)-(-)-myrtenol and triphenylphosphine dibromide as described in the literature;[20] b.p. 50-53 °C/0.1 Torr (lit.[20] b.p. 45-47 °C/0.05 Torr). $\delta(^1H)(CDCl_3)$ 0.83 (s, 3H, CMe^{A}Me^B), 1.18 (d, 1H, *J* 8.8), 1.31 (s, 3H, CMe^{A}Me^B), 2.10 (m, 1H), 2.20-2.37 (m, 3H), 2.45 (m, 1H), 3.96 (m, 2H, CH$_2$Br), 5.68 (m, 1H, C=CH).

Myrtenyl bromide (52.6 g, 245 mmol) was added dropwise with mechanical stirring to neat pyrrolidine (400 cm^3, 4.79 mol) and the mixture was heated under reflux for 8 h. Excess pyrrolidine was removed using a water pump and aqueous potassium hydroxide (265 cm^3 of a 3.5 *M* solution) was added to the residue with stirring. The mixture was then extracted with ether (4 x 150 cm^3) and the ethereal solution was washed with saturated aqueous sodium chloride (2 x 240 cm^3) and dried (Na$_2$SO$_4$). After removal of the ether, the residual brown oil was distilled to give 41 g (82%) of *N*-myrtenylpyrrolidine, b.p. 70-82 °C/0.019 Torr. $\delta(^1H)(CDCl_3)$ 0.84 (s, 3H, CMe^{A}Me^B), 1.15 (d, 1H, *J* 8.4), 1.28 (s, 3H, CMe^{A}Me^B), 1.77 (m, 4H, NCH$_2$CH$_2$), 2.08 (m, 1H), 2.16-2.32 (m, 3H), 2.39 (m, 1H), 2.47 (m, 4H, NCH$_2$), 2.84, 3.06 (AB quartet, 2H, *J* 14, CH$_2$NCH$_2$CH$_2$), 5.38 (m, 1H, C=CH).

BMS (22.0 cm^3, 220 mmol) was added dropwise to a stirred solution of *N*-myrtenylpyrrolidine (45.5 g, 222 mmol) in hexane (100 cm^3) at 0 °C. After the addition, the mixture was stirred at room temperature for 1 h and then re-cooled in an ice-water bath. The white crystalline precipitate was removed by filtration, washed with hexane (4 x 30 cm^3) and dried at 0.01 Torr to give 23.0 g (48%) of *N*-myrtenylpyrrolidine-borane **17**; m.p. 78-79 °C. Found: C, 76.58; H,

12.03; N, 6.45. $C_{14}H_{26}NB$ requires C, 76.72; H, 11.96; N, 6.39%. $\delta(^1H)(CDCl_3)$ 0.81 (s, 3H, C$\underline{Me}^AMe^B$), 1.18 (d, 1H, J 8.8), 1.27 (s, 3H, CMe$^A\underline{Me}^B$), 1.82 (m, 2H), 2.02-2.48 (m, 7H), 2.80 (m, 2H), 2.98 (m, 2H), 3.37 (m, 2H, C=CCH$_2$N), 5.60 (m, 1H, C=CH).

N-Myrtenylpyrrolidine-borane (3.04 g, 13.9 mmol) was transferred to a thick-wall glass tube containing a small Teflon-covered magnetic stirrer bar. Toluene (22 cm^3) was added and the solution was frozen in liquid N$_2$. The tube was attached to the vacuum line, evacuated and flame-sealed. The contents were thawed to room temperature and then heated in an oil bath at 150 °C for 1.5 h. The solution was allowed to cool to room temperature, the tube was cracked open at the neck and the solution was removed by syringe into a conical flask. ^{11}B NMR spectroscopic examination of the solution using a mixture of benzene and C$_6$D$_6$ as solvents showed a main triplet (ca. 90%) at δ -0.97 (J_{BH} 105).

6.8.15 Attempted Synthesis of Cyclic N-Myrtenyldimethylamine-Borane 20

Myrtenyl bromide was prepared as described in the literature.[20] Dimethylamine (140 cm^3, 2.11 mol) was allowed to evaporate into a reaction flask equipped with a condenser containing solid CO$_2$-acetone slush, while the flask was cooled in an ice-salt bath at -10 °C. Myrtenyl bromide (48.9 g, 227 mmol) was added dropwise during 0.5 h and the reaction mixture was then stirred at 0 °C for a further 4.5 h. Excess dimethylamine was allowed to evaporate at room temperature overnight and potassium hydroxide (247 cm^3 of a 20% solution) was added to the residual liquid. The mixture was extracted with diethyl ether (3 x 150 cm^3), the ethereal solution was washed with saturated

aqueous sodium chloride (2 x 200 cm^3) and dried (Na$_2$SO$_4$). After removal of the solvent, the residual liquid was distilled to give 28 g (69%) of N,N-dimethylmyrtenylamine, b.p. 54-64 °C/1.4 Torr (lit.[21] b.p. 40-41 °C/0.6 Torr). δ(^{1}H)(CDCl$_3$) 0.84 (s, 3H, C$\underline{Me}^A$Me^B), 1.14 (d, 1H, J 8.8), 1.28 (s, 3H, CMe$^A\underline{Me}^B$), 2.09 (m, 1H), 2.18 (s, 6H, NMe$_2$), 2.20-2.35 (m, 3H), 2.40 (m, 1H), 2.67, 2.82 (AB quartet, 2H, J_{AB} 12.8), 5.36 (m, 1H, C=CH).

BMS (9.4 cm^3, 94 mmol) was added dropwise to a solution of N,N-dimethylmyrtenylamine (17.0 g, 94.6 mmol) in hexane (43 cm^3) at 0 °C. After the addition, the solution was stirred for 1 h at room temperature before being re-cooled to 0 °C and the precipitated material was removed by filtration. The solid was washed with cold hexane and dried at 0.01 Torr to give 12 g (68%) of N,N-dimethylmyrtenylamine-borane 21, m.p. 75-76 °C. Found: C, 74.41; H, 12.77; N, 7.17. C$_{12}$H$_{24}$NB requires C, 74.63; H, 12.52; N, 7.25%. δ(^{1}H)(C$_6$D$_6$) 0.69 (s, 3H, C$\underline{Me}^A$Me^B), 0.95 (d, 1H, J 8.8), 1.13 (s, 3H, CMe$^A\underline{Me}^B$), 1.85 (m, 1H), 1.92-2.04 (m, 3H), 2.12 (s, 3H, NMe^A), 2.13 (s, 3H, NMe^B), 2.20 (m, 1H), 2.45 (q, 3H, J_{BH} 79, BH$_3$), 3.12 (m, 2H, C$\underline{H}_2$N), 5.07 (m, 1H, C=CH). δ(^{13}C)(C$_6$D$_6$) 21.2 (C$\underline{C}$H$_3$^{A}), 26.1 (C$\underline{C}$H$_3$^{B}), 31.8, 31.9, 37.6 ($\underline{C}$Me$_2$), 40.1 [N(CH$_3$)$_2$], 47.3, 50.1, 69.0 (CH$_2$N), 129.3 (C=$\underline{C}$H), 140.8 ($\underline{C}$=CH). δ(^{11}B)(C$_6$H$_6$ and C$_6$D$_6$) -7.41 (q, J_{BH} 98).

The amine-borane complex (2.64 g, 13.6 mmol) was heated in toluene (19 cm^3) in a sealed tube at 150-160 °C for 1.5 h, as described above. The ^{11}B NMR spectrum showed a triplet at δ +1.45 (J_{BH} 116), which we believe is due to the cyclic complex 20. It also showed a quartet at δ -7.41 (J_{BH} 97) due to the uncyclised amine-borane and a triplet at δ +6.56 (J_{BH} 121), along with other unidentified signals.

6.9 UV Irradiation

The experimental arrangement as shown in Chapter 5, Figure **5.4** was used. All sample tubes and other apparatus through which the photolysing beam passed were made from fused silica.

Reactions were carried out using the dewar cavity insert from a Varian temperature control unit designed for operation with an ESR spectrometer. The upper part of the standard insert was cut off and replaced with a wide-bore section which could accommodate sample tubes up to 9 mm in diameter. Pre-cooled nitrogen was passed through the dewar insert and around the sample to control its temperature, which was monitored by a thermocouple placed alongside the sample. The section of the insert which contained the sample was surrounded by a fused silica tube sealed to the insert with silicone rubber. Through the jacket so formed, which was backed with aluminium foil to act as a reflector, a slow flow of dry argon was maintained to prevent condensation of moisture on the insert. Unfiltered light from a Mazda 250 W high-pressure mercury arc lamp was focussed onto the sample using two lenses of focal length 10 cm (10 cm diameter). The sample temperature during photolysis was estimated by immersing a small thermocouple in an open sample tube containing a solution of DTBP in diethyl ether and relating the temperature of this to the reading obtained from the external thermocouple positioned in the gas flow. Quoted reaction temperatures are considered accurate to ± 5 °C. The lamp could be shuttered to facilitate removal of the sample, which was mixed by shaking at frequent intervals.

6.10 Typical Procedure for Kinetic Resolution

A representative experiment is described. The complex ^{d}IpcC (0.063 g, 0.15 mmol) was first transferred to a dry, argon-filled Suprasil quartz sample tube (9 mm o.d., 1 mm wall). A mixture of racemic methyl 2-phenylpropanoate (250 µl), DTBP (560 µl) and t-butylbenzene (160 µl) was made up in a small pyrex sample tube and kept in an ice bath. An aliquot (485 µl) of this mixture was transferred by a microsyringe to the quartz sample tube. The sample tube was then attached to the vacuum line and the contents were frozen in liquid N_2. The tube was evacuated and oxirane (520 µl) was condensed onto the frozen reagents before the tube was flame-sealed under vacuum. The sample was transferred to a bath containing CO_2-IMS slush (ca. -78 °C) and the contents were mixed thoroughly by repeated inversion of the tube. (The depth of liquid in the sample tube was ca. 2.8 cm). The sample was UV irradiated for 5 h at ca. 196 K with unfiltered light from a Mazda 250 W high-pressure mercury arc lamp. The sample tube was removed from the dewar insert and the contents mixed by shaking every 20-30 min. After photolysis, the tube was cooled to ca. -78 °C and was cracked open at the neck. Toluene (2.0 cm^3) was added, the contents of the tube was transferred into a small pyrex sample tube. The sample was then kept in ice and subjected to GLC analysis, using the t-butylbenzene as internal standard, to determine the ester consumption by comparison with the chromatogram obtained from the stock mixture before photolysis. The solution was then transferred to a round-bottomed flask and volatile material was removed by rotary evaporation at ca. 30 °C. The residue was redissolved in diethyl ether (30 cm^3) and the solution was washed

with 1.8 *M* sulfuric acid (4 x 25 cm³) (to remove the amine-alkylborane or any free amines present, which might otherwise complex to the chiral shift reagent), followed by saturated aqueous sodium hydrogen carbonate (4 x 25 cm³) and then dried (MgSO₄).*⁺ Ether was removed using a rotary evaporator and other volatiles were removed at room temperature by pumping at *ca*. 1.2 Torr; under these conditions, no ester was lost. The residual ester was examined by 400 MHz ¹H NMR spectroscopy in CDCl₃ solvent in the presence of Eu(hfc)₃. The ee was calculated either from the integrals or peak weights for the CH<u>Me</u> doublets from the (*R*)- and (*S*)-enantiomers of the ester.

Pure residual ester could be obtained by column chromatography after the washing procedure* using hexane/diethyl ether (4:1) as

* A control experiment was carried out using (*R*)-methyl 2-phenyl propanoate. The ester (50 μl) dissolved in diethyl ether was washed with 1.8 *M* sulphuric acid (4 x 8 cm³), saturated sodium hydrogen carbonate (4 x 8 cm³) and dried (MgSO₄). The ¹H NMR spectrum of the recovered material in the presence of Eu(hfc)₃ showed that there was no racemisation of the ester under these conditions used.

⁺ For t-butyl 2-phenyl propanoate **39**, the residue was washed with 1.1 *M* sulfuric acid (2 x 30 cm³), saturated aqueous sodium hydrogen carbonate (2 x 25 cm³) and dried (MgSO₄).

* In the case of dimethyl 2,2-dimethyl-1,3-dioxolane-*trans*-dicarboxylate **46**, the residual material after removal of toluene was directly subjected to column chromatography without the washing procedures. Dichloromethane/diethyl ether (9:1) was used as eluant.

eluant, or by HPLC using hexane/ethyl acetate (95:5). The HPLC chromatograms showed two peaks which may correspond to the dehydro dimers **32** and **33**.[22,23] The *meso*-dimer was isolated as a solid. $\delta(^1H)(CDCl_3)$ 1.68 (s, 6H, CMe), 3.74 (s, 6H, CO_2Me), 6.80-7.40 (m, 10H, Ph). [lit.[23] $\delta(^1H)(CCl_4)$ 1.66 (s, 6H, CMe), 3.66 (s, 6H, CO_2Me), 6.6-7.3 (m, 10H, Ph)]. The *dl*-dimer was obtained as a liquid. $\delta(^1H)(CDCl_3)$ 1.78 (s, 6H, CMe), 3.70 (s, 6H, CO_2Me), 6.70-7.20 (m, 10H, Ph). [lit.[23] $\delta(^1H)(CCl_4)$ 1.83 (s, 6H, CMe), 3.66 (s, 6H, CO_2Me), 6.68-7.22 (m, 10H, Ph)].

The ee of the residual esters could also be determined by HPLC analyses using the Chiralcel OD column. The eluant used was usually hexane/isopropyl alcohol (99.95:0.05).[¶] The ee determined by HPLC agreed with that found by the NMR spectroscopic method.

[¶] For the ester **39**, the ee can only be determined by HPLC, using hexane (100%) as eluant.

References to Chapter 6

1. T. Shono, S. Kashimura, and H. Nogusa, *J. Org. Chem.*, 1984, **49**, 2043.

2. C. Aaron, D. Dull, J. L. Schmiegel, D. Jaeger, Y. Ohashi and H. S. Mosher, *J. Org. Chem.*, 1967, **32**, 2797.

3. D. A. Bright, D. E. Mathisen and H. E. Zieger, T. Org. Chem., 1982, 47, 3521.

4. M. F. Hawthorne, *J. Am. Chem. Soc.*, 1961, **83**, 831.

5. G. Hallas, *J. Chem. Soc.*, 1965, 5770.

6. S. M. McElvain and C. L. Stevens, *J. Am. Chem. Soc.*, 1946, **68**, 1917.

7. G. R. Ramage, *J. Chem. Soc.*, 1938, 397.

8. T. Hayashi, M. Konishi, M. Fukushima, K. Kanehira, T. Hioki and M. Kumada, *J. Org. Chem.*, 1983, **48**, 2195.

9. P. A. S. Smith, D. R. Baer and S. N. Ege, *J. Am. Chem. Soc.*, 1954, **76**, 4564.

10. R. Delaby, P. Reynaud and F. Lilly, *Bull. Soc. Chim. France*, 1961, 2067.

11. M. Carmack and C. J. Kelley, *J. Org. Chem.*, 1968, **33**, 2171.

12. H. C. Brown, J. R. Schwier and B. Singaram, *J. Org. Chem.*, 1978, **43**, 4395.

13. B. Singaram and J. R. Schwier, *J. Organomet. Chem.*, 1978, **156**, C1.

14. H. C. Brown, B. Singaram and J. R. Schwier, *Inorg. Chem.*, 1979, **18**, 51.

15. A. K. Mandal, P. K. Jadhav and H. C. Brown, *J. Org. Chem.*, 1980, **45**, 3543.

16. H. C. Brown, R. S. Randad, K. S. Bhat, M. Zaidlewicz, S. A. Weissman, P. K. Jadhav and P. T. Perumal, *J. Org. Chem.*, 1988, **53**, 5513.

17. C. S. Shiner, C. M. Garner and R. C. Haltiwanger, *J. Am. Chem. Soc.*, 1985, **107**, 7167.

18. C. F. Lane, *J. Org. Chem.*, 1974, **39**, 1437.

19. D. E. Ward and C. K. Rhee, *Tetrahedron Lett.*, 1991, **32**, 7165.

20. R. K. d. Richter, M. Bonato, M. Follet and J.-M. Kamenka, *J. Org. Chem.*, 1990, **55**, 2855.

21. S. W. Markowicz, *Polish J. Chem*, 1979, **53**, 157.

22. C. T. Ng, X. Wang and T.-Y. Luh, *J. Org. Chem.*, 1988, **53**, 2536.

23. C. d. Luca, A. Inesi and L. Rampazzo, *J. Chem. Soc., Perkin Trans. 2*, 1982, 1403.

CHAPTER 7

ESR SPECTROSCOPIC STUDIES OF ENANTIOSELECTIVE HYDROGEN-ATOM

### ABSTRACTION REACTIONS

RESULTS AND DISCUSSION

In Chapter 5, the kinetic resolutions of racemic esters were described. In this chapter, we describe the use of ESR spectroscopic methods which permit the elementary enantioselective H-atom transfer steps to be studied in isolation and to allow determination of the relative rates of α-hydrogen-atom abstraction from enantiomeric pairs of esters by chiral amine-boryl radicals.. As in the work involving kinetic resolution, the concept of polarity reversal catalysis[1-3] was utilised to control the chemo- and enantio-selectivity of the H-atom abstraction.

When an oxirane solution containing DTBP (28% v/v) and methyl 2,2-dimethyl-1,3-dioxolane-4-carboxylate 1-R or 1-S (0.83 M) was irradiated with UV light at 188 K, while the sample was in the
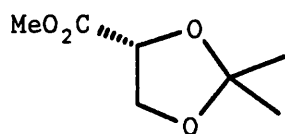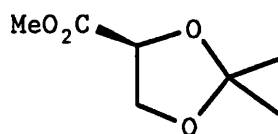
1-R   1-S

microwave cavity of the ESR spectrometer, signals from the radicals 2-E [$a(2H_\beta)$ 22.36, $a(3H_s)$ 1.31 G, and g 2.0041(0) at 188 K], 2-Z [$a(2H_\beta)$ 22.96, $a(3H_s)$ 1.56 G, and g 2.0040(8) at 188 K], and 3 [$a(H_\alpha)$ 12.78, $a(H_\beta)$ 27.40 G, and g 2.0033 at 188 K] were observed along with the spectrum of the oxiranyl radical. The electrophilic t-butoxyl

radical abstracts hydrogen unselectively from the ester and from the solvent. The designations E and Z refer to the eneoxyl resonance forms **4-E** and **4-Z**; the assignments are speculative.

Me $\smallsmile$ O

Me $\smallsmile$ O

MeO$_2$C

2-E

2-Z

3

4-E

4-Z
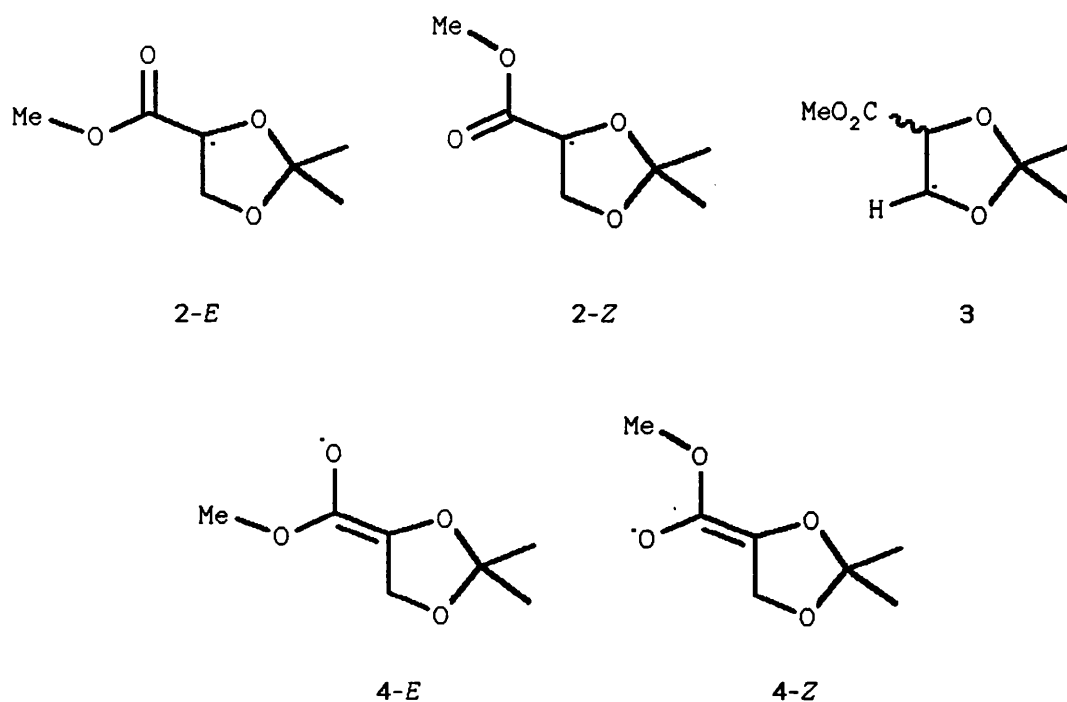
When the experiment was repeated in the additional presence of $Me_3N{\rightarrow}BH_2Bu^n$ (0.15 M), which acts as a polarity reversal catalyst, H-atom abstraction is brought about by $Me_3N{\rightarrow}\dot{B}HBu^n$ **5**, through the catalytic cycle of reactions (7.1) and (7.2), both of which benefit

$$Bu^tO^{\cdot} \ + \ amine{\rightarrow}BH_2R \ \longrightarrow \ Bu^tOH \ + \ amine{\rightarrow}\dot{B}HR \qquad (7.1)$$

$amine{\rightarrow}\dot{B}HR \ +$ MeO$_2$C $\longrightarrow amine{\rightarrow}BH_2R \ +$ MeO$_2$C   (7.2)

1-R or 1-S

2
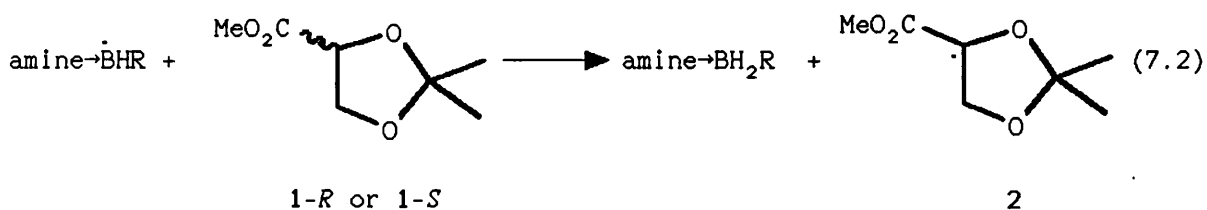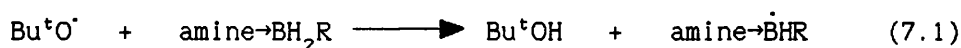
from favourable polar effects. Now, the highly nucleophilic amine-boryl radical abstracts hydrogen exclusively from the C-H group

α to the electron-withdrawing carbonyl function to give only 2-E/Z ([2-E]:[2-Z] = 1:1.4 at 186 K determined by computer simulation) (Figure 7.1).

The isomer ratio [2-E]:[2-Z] varies with the nature of the abstracting radical. By computer simulation of the ESR spectrum, for H-atom abstraction by $Bu^tO\cdot$, the ratio [2-E]:[2-Z] was found to be 1:2.3 at 188 K. Rotation about the $C(O)$-$\dot{C}$ bond must be slow compared to the lifetimes of the radicals (*ca.* 1 ms) for non-equilibrium ratios of rotamers to be detected. Relatively high rotational barriers might be expected for these captodatively-substituted radicals.[4]

The relative reactivities of the enantiomers of 1 (k_{1-R}/k_{1-S}) towards 5 could be determined by competition experiments[1-3] using an achiral competitor and measuring ($k_{1-R}/k_{competitor}$) and ($k_{1-S}/k_{competitor}$) separately. When an oxirane solution containing 1-R (0.75 M), dimethyl methylmalonate (DMMM) (0.51 M), as the achiral competitor, $Me_3N{\rightarrow}BH_2Bu^n$ (0.16 M) and DTBP (27% v/v) was UV irradiated at 188 K, ESR spectra of a mixture of the radicals 2-E/Z and 6 were recorded. Computer simulation or double integration of the ESR spectra provided relative concentrations of the radicals, and hence (k_{1-R}/k_{DMMM}) could be determined. At 188 K the value of (k_{1-R}/k_{DMMM}) was found to be 0.71. Similar experiments using 1-S gave (k_{1-S}/k_{DMMM}) = 0.66. Hence, (k_{1-R}/k_{1-S}) is equal to unity within experimental error, as required because 5 is achiral (Scheme 7.1).

In contrast, when the optically-active amine-boranes 7a-11a (*ca.* 0.07 M) were used in place of $Me_3N{\rightarrow}BH_2Bu^n$ as polarity reversal catalysts, the reactivities of 1-R and 1-S towards the chiral amine-boryl radicals differed and the enantioselectivity constants s
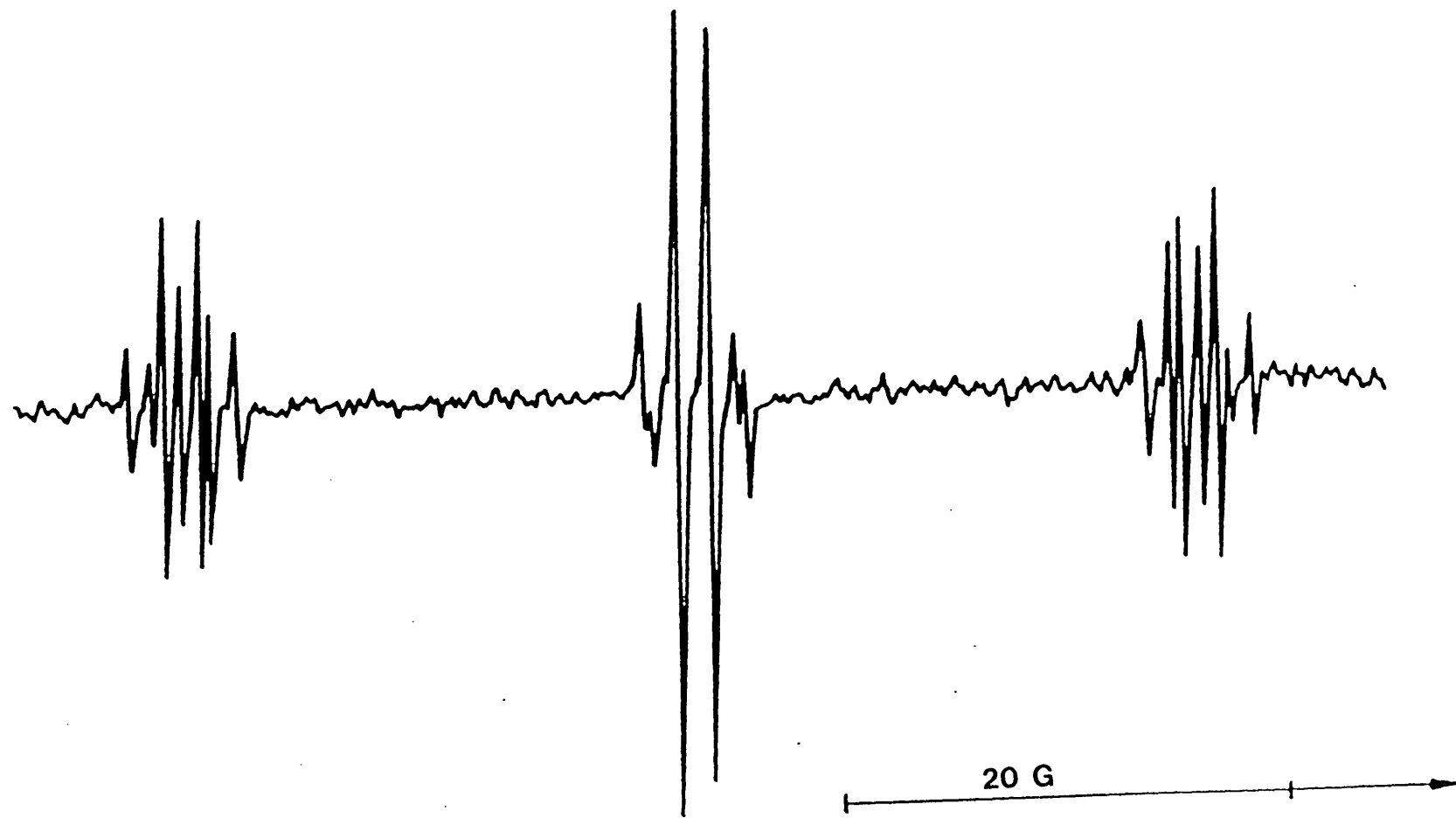
Figure 7.1 ESR spectrum of the radical **2** generated in the presence of **1**-S and $Me_3N{\rightarrow}BH_2Bu^n$ in oxirane at 184 K.

1-*R/S*

$k_{1-R/S}$

in oxirane

at 188 K

k_{DMMM}

DMMM

2-*E/Z*

MeĊ(CO₂Me)₂

6

Scheme 7.1

Me   Me
| |
X   NCH₂CH₂N
| | |
BH←   Me   Me →BH₂
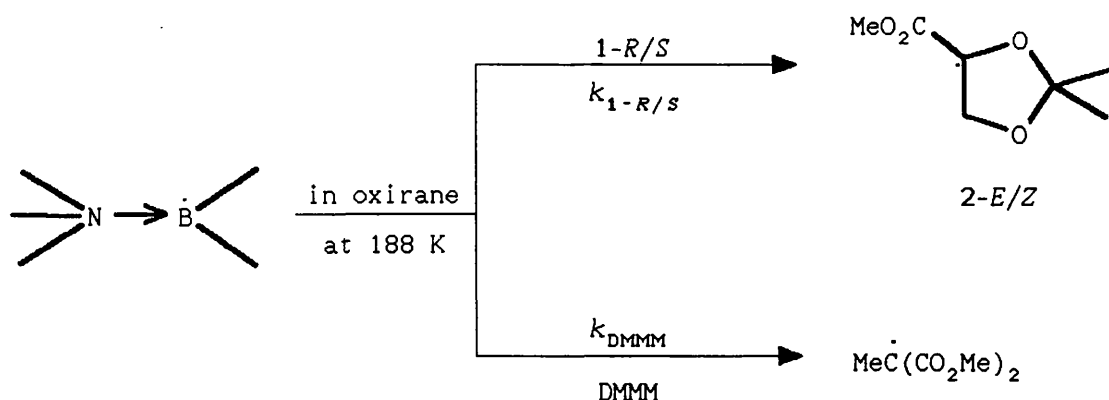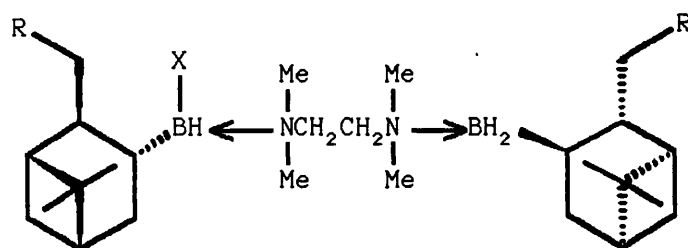
7a; R = H,   X = H

7b; R = H,   X = unpaired electron (u.p.e.)

Me   Me
| |
X   NCH₂CH₂N
| | |
BH←   Me   Me →BH₂
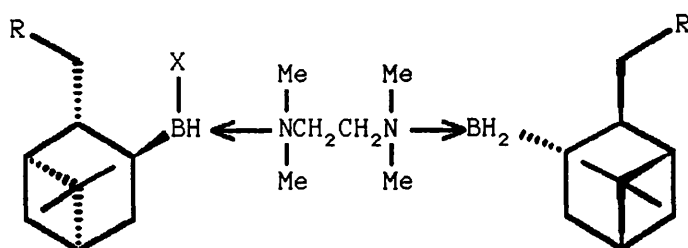
8;   R = H
9;   R = Me   a;   X = H
10; R = CH₂OCH₂Ph   b;   X = u.p.e.
11; R = CH₂OMe

(= $k_{1-R/S}/k_{1-S/R}$) for H-atom abstraction to give **2** are listed in Table **7.1**. Figure **7.2a** shows parts of the spectra of **2-*E/Z*** and **6** obtained from a mixture of **1-*R*** (0.66 *M*), DMMM (0.45 *M*), DTBP (23%

Table **7.1**

Enantioselectivity constants (s) for hydrogen-atom abstraction from **1** in oxirane at 188 K.

Abstracting radical	k_{1-R}/k_{DMMM}	k_{1-S}/k_{DMMM}	Faster reacting enantiomer	s^a
7b	0.68	1.63	S	2.4
8b	1.65	0.67	R	2.5
9b	1.92	1.16	R	1.7^b
10b	2.56	1.23	R	2.1
11b	1.71	0.88	R	1.9

a [Amine-borane] = $ca.$ 0.07 M; s did not change significantly when the catalyst concentration was doubled. b At 202 K.
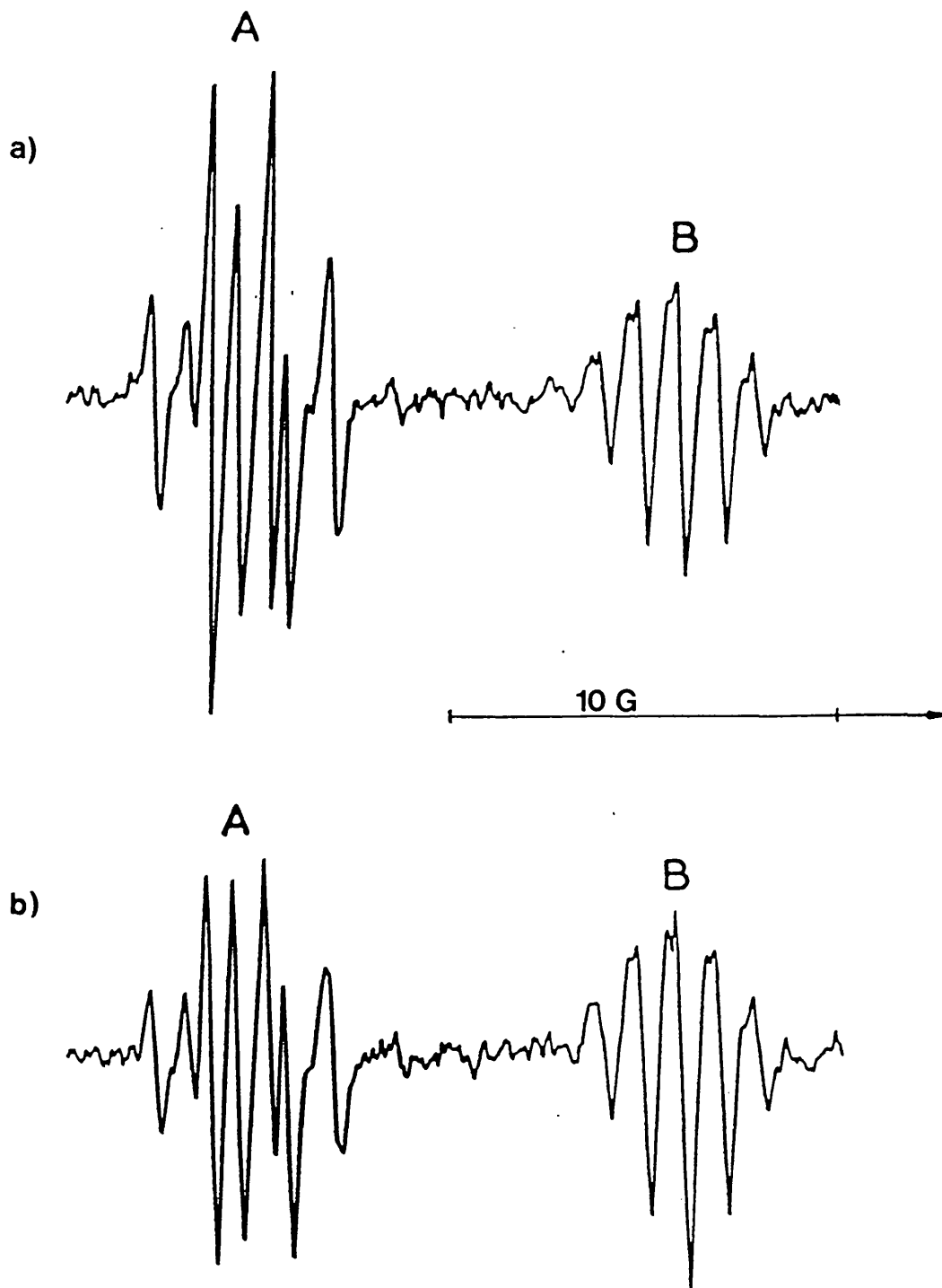
Figure 7.2 Low field regions from the ESR spectra of 2-E/Z and 6 generated from a mixture of 1-R, DMMM and DTBP in oxirane at 184 K. The $M_I(2H_\beta)$ = + 1 lines for 2-E/Z (multiplets A) and the $M_I(3H_\beta)$ = + 1/2 lines for 6 (multiplets B) are shown. (a) Using 8a as catalyst. (b) Using 7a as catalyst.

v/v) and catalyst **8a** in oxirane at 184 K. Figure **7.2b** shows the same region of the spectra obtained from the same mixture, but using the enantiomeric catalyst **7a**. The $E:Z$ rotamer ratios differ slightly for diastereomeric radical-substrate reactant pairs. For example, at 188 K [**2-E**]:[**2-Z**] = 1:1.3 from **7b** + **1-R** and 1:1.6 from **7b** + **1-S**.

Another substrate investigated was dimethyl 2,2-dimethyl-1,3-dioxolane-*trans*-dicarboxylate **12**. When an oxirane solution containing **12-R,R** (0.75 M) and DTBP (28% v/v) was UV irradiated at 198 K, a mixture of the radicals **13-E/Z** and the oxiranyl radical was obtained. However, when the experiment was repeated in the presence of Me$_3$N$\rightarrow$BH$_2$Bu^n (0.25 M), only the radicals **13-E** [a(H$_\beta$) 20.52, a(3H$_\delta$) 1.23 G, and g 2.0039(9) at 201 K] and **13-Z** [a(H$_\beta$) 20.52, a(3H$_\delta$) 1.52 G, and g 2.0039(7) at 201 K] were detected. The Z-rotamer is arbitrarily assumed to predominate and [**13-E**]:[**13:Z**] = 1:1.2 for abstraction by **5** (Figure **7.3**).

12-R,R 12-S,S

13-E 13-Z
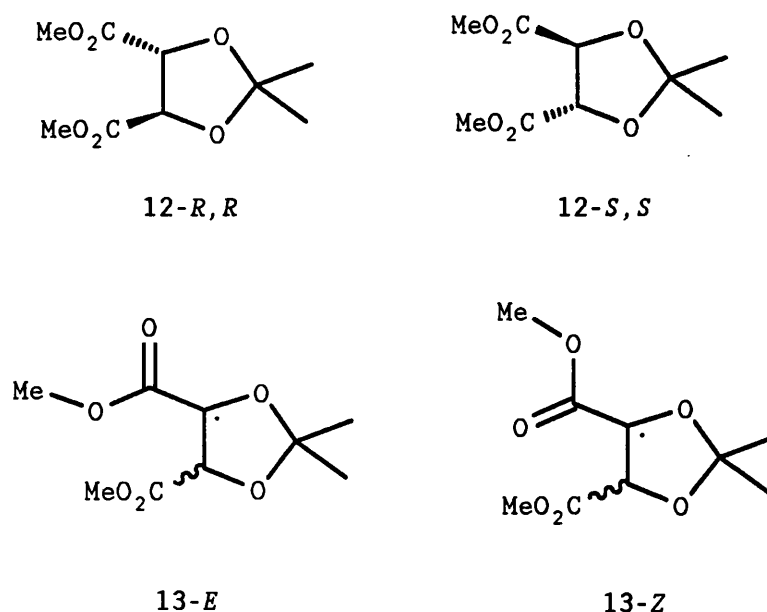
Competition experiments with **12** showed that H-atom abstraction by **7b-11b** to give **13** takes place with very high enantioselectivity.
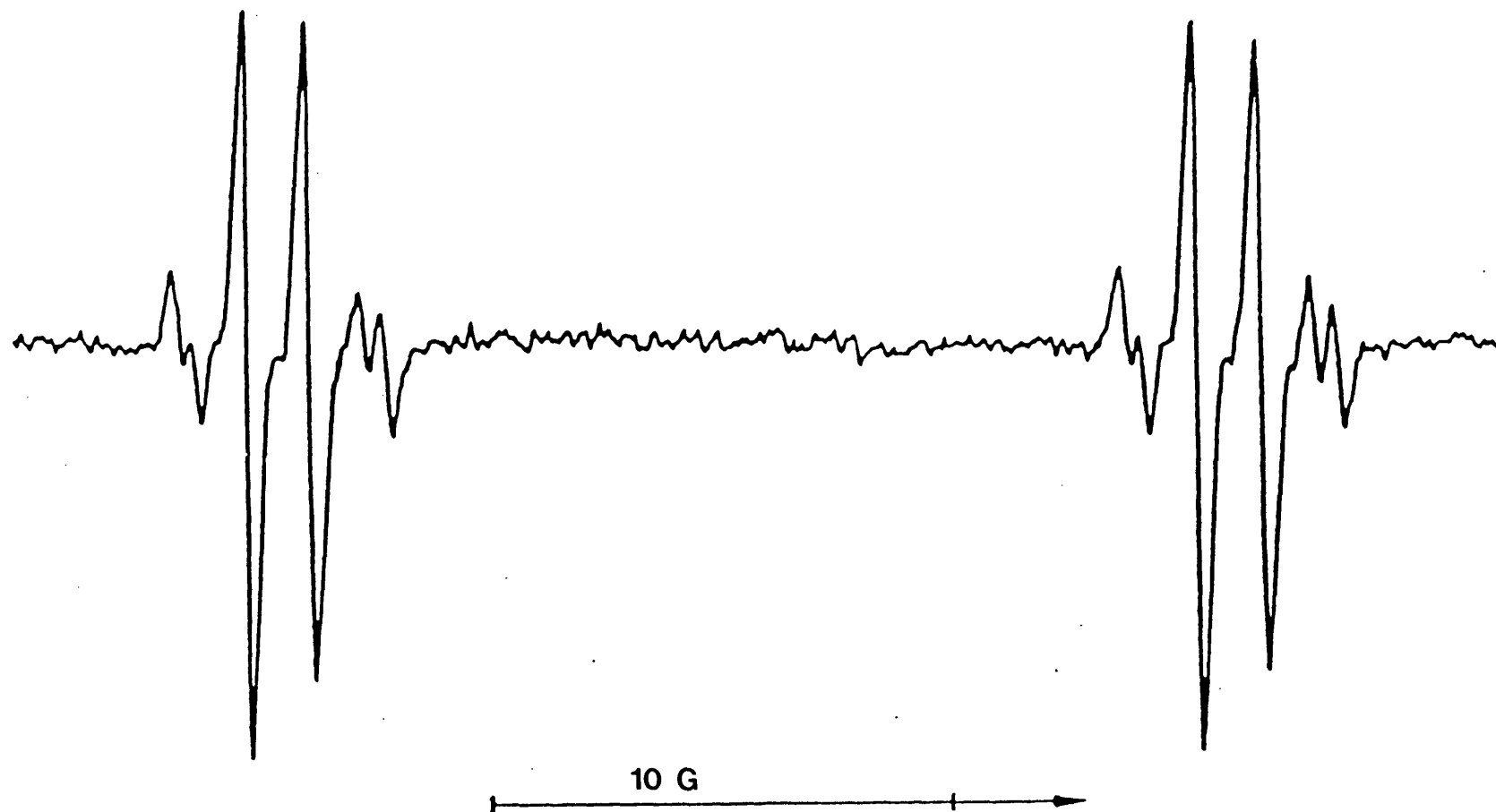
Figure 7.3   ESR spectrum of the radical 13 generated by reaction of
the amine-boryl radical 5 with 12-*R,R* in oxirane at 201 K; both *E*-
and *Z*-rotamers are present.

The reactivities of **12-R,R** and **12-S,S** were determined in separate experiments relative to triethyl methanetricarboxylate (TEMT) (Scheme 7.2).[2] When an oxirane solution containing **12-R,R** (0.49 M), TEMT

Scheme 7.2
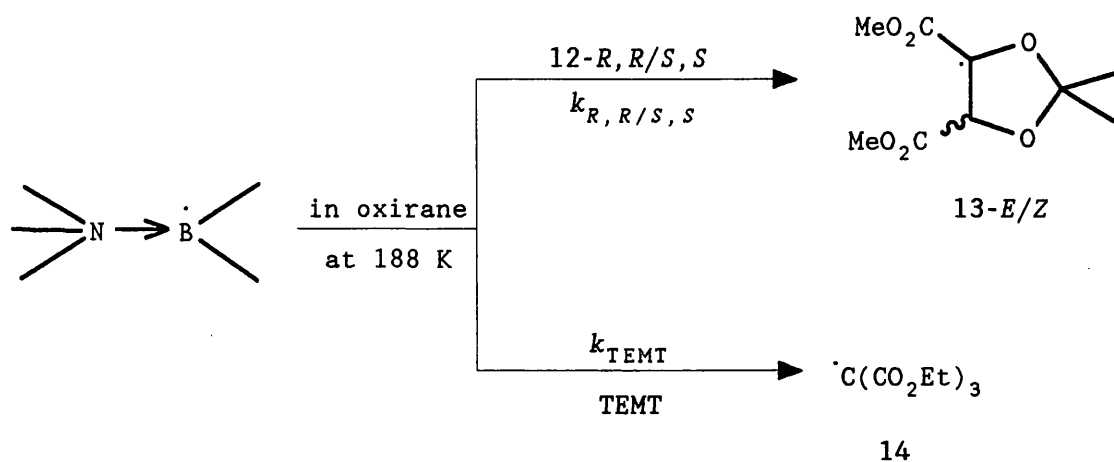
(0.25 M), DTBP (23% v/v) and $Me_3N{\rightarrow}BH_2Bu^n$ (0.15 M) was UV irradiated at 189 K, ESR spectra of a mixture of the radicals **13-E/Z** and **14** were detected. From double integration of the spectra, $(k_{R,R}/k_{TEMT})$ = 1.70. Similar experiments using **12-S,S** showed $(k_{S,S}/k_{TEMT})$ = 1.83. Hence, $(k_{R,R}/k_{S,S})$ is equal to unity within experimental error, as required because **5** is achiral. However, when the chiral amine-boranes **7a-11a** were used, very high enantioselectivities were observed and the derived enantioselectivity constants are given in Table **7.2**.

The high enantioselectivity of H-atom abstraction from **12** is immediately obvious from comparison of Figures **7.4a** and **b**. Figure **7.4a** shows the composite ESR spectra of **13** and **14** recorded during generation of **7b** in the presence of a mixture of **12-S,S** (0.51 M) and TEMT (0.26 M) in oxirane at 187 K, while Figure **7.4b** shows the corresponding spectrum recorded when the enantiomeric amine-boryl

Table **7.2**

Enantioselectivity constants (s) for hydrogen-atom abstraction from **12** in oxirane at 188 K.

Abstracting radical	$k_{R,R}/k_{TEMT}$	$k_{S,S}/k_{TEMT}$	Faster reacting enantiomer	s
7b	0.090	1.91	S,S	21
8b	2.27	0.11	R,R	21
9b	1.11	0.072	R,R	15[a]
10b	5.24	0.23	R,R	23
11b	1.51	0.086	R,R	18

a At 202 K
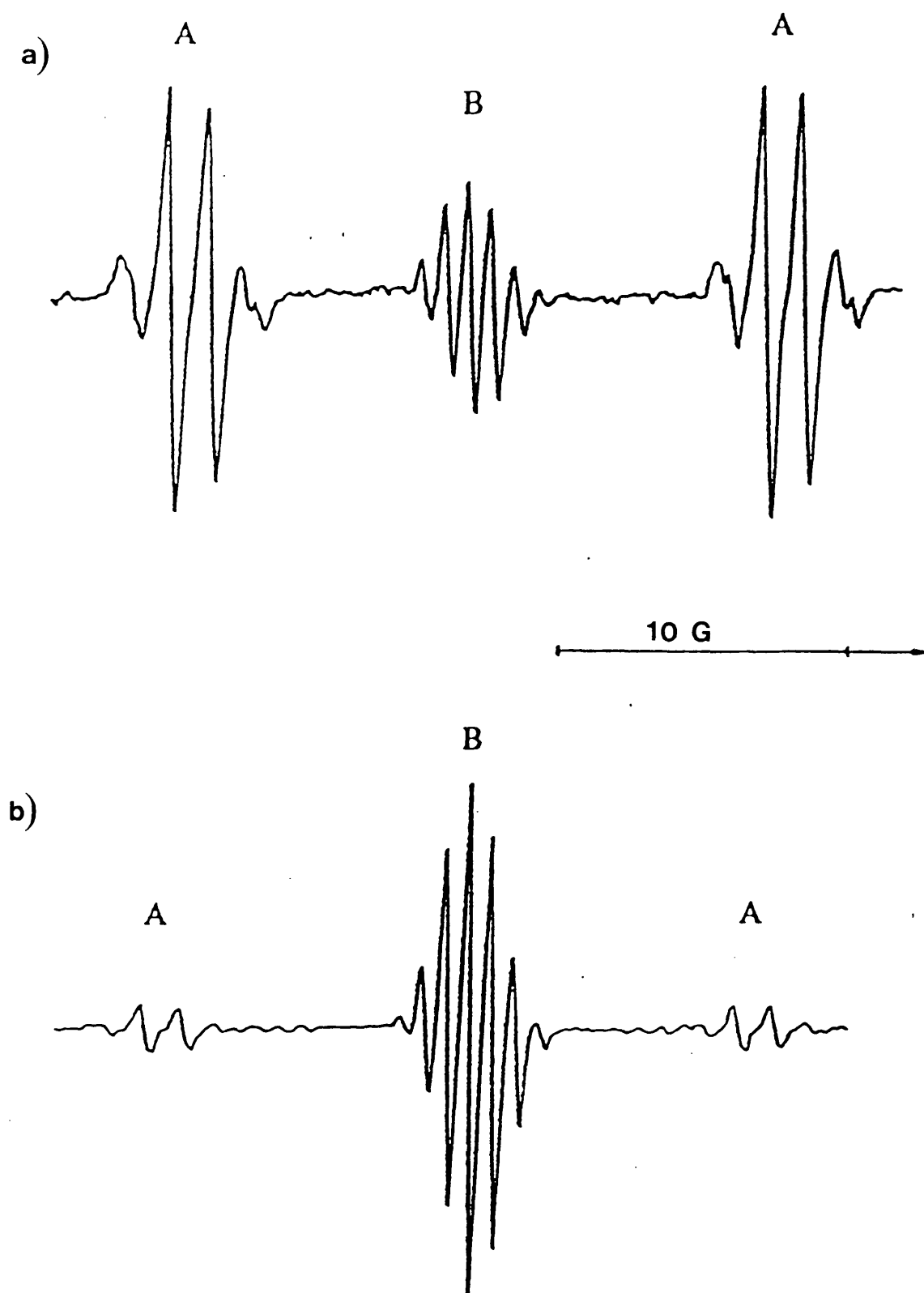
Figure 7.4 ESR spectra of **13** (multiplets A) and **14** (multiplets B), generated at 187 K from a mixture of **12**-*S,S* (0.51 *M*) and TEMT (0.26 *M*). (a) Using **7a** as polarity reversal catalyst. (b) Using **8a** as catalyst.

radical **8b** was generated in the presence of the same mixture of esters.

Results obtained using the direct ESR method for determining enantioselectivities were compared with the values of s calculated from kinetic resolution data using equation (7.3) (see Chapter 5).[5,6]

$$s = (k_A/k_B) = \ln[(1 - C)(1 - EE)]/\ln[(1 - C)(1 + EE)] \qquad (7.3)$$

With racemic **12** and the amine-borane **7a**, $(k_{S,S}/k_{R,R})$ was found to be 14, as described in Chapter 5. With **8a**, the value of $(k_{R,R}/k_{S,S})$ was 12. An accurate value of s will be obtained from equation (7.3) only if strict homogeneity of the reaction mixture is maintained during photolysis. Since samples were unstirred in the experiments, it is possible that the faster-reacting enantiomer could become depleted in the region of the sample nearer to the light source, allowing more of the slower-reacting enantiomer to be consumed, leading to a value of s which is too low. In contrast, in the ESR experiments, the tube was either taken out from the cavity and shaken up after each peak was recorded, or, the spectra were recorded continuously and then extrapolated to zero irradiation time. Considering the sensitivity of s to C and EE when s is large,[5,6] and the fact that C and EE provide only an indirect measure of s using equation (7.3), the agreement with the values determined by ESR spectroscopy is satisfactory.

Control experiments with **1** and **12**, in which the DTBP was replaced with an equal volume of UV-transparent 2,2,5,5-tetramethyltetrahydrofuran **15** were also carried out. When an oxirane solution containing **1**-S (0.65 M), **15** (1.5 M) and the amine-borane **7a** (0.07 M) was UV irradiated at 187 K, a spectrum

attributed to the radical **16** [$a(2H_\beta)$ 27.84, $a(H_\alpha)$ 11.80 G, and g 2.0032 at 187 K] was obtained. Similar experiments using **12**-*R,R* (0.51 *M*), **15** (1.5 *M*) and the amine-borane **7a** (0.08 *M*) at 187 K yielded a weak spectrum of the radical **3**. These radicals are probably formed by Norrish Type 1 photochemical cleavage of the esters [equations (7.4) and (7.5)] and were not detected in the presence of the

$$\text{(structure)} \quad \xrightarrow{h\nu} \quad \text{(structure)} \quad + \quad \cdot CO_2Me \qquad (7.4)$$

16

$$\text{(structure)} \quad \xrightarrow{h\nu} \quad \text{(structure)} \quad + \quad \cdot CO_2Me \qquad (7.5)$$

3
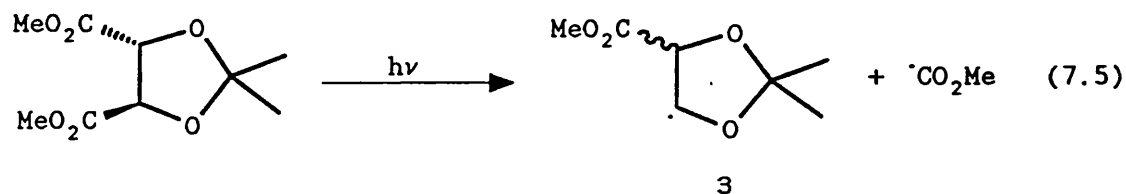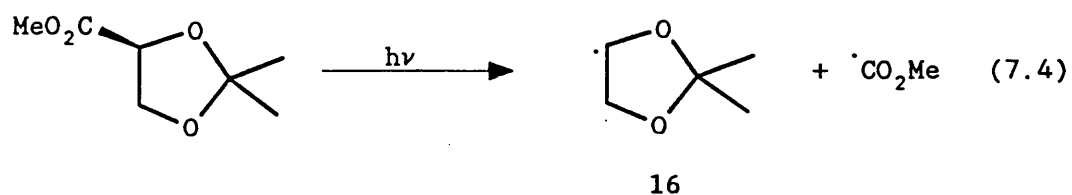
peroxide, which presumably absorbs most of the UV light.

References to Chapter 7

1. V. Paul and B. P. Roberts, *J. Chem. Soc., Perkin Trans. 2*, 1988, 1183.

2. V. Paul, B. P. Roberts and C. R. Willis, *J. Chem. Soc., Perkin Trans. 2*, 1989, 1953.

3. P. Kaushal, P. L. H. Mok and B. P. Roberts, *J. Chem. Soc., Perkin Trans. 2*, 1990, 1663.

4. A. L. J. Beckwith, S. Brumby, *J. Chem. Soc., Perkin Trans. 2*, 1987, 1801.

5. V. S. Martin, S. S. Woodard, Y. Y. Katsuki, M. Ikeda and K. B. Sharpless, *J. Am. Chem. Soc.*, 1981, **103**, 6237.

6. H. B. Kagan and J. C. Fiaud, *Topics Stereochem.*, 1988, **18**, 249.

CHAPTER 8

EXPERIMENTAL

8.1 ESR Spectroscopy

ESR spectra were recorded with a Varian E-109 instrument operating at *ca.* 9.1 GHz. The experimental details, including the method for measuring hyperfine coupling constants and g-values are described in Chapter 9.

Relative radical concentrations were determined by double integration of suitable lines in each spectrum. Some of the radicals exhibited CIDEP effects, such that corresponding hyperfine lines to low- and high-field of the spectrum centre were of unequal intensity (E/A polarisation).[1-3] In these circumstances, relative radical concentrations were determined by taking the average intensity of corresponding low- and high-field lines.[1-3] The rotamer ratios were obtained by computer simulation of spectra using a modified version of Krusic's program ESRSPEC2,[4] as described in Chapter 3.

8.2 Materials

The enantiomers of methyl 2,2-dimethyl-1,3-dioxolane-4-carboxylate **1** and dimethyl 2,2-dimethyl-1,3-dioxolane-*trans*-dicarboxylate (sold as 2,3-*O*-isopropylidene-tartrate) **12** and oxirane (all Fluka) were used as received. Trimethylamine-n-butylborane, the amine-boranes **7a** -**11a** (compound numbers as in Chapter 7), and racemic **12** were prepared as described in Chapter 6.

For competition experiments, a stock mixture of the two reactants was made up accurately by weight and portions of this were used for sample preparation.

References to Chapter 8

1. J. K. S. Wan and A. J. Elliot, *Acc. Chem. Res.*, 1977, **10**, 161.

2. P. J. Hore, C. G. Joslin and K. A. McLauchlan, *Chem. Soc. Rev.*, 1979, **8**, 29.

3. M. Anpo, K. U. Ingold and J. K. S. Wan, *J. Phys. Chem.*, 1983, **87**, 1674.

4. P. J. Krusic, Quantum Chemistry Program Exchange, Program no. 210.

CHAPTER 9

ELECTRON SPIN RESONANCE SPECTROSCOPY

In this chapter the theoretical principles of electron spin resonance (ESR) spectroscopy are discussed briefly. ESR spectroscopy is by far the most useful method for radical detection. As will be apparent later, detailed analysis of an ESR spectrum frequently makes it possible to deduce not only the gross chemical structure of the radical, but also its detailed conformation. Spin populations on various atoms in delocalised radicals may also be obtained. The technique can be applied to the measurement of radical concentrations. ESR spectroscopy is of particular value in that, by use of suitable methods of generation, the spectra of short-lived radicals may be obtained and the sensitivity of the method allows radical concentrations of $\geq 10^{-8}$ M to be detected.

9.1 Principles of ESR Spectroscopy

An unpaired electron possesses spin angular momentum and thus also possesses a magnetic moment. It can thus exist in two spin states, which are of equal energy in the absence of an external magnetic field. In the presence of an applied magnetic field, the magnetic moment of the electron can align itself parallel ($m_s = -1/2$, the α state) or antiparallel ($m_s = + 1/2$, the β state) to this field. The difference in energy of these states is given by equation (9.1).

$$\Delta E = g \mu_B B \qquad (9.1)$$

Here g is a dimensionless proportionality factor, which has the value 2.00232 for a free electron, μ_B is the Bohr magneton, and B is the

strength of the applied magnetic field (more precisely, the magnetic flux density). It is imperative that this field be homogeneous if the absorption peak is not to be broadened with resultant obscuring of the hyperfine splitting, which is so important in determination of radical structures.

Initially, in a bulk sample there are more unpaired electrons in the lower $(m_s = -1/2)$ energy level. The ratio of the numbers of spins in the two energy states at thermal equilibrium is given by equation (9.2), in which n_α and n_β are the numbers of spins in the

$$n_\alpha/n_\beta = \exp(\Delta E/kT) = \exp(g\mu_B B/kT) \quad (9.2)$$

lower and higher states, respectively, and k is Boltzmann's constant. Irradiation with electromagnetic radiation of frequency ν_0 results in transitions from the lower to the higher $(m_s = +1/2)$ energy level when the resonance condition, equation (9.3), is satisfied. Here B_0

$$h\nu_0 = g\mu_B B_0 \quad (9.3)$$

is the resonance field, such that $\Delta E = h\nu_0$. Non-emitting relaxation processes maintain the Boltzmann distribution of the two states and normally prevent saturation.

In general, for the study of organic free radicals, a magnetic field of about 330 mT (3300 gauss) is employed and the value of ν_0 is ca. 9.2 GHz, in the X-band microwave region of the electromagnetic spectrum. In principle, resonance can be achieved either by variation of the irradiation frequency or of the applied field, but invariably the frequency is kept constant and the magnetic field varied. In contrast to NMR spectrometers, ESR spectrometers are arranged to record the first-derivative of the absorption curve, rather than the absorption curve itself. This gives somewhat greater

sensitivity and also better resolution. The area under the absorption curve is proportional to the number of spins in the sample. Integration of the first-derivative to give the absorption curve, followed by integration of this to obtain its area, enables one to determine radical concentrations by comparison of this area with that due to a known concentration of radicals.

9.2 Methods of Radical Production for ESR Studies

Most simple organic radicals are transient species and hence special experimental techniques have to be devised to allow their detection by ESR spectroscopy. Three principal methods are used. (a) Radicals may be generated and immobilised in a rigid matrix. (b) They can be produced by continuous UV or electron irradiation of a solution of a suitable precursor in the cavity of the spectrometer. (c) They may be formed continuously by rapid mixing of reagents just before introduction into the cavity by use of a flow system.

The lifetimes of radicals generated in a matrix are very much greater than would be the case in fluid solution, because the slow rate of diffusion prevents or retards bimolecular radical-radical reactions. The spectra of radicals produced in this way can be complicated by anisotropic Zeeman and hyperfine interactions which are absent in the spectra of liquids, where the tumbling of the radicals averages out such interactions. However, if the radicals are free to tumble within cavities in a rigid matrix, such as adamantane, near-isotropic spectra can be obtained.

For study of the ESR spectra of specific radicals in solution, the most useful procedure involves continuous UV irradiation in the

cavity of the spectrometer, and this is the method used in the present work. ESR spectra were recorded using a Varian E-109 or Bruker ESP-300 instrument operating with a microwave frequency of 9.1-9.4 GHz. The spectrometers were equipped for *in situ* UV irradiation of samples. For each spectrometer, the light source was an Osram HBO-500 W/2 mercury discharge lamp in an Oriel Universal 1 KW housing equipped with an f/0.7 Aspherab fused silica condensing lens. The slightly-converging beam from this was focussed onto the sample, using a fused silica lens (focal length 10 cm, diameter 7.5 cm). The intensity of the incident radiation could be varied by placing metal gauze screens (nominally 30, 10, and 3% transmittance) in the light path. Most of the infrared and much of the visible radiation were removed by passage of the beam through a water-cooled aqueous solution filter (silica cell, path length 3 cm) containing $NiSO_4.7H_2O$ (0.38 *M*), $CoSO_4.7H_2O$ (0.70 *M*) and H_2SO_4 (0.04 *M*). The light reaching the sample was mainly in the wavelength region 240-340 nm and the heating effect of irradiation on the sample was reduced to *ca.* 6-7 °C at full intensity.

The temperature of the sample in the cavity was controlled by a pre-cooled flow of nitrogen using a standard variable temperature unit; it was measured by a thermocouple placed alongside the ESR tube about 2-3 cm from the top of the cavity insert and displayed on a digital thermometer (Comark). The insert thermocouple was calibrated against a second thermocouple contained in a sample tube filled with cyclopentane.

The heating effect of the UV irradiation on the sample was measured utilising the temperature dependence of $a(H_\beta)$ for the isobutyl radical (generated by photolysis of a cyclopropane solution

containing triethylsilane and isobutyl bromide) as a function of light intensity, as described previously.[1] The relationship between $a(H_\beta)$ and the sample temperature is given in equation (9.4).

$$T(°C) = 2.70394[a(H_\beta)]^2 - 198.419[a(H_\beta)] + 3490.41 \qquad (9.4)$$

Extrapolation to zero intensity gives the heating effect, and actual sample temperatures during photolysis are given by the sample temperature in the dark plus this heating correction. In all temperatures quoted in this thesis, the heating effect of the radiation has been accounted for.

9.3 Characteristics of ESR Spectra

Electron spin resonance spectra are characterised by three parameters:[2] the g-factor, the hyperfine splitting constants, and the linewidths. A close study of these parameters and of their temperature dependencies enables much detailed structural information about the particular radical to be gleaned.

9.3.1 g-Factors

In a magnetic field an unpaired electron in a free radical possesses, in addition to its spin angular momentum, a small amount of unquenched orbital angular momentum as a result of spin-orbit coupling. This causes the electron to have a slightly different effective magnetic moment from that which a free electron would possess (g 2.00232). The experimentally-measured isotropic g-factor of a polyatomic free radical as defined by the resonance condition [equation (9.3)] will thus deviate slightly from the spin-only value.

Hence, for a given operating frequency, radicals with different g-factors resonate at different applied field strengths. The difference in the g-factor for a radical and that for the free electron is analogous to the chemical shift in NMR spectroscopy. Differences in g-values are small, e.g. g-values for CH_3· and $HOCH_2$ are 2.0026 and 2.0033, respectively, but are nevertheless significant and can give valuable information about the structure of a radical.

In this work g-values were determined by measurement of the microwave frequency (using an E.I.P. Autohet microwave counter, model 331) and the magnetic field at the centre of the spectrum (using a Varian NMR gaussmeter). The difference in field between the gaussmeter probe and the sample was determined by measuring the g-value of the pyrene radical anion, which is accurately known to be 2.002710,[3] generated by the reduction of pyrene with sodium in THF. The unknown g-value was calculated using the resonance condition shown in equation (9.3).

9.3.2 Hyperfine Splitting Constants

These are by far the most useful characteristics of ESR spectra, both for determining the identity and also the detailed structure of the radical under study. Hyperfine coupling arises from interaction between the unpaired electron and neighbouring magnetic nuclei (^1H, ^{11}B, ^{13}C, ^{14}N, ^{17}O, etc.) present in the radical. The interaction with n equivalent nuclei of spin I results in $(2nI + 1)$ lines and the distance between each of these lines is (to first-order) equal to the hyperfine splitting constant. Since ^{12}C has no magnetic moment, proton hyperfine couplings dominate ESR

spectra of neutral and ionic hydrocarbon radicals. The interaction of the unpaired electron with n equivalent protons ($I = 1/2$) gives ($n + 1$) lines and, furthermore, the relative intensities of these lines are given by the coefficients of the binomial expansion of $(1 + X)^n$, which can be found readily from Pascal's triangle. Although the natural abundance of ^{13}C ($I = 1/2$) is only ca. 1.1%, other elements have non-zero spin isotopes which are present in high abundance. These include ^{10}B ($I = 3$) ca. 19.8%, ^{11}B ($I = 3/2$) ca. 80.2%, and ^{14}N ($I = 1$) 99.6%.

9.4 Origins of Hyperfine Splitting

Anisotropic hyperfine splitting, which arises from magnetic dipolar interactions, is only important in the solid state or in viscous media and will not be considered. In solution, such interactions are averaged to zero by rapid tumbling of the radicals. Isotropic hyperfine splitting only results if the unpaired electron has a finite probability of being at the magnetic nucleus in question. This is usually referred to as the Fermi contact interaction. Thus, coupling might be expected to be observable only when the singly occupied molecular orbital (SOMO) has some s-character, since only then will there be a finite electron density at the nucleus. For π-radicals, no splitting would be expected, since the unpaired electron is in a π-orbital which has a node in the molecular plane which contains all the magnetic nuclei. Experimentally, it is found that though splitting for electrons in orbitals with s-character can be very large (506 G for the hydrogen atom), there is nevertheless also some splitting for π-radicals.

9.4.1 α-Proton Splittings*

Hyperfine interaction of this type can be best illustrated by the methyl radical $H_3C\cdot$. Figure **9.1** shows schematically the <u>spin</u>

Figure 9.1 The spin polarisation mechanism for the methyl radical.

<u>polarisation mechanism</u>, which is responsible for the α-H and α-^{13}C splittings. For the two possible arrangements of electron spins about the trigonal carbon, that shown in Figure **9.1a** is the more probable (Hund's rules). The electrons in the σ bond are not perfectly paired due to an exchange interaction, which causes the σ electron with the same spin as the electron in the SOMO to come closer to this electron than the σ electron of opposite spin [Figure **9.1b**]. The value of $a(H_\alpha)$ will thus be negative while $a(^{13}C_\alpha)$ will be positive.

McConnell[4] has shown for π-radicals that the unpaired spin induced in the H_α-1s orbital is approximately proportional to the

*Throughout this thesis, the common nomenclature used was for hydrogen positions with reference to atom X : $-CH_2-CH_2-\overset{\cdot}{X}-H$
γ   β   α

unpaired spin population on the adjacent carbon atom, $\rho^\pi_{C\alpha}$. This can be expressed by equation (9.5), in which Q is a proportionality

$$a(H_\alpha) = Q\rho^\pi_{C\alpha} \qquad (9.5)$$

constant, which has a value between -20 and -30 G, depending on the particular type of radical.

9.4.2 β-Proton Splittings

Since spin polarisation depends strongly on the distance between the unpaired electron and the interacting nuclei another mechanism must be operative in transferring spin density to a β-proton. As commonly accepted, this is the hyperconjugation mechanism, which allows some of the unpaired α-spin density to appear at the β-proton, producing a positive coupling constant [see the canonical structures **9.2**].

9.2a   9.2b
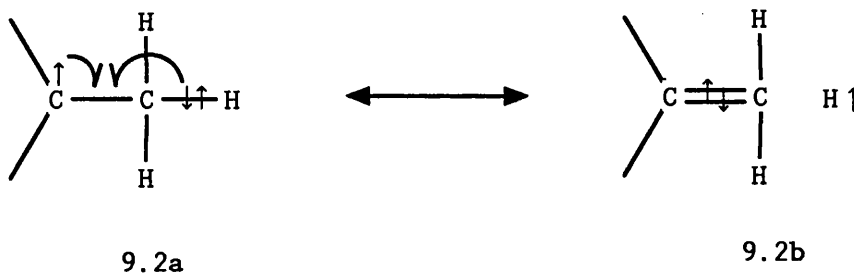
The hyperconjugation mechanism can be explained using simple molecular orbital theory, and can be visualized in Figure **9.3** for the ethyl radical. The basic concept is that there must be overlap between one or more sigma C-H bonds and the C_α-2pπ orbital which formally contains the unpaired electron. This interaction follows a $\cos^2\theta$ law, as shown by the Heller-McConnell equation[5,6] (9.6), in which A is a spin-polarisation parameter of small value (*ca.* 1 G),
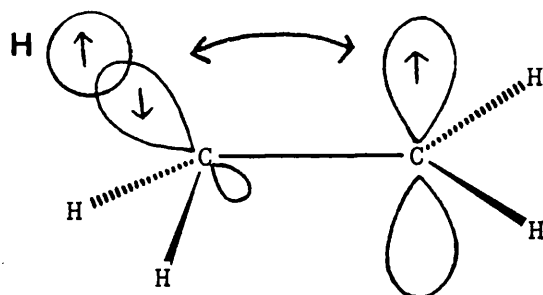
Figure 9.3 The hyperconjugation mechanism for the ethyl radical

$$a(H_\beta) = (A + B\cos^2\theta)\ \rho^\pi_{C\alpha} \qquad (9.6)$$

often neglected, and B is the hyperconjugation parameter of value 58.5 G. The angle θ is defined as the dihedral angle between the C_α-2pπ orbital and the C-H bond (Figure **9.4**). The coupling constant
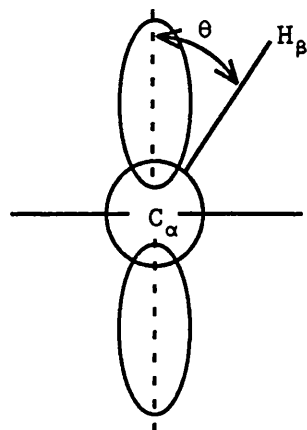

Figure 9.4

with a β-proton is thus at a maximum when it is in the same plane as that of the C_α-2pπ orbital *i.e.* when θ is zero.

9.4.3 Long-Range Proton Splittings

Long-range hyperfine interactions with γ and δ hydrogens are usually rather small, and positive and negative contributions to them

often cancel each other. They are very dependent on stereochemistry. An extensive review of this subject has been given by King.[7] Ellinger *et al.*[8] have given theoretical analyses of long-range hyperfine interactions in both simple aliphatic and bicyclic free radicals. Figure **9.5** illustrates the so-called "W" and "anti-W"
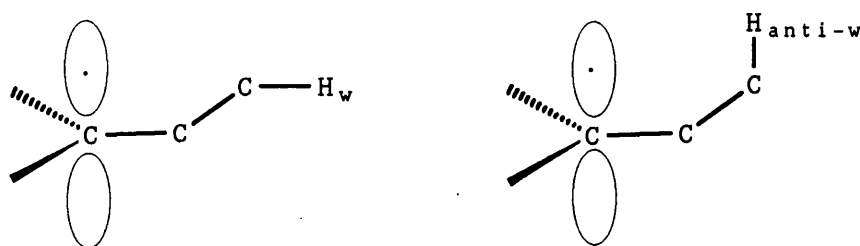

Figure 9.5   "W" and "anti-W" protons

rules. The former type of interaction leads to the larger value of $a(\mathrm{H}_\gamma)$ because contributions from spin-delocalisation and spin-polarisation are both positive, whereas they cancel for the latter.

9.5 Second-Order Effects

The analysis of hyperfine splittings which has been presented here is valid only in cases where the coupling energy is very much smaller than the electronic Zeeman energy. When hyperfine coupling constants are very large or the applied magnetic field is very small, additional splittings can occur which arise due to the removal of the degeneracy of certain Zeeman energy levels. Furthermore, lines can be shifted from the positions predicted by simple theory. These phenomena are referred to as second-order effects. Line shifts from the first-order positions are of the order $(a^2/4B_0)$ where a is the hyperfine coupling constant and B_0 is the applied magnetic field at

the centre of the spectrum.[9]

For example, to second-order, coupling of the unpaired electron with three equivalent protons actually gives rise to the splitting pattern shown below rather than to a simple 1:3:3:1 quartet.

First-order

Second-order

Intensity	1		1	2		1	2		1

Shift from first order position in units of $(a^2/4B_0)$

	3		7	1		7	1		3
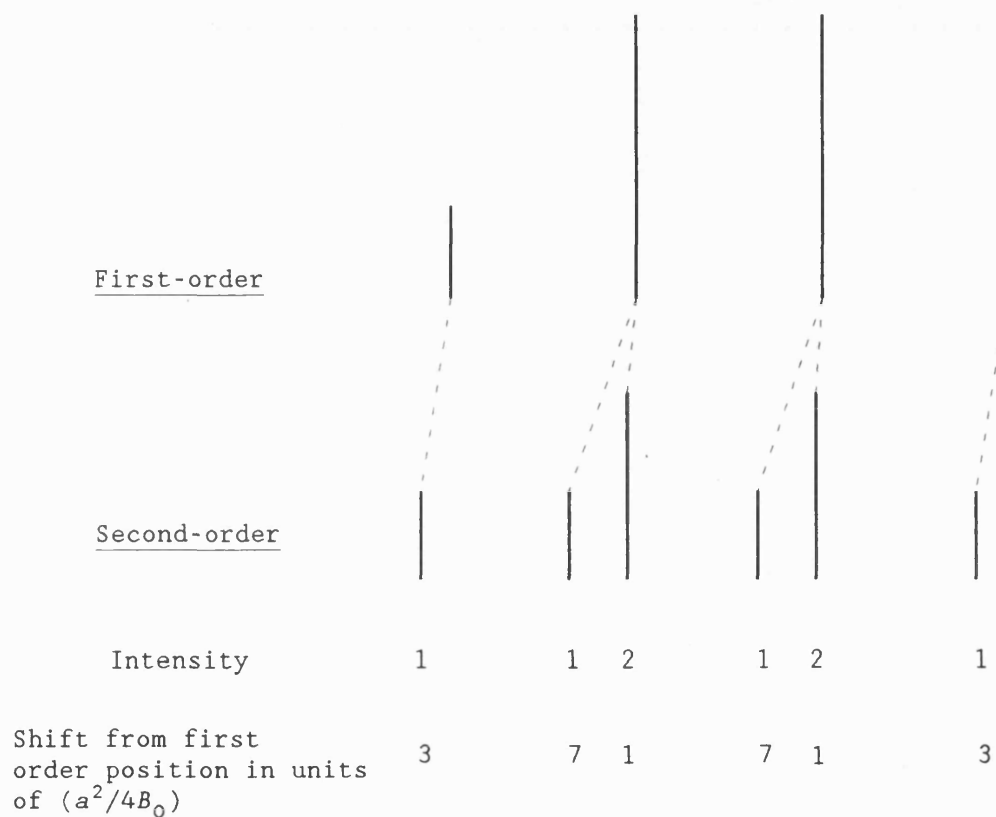
References to Chapter 9

1. J. A. Baban and B. P. Roberts, *J. Chem. Soc., Perkin Trans. 2*, 1981, 161.

2. J. E. Wertz and J. R. Bolton, "Electron Spin Resonance Elementary Theory and Practical Applications", McGraw-Hill, 1972.

3. B. G. Segal, M. Kaplan, and G. K. Fraenkel, *J. Chem. Phys.*, 1965, **43**, 4191.

4. H. M. McConnell, *J. Chem. Phys.*, 1956, **24**, 632, 764.

5. C. Heller and H. M. McConnell, *J. Chem. Phys.*, 1960, **32**, 1535.

6. J. K. Kochi, *Adv. Free Radical Chem.*, 1975, **5**, 189.

7. F. W. King, *Chem. Rev.*, 1976, **76**, 157.

8. (a) Y. Ellinger, A. Rassat, R. Subra, and G. Berthier, *J. Am. Chem. Soc.*, 1973, **95**, 2372. (b) Y. Ellinger, R. Subra, and G. Berthier, *ibid.*, 1978, **100**, 4961.

9. R. W. Fessenden, *J. Chem. Phys.*, 1962, **37**, 747.